

THE FORMATION OF NITRIC OXIDE FROM ORGANIC
NITROGEN CONTAINED IN FOSSIL FUELS

by

RICHARD CHARLES FLAGAN

B.S.E., University of Michigan
(1969)

S.M., Massachusetts Institute of Technology
(1971)

SUBMITTED IN PARTIAL FULFILLMENT
OF THE REQUIREMENTS FOR THE
DEGREE OF DOCTOR OF
PHILOSOPHY

at the

MASSACHUSETTS INSTITUTE OF TECHNOLOGY

May 1973

Signature of Author Signature redacted
Department of Mechanical Engineering, May 10, 1973

Certified by Signature redacted
" Thesis Supervisor

Accepted by Signature redacted
Chairman, Departmental Committee on Graduate Students





77 Massachusetts Avenue
Cambridge, MA 02139
<http://libraries.mit.edu/ask>

DISCLAIMER NOTICE

The pagination in this thesis reflects how it was delivered to the Institute Archives and Special Collections.

Missing page 97

THE FORMATION OF NITRIC OXIDE FROM ORGANIC NITROGEN
CONTAINED IN FOSSIL FUELS

by

Richard Charles Flagan

Submitted to the Department of Mechanical Engineering on May 10, 1973,
in partial fulfillment of the requirements for the degree of Doctor
of Philosophy.

ABSTRACT

Experiments, carried out in an atmospheric pressure oil-fired burner, which were designed to investigate the formation of nitric oxide from organic nitrogen contained in fossil fuels show that turbulent mixing significantly affects the NO emissions. In combustion characterized by poor initial fuel:air mixing, the exhaust NO concentration is much less than that observed in a flow of more uniform composition. A kinetic model for the conversion process is deduced from the results of premixed flame experiments. The interaction of chemical kinetics and turbulent mixing is explored, and a statistical collision model for the interaction is developed. The kinetic model is incorporated into a simple model describing the flow nonuniformities in the burner and is shown to predict the observed NO emissions.

Thesis Supervisor: John P. Appleton
Title: Professor of Mechanical Engineering

Acknowledgments

The author wishes to thank Professor John P. Appleton for his guidance and encouragement during the course of this work, Professor John B. Heywood, Professor James C. Keck, and Professor Adel F. Sarofim for participating in his thesis committee and their many helpful suggestions, Mr. Serge Galant for assistance in many aspects of this thesis, particularly in the application of his constrained equilibrium computer program, and Mr. Frank Pompei for assistance during the early experiments.

The author was supported during the final year of this study by a Sloan Research Traineeship.

TABLE OF CONTENTS

	<u>Page</u>
Abstract	2
Acknowledgments.	3
1. Introduction	6
2. Turbulent Flow Combustor Experiments	11
2.1 Experimental Details.	11
2.2 Exhaust Nitric Oxide Concentrations	12
2.3 Axial Nitric Oxide Concentration Profiles	13
2.4 Detection of HCN in the Exhaust Gases	14
3. Kinetic Model for Fuel-Nitrogen Conversion	15
3.1 Premixed Flame Experiments	15
3.2 Kinetic Model for Nitric Oxide Formation from Fuel Nitrogen	17
3.3 Slow Removal of Bound Nitrogen	19
3.4 Rapid Removal of Bound Nitrogen	26
4. Turbulent Mixing Processes	34
4.1 Introduction	34
4.2 General Considerations	35
4.3 Determination of β	37
4.4 Applications to CO Oxidation and Thermal NO Formation	39
4.5 Statistical Collision Model	40
4.6 Evaluation of the Distribution Function	44
5. Fuel Nitrogen Conversion in a Practical Combustor	48
5.1 Introduction	48

	<u>Page</u>
5.2 A Simple Mixing Model for Fuel-Nitrogen Conversion49
5.3 An Approximate Model of the Fuel-Nitrogen Conversion51
5.4 An Estimate of the Unoxidized Fuel-Nitrogen	52
6. Conclusions.	55
Table I	58
Table II	59
Figures60 - 97
References98 - 100
Appendix102 - 103
Biographical Note104

1. Introduction

As a consequence of recent system and engineering research studies,⁽¹⁻⁷⁾ it has now come to be recognized that, in addition to the formation of nitrogen oxides (NO_x) via the well-known Zel'dovich mechanism, the organic nitrogen contained in fossil fuels could be an important source on NO_x emissions from stationary combustion sources.

Unfortunately, with the current limited data on the total quantity of organic nitrogen present in the various grades and types of fuel oil and coal which are presently being used in the U.S., and our even more limited understanding of the chemical processes which are responsible for the conversion of fuel nitrogen to NO_x , it is difficult to make accurate assessments of the present and possible future magnitudes of the problem. In an attempt to do this, we observed that in 1968 electric utility and industrial combustion sources were estimated^(1,2) to account for 7.4×10^6 tons of the total 16.0×10^6 tons of NO_x (calculated as NO_2) emitted into the atmosphere of the continental United States by human activities. Based on figures taken from the Bureau of Mines' Simulated Model for Future Energy Demands,⁽⁸⁾ we estimate that these industries consumed approximately 4.6×10^8 tons of bituminous coal and 9.08×10^8 bbl. ($\approx 1.3 \times 10^8$ tons) of petroleum and natural gas liquids. As mentioned previously, estimates of the amount of elemental nitrogen contained in coal and fuel oils are varied and uncertain. However, analyses⁽⁹⁾ on the distribution of nitrogen in Wilmington (California) crude oil give an average of 0.64 per cent by weight, and

because the majority of the organic nitrogen compounds identified in the crude oil only begin to distil out significantly at temperatures greater than 400°C, the average concentration of elemental nitrogen in the residual grades of the oil is higher, typically greater than 1 per cent by weight. For U.S. coals, Spiers ⁽¹⁰⁾ compiled data which indicate that they contain an average of between 1 per cent and 1.75 per cent nitrogen by weight. (European soft coals appear to contain a greater percentage.)

The Esso NO_x System Study ⁽²⁾ has reported field data from a West Coast Utility Company which indicate that for power stations having capacities in the range 175-480 M.W. and burning fuel oil containing 1 per cent nitrogen by weight, between 12 per cent and 20 per cent of this may be converted to NO. Controlled laboratory studies, ⁽³⁻⁶⁾ on the other hand, indicate that nitrogen contained in additives of the types found in residual fuel oils and coal is converted to NO via combustion in somewhat larger proportions than the limited field studies indicate. If we therefore take a 20 per cent conversion as being a conservative figure, it appears that in 1968 about 3.8×10^6 tons or slightly more than one-half of the NO_x emitted by electric utilities and industrial combustion may well have been derived from nitrogen contained in the fuel.

The importance of the fuel nitrogen in the production of NO_x is clearly illustrated by the trends of the emissions from stationary combustion sources in the Los Angeles County Air Pollution Control District since 1959, ⁽¹¹⁾ see Figure 1. In 1959, Rules 62 and 62.1

of the A.P.C.D. prohibited the combustion of any fuel containing more than 0.5 per cent sulfur by weight.⁽¹²⁾ Prior to 1967 this was accomplished by replacing high-sulfur fuel oils (primarily Californian residuals) with natural gas to the extent of available supplies, increasing the proportion of stationary combustion fueled by natural gas from 50 per cent to 80 per cent of the total fuel consumed. In 1967 the natural gas was supplemented with low-sulfur fuel oils from Indonesia and Alaska, virtually eliminating the combustion of high sulfur oils in the Los Angeles Basin. The bound nitrogen content of natural gas is negligible and the Indonesian and Alaskan oils have a small concentration of organic nitrogen. The Californian crudes, on the other hand, have a high nitrogen content.⁽¹⁰⁾ Thus, the reduction of NO_x emissions from stationary sources during a time of steadily increasing electric power production may be, at least in part, attributed to the decreased fuel bound nitrogen, a side effect of the efforts to reduce the SO_2 emissions.

The fact that this source of NO_x could become even more important over the next few decades is made evident by the following considerations: (1) Bituminous coal deposits, which probably contain more than 1 per cent of elemental nitrogen, form the world's largest fossil fuel reserve.⁽¹³⁾ The Bureau of Mines'⁽⁸⁾ estimate of the coal demand of U.S. industry and the electrical utilities indicate that it may double between the years 1966 and 2000.⁽²⁾ Shale oil and tar sand deposits, which will probably assume increasing importance as sources of primary hydrocarbons in the U.S., are known to contain a high proportion of nitrogen-bearing compounds.

A recent analysis⁽⁹⁾ of typical gas oils prepared from Green River (Colorado) oil shale was shown to contain between 1.37 per cent and 1.79 per cent by weight of elemental nitrogen.

Various control methods for limiting NO_x emissions from large-scale stationary sources are actively being investigated. Reference 14 contains a detailed review of those techniques currently in use. Methods which seek to remove NO by scrubbing the flue gases may prove too costly and, even if economically feasible processes are developed, may be undesirable due to the reduced plume buoyancy as a result of the scrubbing process, thereby making the dispersion of remaining pollutants less efficient.⁽¹⁴⁾ Those methods which attempt to reduce the NO formation by changing the combustion conditions are based upon the Zel'dovich mechanism for the formation of NO from nitrogen in the air.⁽¹⁴⁾ It is not immediately apparent that such methods will work for the elemental nitrogen contained in fuels. Recent experimental evidence⁽⁶⁾ suggests that cooled flue gas recirculation, which acts to reduce the peak flame temperatures, is effective in reducing thermal NO but not fuel nitrogen conversion. On the other hand, two stage combustion, in which the fuel is initially burned under rich conditions and then diluted with additional air to allow complete combustion, may reduce NO formation due to both mechanisms. As of this writing, there is no proposed or tested kinetic scheme which could claim to explain how NO is formed from the fuel nitrogen.

In this thesis experimental measurements are reported which indicate that, in a practical combustor, fluid mechanical mixing plays a major

role in determining the net conversion of fuel-nitrogen to nitric oxide. In combustion characterized by poor fuel:air mixing, the exhaust NO concentration is less than that observed in a flow of more uniform composition. In order to understand these results a kinetic model is deduced from the results of recent premixed flame experiments. (15, 16) In addition, models of the interaction of chemical kinetics and turbulent mixing processes are explored. The kinetic model is incorporated into a simple model which describes the flow nonuniformities in the burner and is shown to predict the observed NO emissions.

2. Turbulent Flow Combustor Experiments

2.1 Experimental Details

Experiments to simulate the conversion of fuel nitrogen to NO in realistic combustion systems were carried out using a tubular combustor (4 inch internal diameter; 24 inch overall length) which was originally constructed as a practical model to study the effects of standard burner design and operating variables and to provide a reasonably simple flow pattern. Kerosene fuel was burned at a rate of about 1.3×10^5 BTU hr.⁻¹, the resulting combustion intensity of 10^6 BTU hr.⁻¹ ft.⁻³ atm.⁻¹ is, thus, in the range of current steam and gas turbine designs. Figure 2 is a schematic of the combustor. Fuel was admitted through a pneumatic atomizing nozzle using compressed air. Varying the air pressure had the effect of altering the initial fuel distribution in the combustor, i.e., a high atomizing pressure (29 psig) resulted in rapid fuel:air mixing, while a low atomizing pressure (12 psig) resulted in poor mixing. Combustion air (about 95 per cent of the total air flow) was supplied at atmospheric pressure and given swirl by a stationary 45° blade angle swirler. The total air flow of about 125 lbm. hr.⁻¹ was kept constant while the fuel flow rate was changed to obtain variable equivalence ratio.

Sample gases were removed using a water-cooled, stainless-steel probe and then subject to analysis. The variation in gas composition across any cross section of the burner was measured to be less than ± 20 per cent of the centerline value. Carbon monoxide and carbon dioxide were measured with Beckman Model 315A Nondispersive Infrared Analyzers, nitric oxide with a Thermo Electron Model 10A Chemiluminescent Analyzer,

and oxygen with a Beckman Model 777 Oxygen Analyzer. The measured data were corrected for water removal in the condensor and presented on a "wet" basis. More detailed descriptions of the combustor and instrumentation may be found in Reference 17.

In order to simulate the combustion of fuel oils containing organically bound nitrogen, the kerosene (see Table I for an analysis of the fuel) was doped with pyridine or pyrrole to amount to 1/4, 1/2, and 1 per cent of nitrogen by weight. These additives were chosen as typical of the forms in which nitrogen is found in residual fuel oils and the concentrations span the range found in most such oils without being so large as to significantly affect the combustion. Preliminary results of these experiments have been presented previously in References 18 and 19.

2.2 Exhaust Nitric Oxide Concentrations

Figures 3a to 3c show the NO concentrations (ppm) measured at the end of the combustor as a function of the overall fuel:air equivalence ratio. The solid points represent the measurements obtained with a pyridine additive, and the open points are the pyrrole data. For any atomizing pressure, there are no systematic differences between the two sets of data. All of the measurements were made after the combustor had achieved steady-state operating conditions. Furthermore, since the small amounts of additive did not significantly affect the heating value of the fuel, the thermal fixation of atmospheric nitrogen should not be affected at local equivalence ratios where the total NO level is much below equilibrium. (N.B. There was no difference between the exhaust CO concentrations with or without the additive, see Figure 4)

The full lines in Figures 3a to 3c represent the total amount of nitrogen added to the fuel. The broken lines add to this the total local nitric oxide due to thermal fixation. These thermal fixation estimates were shown, in Reference 17, to be in good agreement with measured levels of NO in the combustion of pure kerosene. At high atomizing pressures (good fuel:air mixing) and lean combustion with 0.25 per cent N by weight in the fuel, the measured [NO] amounts to complete conversion of the fuel nitrogen plus the full thermal NO formation. For larger amounts of additive the degree of conversion is somewhat less, about 90 per cent for 0.51 per cent N and about 80 per cent for 1.05 per cent N. Under rich conditions the conversion to nitric oxide decreases significantly. Poor fuel:air mixing (low atomizing pressures also results in reduced conversion. This might suggest that the NO formation is not kinetically controlled, but, rather, is controlled by the turbulent mixing process. The fact that this cannot be the case over the entire length of the burner is made apparent by the following observations.

2.3 Axial Nitric Oxide Concentration Profiles

Figure 5 shows the axial variation of NO as a function of distance along the length of the combustor for stoichiometric combustion and three different atomizing pressures. In each case it is clear that the NO concentrations rises rapidly to a plateau in a distance which probably contains the bulk of the nonequilibrium reaction zone (about 20 cm., 2 diameters). The CO concentration, on the other hand, was observed to continually decrease with axial distance down the combustor, as is shown

in Figure 6. This implies that, whereas the CO concentration changed as the combustion gases became better mixed, and, therefore, was mixing controlled, NO was formed primarily in the early part of the combustor which contained the radical rich turbulent flame reaction zone and was, therefore, kinetically controlled.

2.4 Detection of HCN in the Exhaust Gases

Since under poor fuel:air mixing conditions a considerable portion of the fuel nitrogen is not observed in the exhaust gases as NO, and further, since the possibility exists that some of the fuel nitrogen may have remained in a form other than NO or N₂, an attempt was made to measure HCN in the exhaust gases. Samples of the exhaust were passed through a gas bubbler in an attempt to dissolve any HCN in a basic solution of potassium hydroxide. Titration of this solution with silver nitrate⁽²⁰⁾ was followed by the standard confirmatory test⁽²¹⁾ for CN. Our CN⁻ ion analysis of a sample from the stoichiometric combustion of fuel doped with 0.51 per cent N at an atomizing pressure of 12 psig yielded an exhaust gas composition of about 30 ppm HCN. However, a second bubbler in series with the first collected a CN concentration only slightly less than the first, indicating that the efficiency of the system for the dissolution of HCN was poor. For this reason the figure of 30 ppm HCN may be considered to be a lower limit.

3. Kinetic Model for Fuel-Nitrogen Conversion

3.1 Premixed Flame Experiments

Recently Fenimore⁽¹⁵⁾ has presented a series of measurements on the formation of nitric oxide from fuel nitrogen in premixed ethylene flames. The experiments were performed at atmospheric pressure with the flame shielded from the surrounding air with a flow of nitrogen or argon. The reactants were mixtures of ethylene and oxygen, with either nitrogen or argon as a diluent, and the nitrogen containing additives. Four additives (pyridine, C_5H_5N , methacrylonitrile, $CH_2C(CH_3)CN$, methyl amine, CH_3NH_2 , and ammonia, NH_3) were used with the same resultant yields of nitric oxide for all the additives. The temperature was varied in flames of constant equivalence ratio by changing the proportion of molecular nitrogen or argon in the flow. The "oxygen index" was defined as

$$OI = \frac{(O_2)}{(O_2) + (\text{inert gas})} \quad (3.1-1)$$

to describe this dilution (note that for air $OI = 0.209$). Flame temperatures were measured using sodium line reversal techniques.

The burnt gas was sampled using a quartz probe in a region 0.5 cm. to 3.0 cm. downstream of the reaction zone. If the nitric oxide levels (measured with a slightly modified phenoldisulfonic acid technique) changed significantly in this region, the levels reported were those obtained at the minimum distance; hence 0.5 cm. may be taken as typical. Flow velocities were not measured, however, an estimate of the cold gas velocity upstream of the reaction zone has been obtained⁽²²⁾ (typically, 20 cm. sec.⁻¹ to 40 cm. sec.⁻¹). The typical hot gas residence time

prior to sampling was, thus, between 2 - 4 milliseconds.

The results of these experiments are shown in Figure 7a. The temperatures listed are the calculated adiabatic flame temperatures rather than the measured values (see Table II for a comparison of the two estimates). The differences between the two determinations is small, less than +12 per cent for all of the data, and within the range of uncertainty of the measurement technique. This data has been empirically correlated with a factor X which is determined for each equivalence ratio and degree of dilution (see Figure 7b). Numerically, X is the maximum concentration of NO formed when, for very large amounts of additive, the NO concentration becomes independent of the amount of additive. Fenimore postulated that intermediary species are formed, directly from the fuel nitrogen, which are then rapidly oxidized to form NO. Some of this NO is then removed by reactions forming N_2 . These arguments were entirely qualitative, however, and no detailed kinetics were proposed.

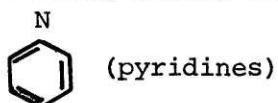
Additional experimental data on fuel nitrogen conversion in premixed flames has recently been obtained by Johnson⁽¹⁶⁾ at M.I.T. for methane/air flames using ammonia as an additive. In these experiments gas samples were extracted using a water-cooled stainless-steel probe and analyzed using a chemiluminescent analyzer. Again, the hot gas residence time is not well defined, but has been estimated to be between 5 and 10 milliseconds.

These experiments provide a convenient test for a kinetic model since the complications of heat transfer and turbulent mixing are avoided. A

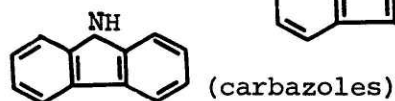
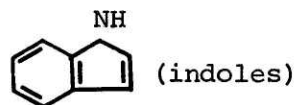
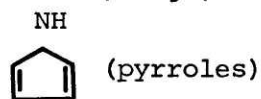
detailed development of the chemical kinetic model is described in the following sections.

3.2 Kinetic Model for Nitric Oxide Formation from Fuel Nitrogen

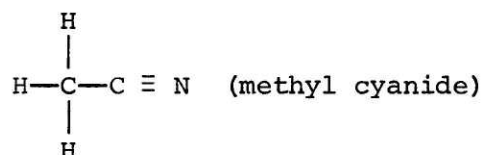
There are a wide variety of organic nitrogen bearing compounds contained in coals and crude oils. (9, 10) Organic chemists categorize them as being basic, e.g.,



and nonbasic, e.g.,

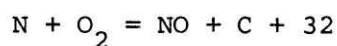
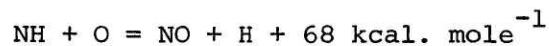


It is noticeable that in most of these compounds the bonds between the nitrogen atom and the remainder of the molecule are considerably weaker than the bond dissociation energy of N_2 (225 kcal. mole⁻¹). Even for nitriles, e.g.,



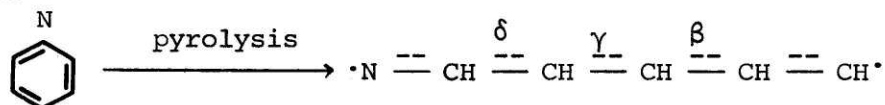
the bond energy of the CN triple bond is about 13 kcal. mole⁻¹ less than the dissociation energy of N_2 . Thus, it is not surprising that these organic molecules can yield larger quantities of NO when undergoing combustion than is derived by the thermal fixation of N_2 .

A reasonable kinetic explanation appears to be that these nitrogen compounds give radicals such as CN and NH during their decomposition within the nonequilibrium flame reaction zone, and that these processes are followed by fast O-atom attack, viz.



All of these reactions are exothermic, spin allowed, and therefore likely to be fast.

It is not difficult to surmise how radicals such as NH and CN are formed in the reaction zone, although such processes have not been investigated in any detail. If we consider pyridine as a representative nitrogen compound, it seems likely, following the suggestion of Hurd, et al.,⁽²³⁾ that pyrolysis will be initiated by rupture at the hetero (C-N) bond:



and that this will be followed by subsequent cleavage at the positions marked δ and γ . (The absence of acetylene, C_2H_2 , in the pyrolysis products⁽²³⁾ indicates that cleavage at the β bond does not occur.) Certainly, it should be anticipated that the above radicalized open-chain structure should undergo rapid decomposition and oxidation in the flame reaction zone in much the same way as does any other hydrocarbon fuel molecule. Having thus formed CN or, via hydrogen exchange reactions, NH, rapid oxidation as described above appears to be the next logical step.

In the following discussion a kinetic model is proposed to describe the nitric oxide formation from the fuel nitrogen and the subsequent removal of NO by the formation of N_2 . Since such a model necessarily

requires consideration of a large number of chemical species and a variety of reactions which occur on widely differing time scales, the concept of a constrained equilibrium will be employed. Specifically, the "rate controlled partial equilibrium method" advanced by Keck and Gillespie⁽²⁴⁾ will be applied to model the chemical relaxation due to a limited number of rate-limiting reactions. This technique implies the specification of certain constraints or "passive resistances" on the chemical composition of the gas. For example, one constraint which will be used is based upon the assumption that the shuffle reactions between the various single nitrogen species, i.e., N, NO, NH, NH₂, NH₃, CN, HCN, etc., occur on a much shorter time scale than do the recombination reactions which result in the formation of N₂. Thus, the formation of N₂ is the rate limiting step and, initially, the fuel nitrogen will be distributed in local equilibrium proportions among the single nitrogen, RN, species. As time progresses, the total RN concentration will decrease as the N₂ concentration increases. The time varying constraint would thus be the total RN concentration, X_{RN} (with units of moles per unit volume). The partial equilibrium method will be applied using a computer code developed by Galant⁽²⁵⁾ which couples the constrained equilibrium concept with the chemical rate equations and the one dimensional flow equations.

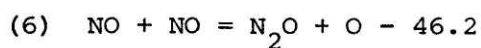
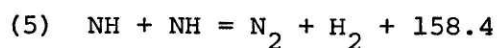
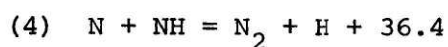
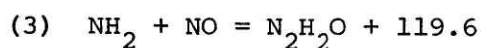
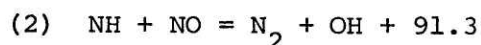
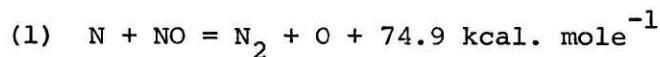
3.3 Slow Removal of Bound Nitrogen

If it is assumed that the rapid oxidation of the fuel nitrogen occurs with no net effects on the total constraint, X_{RN} , the behavior of the nitric oxide may be modelled using a single constraint. Once an

equilibrium distribution is established among the single nitrogen species, at any equivalence ratio less than about 2, the partial equilibrium calculations show that NO will be the predominant form of the fuel nitrogen. (Note: Appendix I presents a method for testing the validity of the constrained equilibrium assumption.) Between $\phi = 2$ and $\phi = 3$, NH_3 will account for most of the single nitrogen, and for ϕ greater than about 3 HCN or other nitrogen containing hydrocarbons will be more likely. This partial equilibrium distribution of the single nitrogen species is illustrated in Figure 8. Since the maximum equivalence ratio of the premixed flame data is 1.72, NO is the predominant form for all the data according to this model.

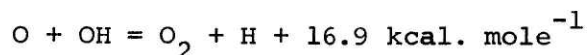
In addition to forming NO, the single nitrogen species may recombine to form N_2 . It is only in this step, the formation of the very stable N-N bond, that the oxidation of the fuel-N differs significantly from the oxidation of the carbon in the fuel, i.e., the carbon atom has no stable form analogous to N_2 .

The major reactions in this recombination step are likely to be the following exchange reactions:



Except for reaction (6) these reactions are exothermic and spin allowed

and, therefore, likely to be fast, certainly much faster than three body recombination reactions. Reaction (1) is the first step of the well-known Zel'covich mechanism for the thermal fixation of N_2 . The rate coefficient taken for this reaction is that of Baulch, et al.,⁽²⁶⁾ i.e., $k_1^+ = 6.43 \times 10^9 T \exp(-6250/RT) \text{ cm}^3 \text{ mole}^{-1} \text{ sec}^{-1}$. Two different values for the rates of reactions (2) and (3) have been suggested. Fenimore and Jones⁽²⁷⁾ have suggested that reaction (3) is much faster than reaction (2). Kaskan and Hughes⁽²⁸⁾ in a recent paper have utilized optical measurements of NH_3 , NH , NO , and OH in the flame gases of an NH_3/O_2 flame to estimate upper bounds on the rate coefficients of these reactions at a temperature of 2010°K. These rates, $k_2^+ = 2.41 \times 10^{13} \text{ cm}^3 \text{ mole}^{-1} \text{ sec}^{-1}$ and $k_3^+ = 1.2 \times 10^9 \text{ cm}^3 \text{ mole}^{-1} \text{ sec}^{-1}$, satisfactorily accounted for the observed NO decay while the faster rates estimated from Fenimore and Jones⁽²⁷⁾ data suggest a much more rapid decay of NH_3 and NO . MacLean and Wagner⁽²⁹⁾ also suggest that reaction (3) does not play the dominant role in the removal of NO formed in ammonia/oxygen flames. Thus, the rates determined by Kaskan and Hughes are used in the present study. No rate for reaction (4) has been measured or estimated, however, by drawing a parallel with the reaction



it may be expected to be relatively fast, with a rate of perhaps $k_4^+ = 10^{13} \text{ cm}^3 \text{ mole}^{-1} \text{ sec}^{-1}$. Reaction (5) undoubtedly proceeds through some intermediate species, Bahn suggests a rate coefficient of $k_5^+ = 3.6 \times 10^{11} T^{0.5} \exp(-1900/RT)$.⁽³⁰⁾ The rate of reaction (6) is taken to be $k_6^+ = 10^{14} \exp(-76000/RT) \text{ cm}^3 \text{ mole}^{-1} \text{ sec}^{-1}$.⁽²³⁾ Due to its high endothermicity,

this reaction is unimportant at the temperatures of atmospheric pressure combustion.

A single constraint equation may now be written to describe the decay of X_{RN} , i.e.,

$$\begin{aligned} \frac{dX_{RN}}{dt} = & -2k_1^+ [N] [NO] - 2k_2^+ [NH] [NO] - 2k_3^+ [NH_2] [NO] \\ & - 2k_4^+ [N] [NH] - 2k_5^+ [NH] [NH] - 2k_6^+ [NO] [NO] \\ & + 2k_1^- [N_2] [O] + 2k_2^- [N_2] [OH] + 2k_3^- [N_2] [H_2O] \\ & + 2k_4^- [N_2] [H] + 2k_5^- [N_2] [H_2] + 2k_6^- [N_2O] [O] \end{aligned} \quad (3.3-1)$$

where, to be consistent with the rate coefficients previously given, the concentrations X_{RN} and $[]$ have the units mole cm^{-3} . It is to be noted that, even at the greatest equivalence ratio of the premixed flame experiments, 1.72, $[NO]$ is much greater than the concentration of any other RN species. Therefore, the contribution due to reactions (4) and (5) will be small. The NH concentration is no more than 2 orders of magnitude less than $[NH_2]$. Hence, the contribution due to reaction (3) will also be small. Furthermore, due to the endothermicity of reaction 6, it does not contribute significantly to the total rate of N_2 formation.

In naturally occurring fuels, the nitrogen content rarely accounts for more than 2500 ppm of the combustion products. With such a small constrained species concentration, the relaxation of X_{RN} toward its equilibrium level will certainly have only minor effects on the gas temperature and the concentrations of species such as OH , O , and H which maintain the equilibrium proportions among the RN species.

It will be seen that, even in the experiments with extremely large additive concentrations, this assumption appears to be reasonable.

This allows us to define constants, $\alpha_{NO} = [NO]/X_{RN}$, $\alpha_N = [N]/X_{RN}$, $\alpha_{NH} = [NH]/X_{NH}$, etc., which are functions of only ϕ and T. Equation (3.3-1) may thus be written in the simplified form,

$$\begin{aligned} \frac{dX_{RN}}{dt} = & -2X_{RN}^2 (k_1^+ \alpha_N \alpha_{NO} + k_2^+ \alpha_{NH} \alpha_{NO}) \\ & + 2[N_2] (k_1^- [O] + k_2^- [OH]) \end{aligned} \quad (3.3-2)$$

Figure 9 illustrates the numerical integration of equation (3.3-1) using the partial equilibrium program of Galant⁽²⁵⁾ compared with the result of the above approximate expression at $\phi = 1.72$, $T = 2540^\circ K$, and both 2500 ppm and 13020 ppm of added nitrogen. It is clear that, even with the extremely large amount of additive, the error introduced by the constant temperature approximation is small, about 10 per cent, whereas the saving in complexity of computation is large, i.e., a first order differential equation with constant coefficients is solved rather than computing the partial equilibrium composition of the gas at each integration step.

The results of the integration of equation (3.3-2) are compared with Fenimore's premixed flame data in Figures 10a and 11a to 11c and with Johnson's data in Figures 10b and 12a to 12d. The rate equations were integrated to hot gas residence times typical of each set of experimental data, i.e., for Fenimore's rich, high temperature data and lean data, $t = 4$ msec, for Fenimore's rich, low temperature data, $t = 2$ msec, and for Johnson's data, $t = 5$ msec and $t = 10$ msec. Clearly,

this model (dashed lines in Figures 10a and 10b) is inadequate to describe the lean data since the model predicts the retention of all of the fuel-N as NO, whereas the experiments show a definite decrease in yield as the additive concentration is increased. We shall return to this point in the following section.

Fenimore's rich, high temperature measurements (●) are compared with the calculated yield of NO (—) in Figure 11a to 11c. In all of these cases both the magnitude and the slope of the measurements are predicted. The magnitude of the yield of NO predicted for the methane flames, Figures 12a to 12d, agrees with the measured levels, but the slope of the experimental data is not reproduced. The observation that, in contrast to Fenimore's data, the fractional yield of NO does not tend toward unity as the amount of additive is decreased, suggests that some difficulty with the experimental data. This might be due to a non-constant residence time.

The calculated conversion for Fenimore's rich, low temperature experiments (---- in Figures 10a to 10c) lies significantly above the measured values (○). Furthermore, as the equivalence ratio is increased, the discrepancy rapidly becomes large. This suggests that the primary assumption of this calculation, namely that in the radical rich region of the flame, the nitric oxide concentration achieves equilibrium with the other single nitrogen species, is no longer valid. At low temperatures and very rich conditions the oxygen containing species involved in the formation of NO may not be present in sufficiently high concentrations for this equilibration to occur within the time of the

radical overshoot. Thus, significant amounts of single nitrogen would likely be found in forms other than NO. Indeed, Fenimore did observe this behavior for rich combustion with large additive concentrations.⁽¹⁵⁾ To remove this assumption would require consideration of the hydrocarbon oxidation mechanism, which will be discussed in the next section.

The fuel nitrogen levels for the rich experiments are far in excess of the full thermodynamic equilibrium levels of [NO]. Therefore, the net reverse rates of the N₂ formation reactions are much slower than the forward rates. Equation (3.3-2) may be simplified to

$$\frac{d(X_{RN}/X_{RN0})}{dt} = \frac{-(X_{RN}/X_{RN0})^2}{\tau} \quad (3.3-2)$$

where the characteristic time of the reaction, τ , is defined as

$$\tau \equiv 2X_{RN0} (k_1^+ \alpha_N \alpha_{NO} + k_2^+ \alpha_{NH} \alpha_{NO} + k_3^+ \alpha_{NH_2} \alpha_{NO}) \quad (3.3-4)$$

and X_{RN0} is the initial fuel nitrogen concentration. The solution to equation 3.3-4 is

$$\frac{X_{RN}}{X_{RN0}} = \frac{1}{(1 + t/\tau)} \quad (3.3-5)$$

where t is the hot gas residence time prior to sampling. Again taking the residence times characteristic of the various experiments, all of the rich data have been plotted as a function of the calculated t/τ in Figure 13. It is readily apparent that, with the exception of Fenimore's low temperature measurements (half solid points), all of the data is fairly well correlated with this universal curve (plotted as a full line).

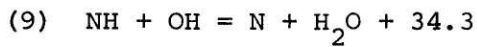
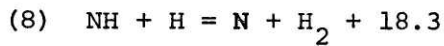
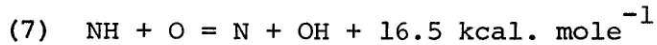
3.4 Rapid Removal of Bound Nitrogen

We now return to a consideration of NO formation for lean combustion conditions. The results of the simple, one constraint, model indicated that, once NO had been formed, its reduction was negligible whereas the experiments show a significant reduction. Therefore, the reactions occurring on a shorter time scale must be considered. To overcome this difficulty we have removed the restriction that the N and NO concentrations are in local thermodynamic equilibrium with the remaining single-N species.

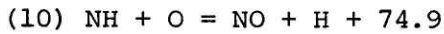
In modelling the results of premixed ammonia/oxygen flame experiments, Kaskan and Hughes⁽²⁸⁾ have applied a kinetic scheme very similar to that proposed below. Calculation using this mechanism for the ammonia flames suggest that the N atom concentration was depressed to only 2 or 3 per cent of its equilibrated value whereas the NH concentration was only depressed to about 80 per cent of its equilibrium value. Spectroscopic absorption measurements confirm the estimate of a near equilibrium NH concentration. Thus, of all the RN species other than NO, the nitrogen atom concentration appears to be most likely to be depleted by the reactions forming N₂. Furthermore, [N] is much greater than [NH] for lean combustion conditions and is, therefore, more important in the removal of the bound nitrogen. Thus, it is logical to constrain the nitrogen atom concentration to determine if any species involved in the RN removal reactions is depressed significantly below its equilibrium concentration.

Initially all of the fuel nitrogen is assumed to be in an equilibrium

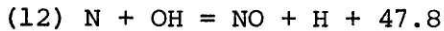
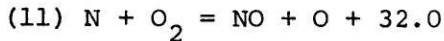
distribution among the single nitrogen species with the additional constraints that the N concentration, X_N , and oxidized species concentration, $X_{NO} = [NO] + [HNO] + [NO_2] + \text{etc.}$, are assumed to be zero. Shuffle reactions involving the removal of a hydrogen atom from NH produce free nitrogen atoms; likely reactions are:



Nitric oxide may be formed directly from NH,



or from N via the reactions of the Zel'dovich mechanism,



Estimates for the rates of reactions (7-10) have been taken from Bahn.⁽³⁰⁾

These are: $k_7^+ = 10^{12} T^{0.5} \exp(-100/RT)$, $k_8^+ = 7.1 \times 10^{11} T^{0.67} \exp(-1500/RT)$, $k_9^+ = 1.6 \times 10^{12} T^{0.56} \exp(-1500/RT)$, and $k_{10}^+ = 5 \times 10^{11} T^{0.5} \exp(-5000/RT)$, all with the units $\text{cm}^3 \text{ mole}^{-1} \text{ sec}^{-1}$. The expression of Baulch, et al,⁽²⁶⁾ $k_{11}^+ = 6.43 \times 10^9 T \exp(-6250/RT) \text{ cm}^3 \text{ mole}^{-1} \text{ sec}^{-1}$, correlates the data of a number of experiments. The measurement of Campbell and Thrush⁽³¹⁾, $k_{12}^+ = 4.2 \times 10^{13} \text{ cm}^3 \text{ mole}^{-1} \text{ sec}^{-1}$, has been used for reaction 12.

Three constraints must now be considered to model the system.

These are $X_N = [N]$, $X_{NO} = [NO] + [NO_2] + [HNO] + \text{etc.}$, and X_{RN} .

Note that an additional constraint may be defined as $X_{bN} = X_{RN} -$

$X_N - X_{NO}$; simply, this is the sum of the initial decomposition products

of the fuel, NH_3 , NH_2 , NH , CN , HCN , etc., excluding N and NO . Immediately after equilibration of the hydrocarbon system, $X_{\text{bN}} = X_{\text{RN}}$. Reactions 7 through 12 result in N and NO formation as described by the additional constraint equations:

$$\begin{aligned} dx_{\text{N}}/dt = & -k_1^+ [\text{N}] [\text{NO}] + k_1^- [\text{N}_2] [\text{O}] - k_4^+ [\text{N}] [\text{NH}] + k_4^- [\text{N}_2] [\text{H}] \\ & + k_7^+ [\text{NH}] [\text{O}] - k_7^- [\text{N}] [\text{OH}] + k_8^+ [\text{NH}] [\text{H}] - k_8^- [\text{N}] [\text{H}_2] \\ & + k_9^+ [\text{NH}] [\text{OH}] - k_9^- [\text{N}] [\text{H}_2\text{O}] - k_{11}^+ [\text{N}] [\text{O}_2] + k_{11}^- [\text{NO}] [\text{O}] \\ & - k_{12}^+ [\text{N}] [\text{OH}] + k_{12}^- [\text{NO}] [\text{H}] \end{aligned} \quad (3.4-1)$$

and

$$\begin{aligned} dx_{\text{NO}}/dt = & -k_1^+ [\text{N}] [\text{NO}] + k_1^- [\text{N}_2] [\text{O}] - k_4^+ [\text{NH}] [\text{NO}] + k_4^- [\text{N}_2] [\text{OH}] \\ & - k_3^+ [\text{NH}_2] [\text{NO}] + k_3^- [\text{N}_2] [\text{H}_2\text{O}] - 2k_6^+ [\text{NO}] [\text{NO}] + 2k_6^- [\text{N}_2\text{O}] [\text{O}] \\ & + k_{10}^+ [\text{NH}] [\text{O}] - k_{10}^- [\text{NO}] [\text{H}] + k_{11}^+ [\text{N}] [\text{O}_2] - k_{11}^- [\text{NO}] [\text{O}] \\ & + k_{12}^+ [\text{N}] [\text{OH}] - k_{12}^- [\text{NO}] [\text{OH}] \end{aligned} \quad (3.4-2)$$

The chemical relaxation may now be described by the integration of equations (3.3-1), (3.4-1), and (3.4-2) with the initial conditions $X_{\text{N}} = X_{\text{NO}} = 0$ and X_{RN} representing the total fuel nitrogen concentration. Again, to simplify the numerical integration, it may be assumed that the temperature and, thus, the relative concentrations of the species within any one constraint are constant. This is accomplished by defining the constants: $\gamma_{\text{NO}} = [\text{NO}]/X_{\text{NO}}$, $\gamma_{\text{NH}} = [\text{NH}]/X_{\text{bN}}$, $\gamma_{\text{NH}_2} = [\text{NH}_2]/X_{\text{bN}}$, etc., to compute the concentrations as the values of the constraints change. Figure 14 shows the resultant NO concentrations using the exact and approximate forms of this expression at an equivalence ratio of 0.9

with 16150 ppm of N added as NH_3 for Fenimore's lean experiments. ⁽¹⁵⁾

The deviation of the approximate calculation is small, about 20 per cent, even for this extreme additive concentration.

The characteristic behavior of the constraints may be seen in Figure 15. X_{bN} decays very rapidly; X_{N} rises to a maximum and then decays. The level of X_{N} during the decay exceeds that of X_{bN} . The NO yield rises to a plateau significantly below the 100 per cent conversion level although the great majority of the single nitrogen is in the form of NO. The total time scale of this transient behavior is on the order of 5 microseconds, three orders of magnitude shorter than that of the slow RN kinetics previously discussed and comparable to the time scale of the hydrocarbon oxidation reactions. The assumption of equilibration of the hydrocarbon system prior to any oxidation of the fuel nitrogen is, therefore, suspect. We shall return to this point shortly.

The reasons for this rapid decay are readily apparent. For a short time during the formation of NO, the concentrations of NO, N, and NH are comparable, allowing reactions 1 and 2 to proceed much more rapidly than will occur once a steady state has been reached between these species. This behavior is expected only during lean combustion since under rich conditions the N and NH concentrations do not approach the NH_3 concentration.

The solid lines in Figures 10a and 10b are the calculated yields of NO for the lean, premixed flame data. The present calculation (full lines) clearly predicts the observed trends much better than did the model using a single constraint (broken lines). However, the calculated

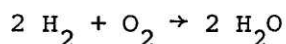
yields of NO are significantly below the measured values. The reason for this may, perhaps, be explained by the following. It has been assumed that the hydrocarbon system is equilibrated prior to any relaxation of the fuel nitrogen chemistry. The calculations have shown that the time scale of the RN relaxation is on the order of microseconds and, thus, on the same scale as the hydrocarbon oxidation kinetics. During the hydrocarbon oxidation process the concentrations of radical species such as OH, O, and H may significantly overshoot their final levels. The result of superequilibrium radical concentrations is to increase the yield of NO by further reducing the time required for the formation of N and NO. This effect is demonstrated in Figure 10a where the O, OH, and H concentrations have been arbitrarily increased by a factor of 3 (Δ) and a factor of 10 (O) times their equilibrium value. As with very rich, low temperature conditions a proper description of this effect requires a kinetic model to describe the hydrocarbon oxidation system. However, at the concentrations likely to be found in realistic fossil fuels, less than 2500 ppm in the exhaust gases at stoichiometric, the error appears to be less than about 30 per cent of the total exhaust NO concentration. For this reason, the additional modelling has not been undertaken.

In summary, a relatively simple kinetic scheme has been developed which predicts the trends of the premixed flame data for the conversion of fuel-nitrogen to NO. It appears that any fuel-N which is not observed in the exhaust as NO has been converted to N_2 except at extremely rich combustion conditions. The primary source of error in this model is in

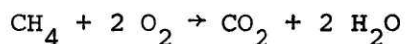
the assumption of rapid equilibration of the hydrocarbon species, which for lean combustion and very rich combustion is probably not complete within the time scale of the nitrogen conversion reactions.

We may speculate on possible improvements in the model calculations. For lean combustion conditions, it was observed that superequilibrium radical species concentrations might explain the discrepancy between the kinetic model calculations and the measured yields of NO. This is due to the higher steady-state nitrogen atom concentration reducing the time scale of NO formation more rapidly than the net rate of the N_2 forming reactions is increased.

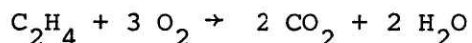
The magnitudes and even the existence of such radical overshoots in different hydrocarbon flames are not well established. In a hydrogen/oxygen flame a radical overshoot must occur due to the net reduction in the number of moles in the oxidation reaction,



i.e., 3 moles of reactants yield 2 moles of products, whereas in the combustion of methane,



or ethylene



the number of moles of reactants and the number of moles of products are the same. Thus, for these fuels a radical overshoot must be the result of dissociation or unimolecular reactions. Westenberg and Fristrom⁽³²⁾ have measured superequilibrium oxygen and hydrogen atom concentrations in ethylene flames. Detailed calculations of the hydrocarbon oxidation

kinetics for combustion of methane in shock tube experiments have suggested that, whereas significant overshoots of [O] and [OH] occur at stoichiometric conditions,⁽³³⁾ no such overshoots exist for lean combustion⁽³⁴⁾, $\phi = 0.5$.

In the absence of a significant radical overshoot, the formation of nitric oxide at an earlier stage of the hydrocarbon combustion than has been assumed in our kinetic calculations may still explain the discrepancy. At a lower temperatures, due to incomplete combustion, the steady state N and, possibly, NH concentrations may be reduced. This results in a reduction in the net rate of N_2 formation during the time in which NO is being formed.

Without modelling the entire hydrocarbon oxidation mechanism, an improved model of the fuel-nitrogen kinetics may be developed by dividing the flame reaction zone into two regions as described by Westenberg.⁽³⁵⁾ There is a relatively thin primary reaction zone in which free atoms and radicals (O, H, OH) are produced and react rapidly with the fuel. In this zone most of the carbon in the fuel is oxidized to form CO and most of the heat is released. The primary zone is followed by a much thicker secondary reaction zone in which the CO is oxidized to form CO_2 and any free atoms and radicals which are present in greater than equilibrium concentrations recombine by slow three-body reactions, thereby reducing the total number of moles in the system. To use such a model, the composition of the gas at the end of the primary reaction zone must first be estimated. Then, in addition to the fuel nitrogen relaxation of the constraints of [CO] and on the total number of moles, M, must be

followed by integrating the appropriate rate equations. Although the description of the secondary zone may improve the model of the fuel-nitrogen kinetics, it should be noted that this approach still avoids the problem of modelling the formation of NO when it probably occurs, on the same time scale of the CO formation reactions.

4. Turbulent Mixing Processes

4.1 Introduction

In practical continuous flow combustors where the fuel and air enter the burner separately, significant nonuniformities exist within the flow. A complex turbulent mixing-controlled flame structure is the result of a nonuniform fuel distribution in the burner reaction zone. In a liquid-fueled burner the fuel atomization, the details of the droplet trajectories and fuel vaporization rates, the air motion and the recirculation pattern all play a part in determining the extent of the nonuniformities in the flow. ⁽¹⁹⁾

It is well-known that poor mixing and excessively fuel-rich regions within the reaction zone result in soot formation. Furthermore, it has been demonstrated that combustion enhances the turbulent mixing, even in a premixed flame. ⁽³⁶⁾ Thus, the fuel-air mixing process affects the details of the flame structure. Also, the burnt gas pockets or eddies downstream of the reaction zone would not be expected to be uniform in composition. Depending on how the fuel has been distributed throughout the reaction zone, the fuel fraction in burnt gas eddies will be distributed about some mean value. As the flow moves through the burner, the action of turbulence and molecular diffusion will change this distribution.

Experimental results have previously been presented which illustrate the effects of turbulent mixing on the thermal fixation of atmospheric nitrogen and on the oxidation of carbon monoxide. ⁽¹⁷⁾ Simple models of the interactions of turbulent mixing and chemical kinetics have been successfully applied to these reactions. ^(17, 37) In this section these

simple models will be discussed and justified in the light of a statistical collision mixing model which will be described.

4.2 General Considerations

To develop a mixing model, we first write a conservation equation for a chemical species i which has a local concentration Γ_i ,

$$\frac{\partial \Gamma_i}{\partial t} + \frac{\partial}{\partial x_j} (\Gamma_i v_j) = D \nabla^2 \Gamma_i + R_i(\bar{\Gamma}) \quad (4.2-1)$$

where $\bar{\Gamma}$ is the vector of all species concentrations, $(\Gamma_1, \Gamma_2, \dots, \Gamma_i, \dots, \Gamma_n)$, R_i is a term which describes the net rate of production of Γ_i due to chemical reactions, and D is the molecular diffusivity which is assumed to be the same for all chemical species. Following the method of Corrsin⁽³⁸⁻⁴⁰⁾ an ensemble average may be taken over Eq. (4.2-1) to yield:

$$\frac{\partial \langle \Gamma_i \rangle}{\partial t} + \frac{\partial}{\partial x_j} (\langle \Gamma_i \rangle \langle u_j \rangle + \langle \gamma_i u_j \rangle) = D \nabla^2 \langle \Gamma_i \rangle + \langle R_i(\bar{\Gamma}) \rangle \quad (4.2-2)$$

in which γ_i and u_j represent the fluctuating components of Γ_i and u_j .

By restricting our discussion to flows with local homogeneity, i.e.,

$\frac{\partial}{\partial x_j} \langle \rangle \equiv 0$, Eq. (4.2.-2) becomes

$$\frac{d \langle \Gamma_i \rangle}{dt} = \langle R_i(\bar{\Gamma}) \rangle \quad (4.2-3)$$

or in the absence of chemical reactions affecting Γ_i ,

$$\frac{d \langle \Gamma_i \rangle}{dt} = 0 \quad (4.2-4)$$

We now subtract Eq. (4.2-2) from Eq. (4.2-1), multiply by γ_i , and again

take an ensemble average to find an equation for the time rate of change of the variance of the concentration:

$$\frac{d\langle\gamma_i^2\rangle}{dt} = -2D\left\langle\left(\frac{\partial\gamma_i}{\partial X_j}\right)\left(\frac{\partial\gamma_i}{\partial X_j}\right)\right\rangle \quad (4.2-5)$$

Finally, by assuming local isotropy, the three mean square derivatives in Eq. (4.2-5) may be characterized by a single length scale, ℓ , analogous to Taylor's "microscale" of turbulence, to give

$$\frac{d\langle\gamma_i^2\rangle}{dt} = -\frac{12D\langle\gamma_i^2\rangle}{\ell^2} \quad (4.2-6)$$

We may now define a mixing intensity,

$$\beta \equiv \frac{12D}{\ell^2} \quad (4.2-7)$$

Corrsin⁽³⁸⁾ has related β to the specific kinetic energy, ϵ , and a characteristic dimension of the reactor,

$$\beta \propto \left(\frac{\epsilon}{L^2}\right)^{1/3} \quad (4.2-8)$$

for fully developed turbulence. Equations (4.2-3) and (4.2-6) may be solved exactly only for very simple reactions with constant rate coefficients. Consider an n^{th} order chemical reaction for the irreversible elimination of Γ , i.e.,

$$R(\Gamma) = -k_n \Gamma^n \quad (4.2-9)$$

Equations (4.2-3) and (4.2-6) now become

$$\frac{d\langle\Gamma\rangle}{dt} = -k_n \langle(\langle\Gamma\rangle + \gamma)^n\rangle \quad (4.2-10)$$

and

$$\frac{d\langle\gamma^2\rangle}{dt} = -2\beta\langle\gamma^2\rangle - 2k_n \langle(\langle\Gamma\rangle + \gamma)^n\rangle \quad (4.2-11)$$

These results are simple enough for a zeroth order reaction

$$\frac{d\langle\Gamma\rangle}{dt} = -k_0 \quad (4.2-12)$$

$$\frac{d\langle\gamma^2\rangle}{dt} = -2\beta\langle\gamma^2\rangle \quad (4.2-13)$$

or a first order reaction

$$\frac{d\langle\Gamma\rangle}{dt} = -k_1 \langle\Gamma\rangle \quad (4.2-14)$$

$$\frac{d\langle\gamma^2\rangle}{dt} = -2\beta\langle\gamma^2\rangle - 2k_1\langle\gamma^2\rangle, \quad (4.2-15)$$

i.e., the net rates are independent of the mixing process. However, when a second or higher order reaction is considered, it is seen that the mean is dependent upon the variance,

$$\frac{d\langle\Gamma\rangle}{dt} = -k_2(\langle\Gamma\rangle^2 + \langle\gamma^2\rangle) \quad (4.2-16)$$

and the variance upon the skewness of the distribution,

$$\frac{d\langle\gamma^2\rangle}{dt} = -2\beta\langle\gamma^2\rangle - 4k_2\langle\Gamma\rangle\langle\gamma^2\rangle - 2k_2\langle\gamma^3\rangle \quad (4.2-17)$$

Thus, the familiar closure problem of turbulence appears. Since this difficulty arises so readily for even a simple reaction with a single rate determining species, direct solutions for more general reaction systems should be expected only in some simple limiting cases.

4.3 Determination of β

Before proceeding to explore cases for which the above formulation may be directly applied, it is useful to consider how the mixing intensity may be measured in a combustion system. If β is a constant, its value may be determined by observing the decay in the variance of the

concentration of a nonreacting species. For example, if the fuel were a hydrocarbon, C_xH_y , then Γ could be defined as the sum of the concentrations of all carbon containing molecules, i.e.,

$$\Gamma = X(C_{xH_y}) + 2(C_2) + (CO) + (CO_2) + \text{etc.}$$

and would be unaffected by chemical reactions. Given an initial variance, $\langle \gamma^2 \rangle_0$, the decay of the variance may be described by the solution to Eq. (4.2-6):

$$\langle \gamma^2 \rangle = \langle \gamma^2 \rangle_0 \exp(-\beta t) \quad (4.3-1)$$

The variance of the carbon concentration may be determined by measuring the mean oxygen concentration during stoichiometric combustion if the form of the distribution function, $f(\Gamma)$, is known. Any lean fluid will have a significant oxygen concentration while any rich fluid which has undergone complete combustion will have a negligible oxygen concentration (the oxygen concentration is very nearly a function of the stoichiometry alone).

Pompei and Heywood⁽¹⁷⁾ assumed the distribution function to be gaussian in the equivalence ratio, i.e.,

$$f(\phi) = \frac{1}{\sigma\sqrt{2\pi}} \exp(-(\phi-\phi_0)^2/2\sigma^2) \quad (4.3-2)$$

Based upon the variance, $\sigma^2 = \langle \gamma_\phi^2 \rangle$, determined in the manner described above, an "unmixedness" parameter, $s = \sigma/\phi_0$, was defined and assumed to be a function of the initial degree of uniformity in the distribution of fuel and air and of the residence time of the fluid in the combustor, but not a function of the overall equivalence ratio, ϕ_0 . The quantity, s^2 , was observed to decay as described by Eq. (4.3-1) with a high value of β in the combustion zone of the burner and a lower value thereafter.

4.4 Applications to CO Oxidation and Thermal NO Formation

The oxidation of carbon monoxide and the thermal fixation of atmospheric nitrogen have previously been modelled using approximate solutions to Eq. (4.2-1) by Pompeii and Heywood⁽¹⁷⁾. These two problems will now be explored as examples of the approximate application of the mixing calculations.

If the residence time of the combustion gases at high temperature is short enough that the equilibrium NO concentration is not approached, the nitric oxide formation via the Zel-dovich mechanism may be described by a very simple rate expression,

$$\frac{d[\text{NO}]}{dt} = 2k[\text{N}_2][\text{O}] \quad (4.4-1)$$

Since the oxygen atom concentration may be assumed to be in equilibrium with the hydrocarbon system, Eq. (4.4-1) is a function of the local equivalence ratio and the net heat transfer from the fluid element, i.e., the rate of NO formation is a function of ϕ and time along, $R(\phi, t)$. Thus, the mean NO formation rate may be expressed as

$$\frac{d\langle[\text{NO}]\rangle}{dt} = \langle R(\phi, t) \rangle \quad (4.4-2)$$

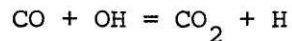
If the distribution function as a function of time, $f(\phi, t)$, is known, the ensemble average rate of NO formation at time t is simply

$$\langle R(\phi, t) \rangle = \int_0^{\infty} R(\phi, t) f(\phi, t) d\phi \quad (4.4-3)$$

and the mean NO concentration is given by

$$\langle[\text{NO}]\rangle_t = \int_0^t \int_0^{\infty} R(\phi, \tau) f(\phi, \tau) d\phi d\tau \quad (4.4-4)$$

The kinetics of the primary carbon monoxide oxidation reaction



under the conditions of Pompei's experiments were sufficiently fast for the CO to be assumed to be in local thermodynamic equilibrium over most of the length of his combustor. The local CO concentration is, therefore, a function of only the local fuel air equivalence ratio and the temperature, which is time dependent due to heat transfer. Thus, the mean CO concentration may be described by

$$\langle [\text{CO}] \rangle = \int_0^{\infty} [\text{CO}]_{\phi, t} f(\phi, t) d\phi \quad (4.4-5)$$

Using Equations (4.4-4) and (4.4-5) with the assumption of a decaying gaussian distribution in ϕ , Pompei was able to predict the exhaust CO and NO levels in his experiments.⁽¹⁷⁾ Clearly, the assumed gaussian distribution function is not initially valid when the fuel and air are injected separately into the combustor. In order to understand why Pompei and Heywood obtained such good results using their simple model, we shall now use a statistical collision model to simulate the turbulent mixing process and, thus, to study the evaluation of the distribution function.

4.5 Statistical Collision Model

The gaussian distribution function in ϕ , which was assumed in the simple mixing models previously discussed, is clearly not valid initially, when the fuel and air are injected separately into the combustor. Nonetheless, these simple models yielded estimates of [CO] and [NO] due to thermal fixation which agree with the experimental measurements. A statistical collision model for the turbulent mixing process will be

developed in this section. This model will allow us to study the form of the distribution function during its development and, thus, to understand the success of the simple models.

The turbulent mixing process will be viewed, in the present development, as a system of two-body fluid particle interactions in a manner similar to that described by Curl,⁽⁴¹⁾ Evangelista,^(42, 43) and others.⁽⁴⁴⁻⁴⁶⁾ In any collision between two equal mass fluid particles, i and j , whose composition is described by the concentration vectors $\bar{\Gamma}'_i$ and $\bar{\Gamma}'_j$ before collision, the composition of the two new particles created after the collision is assumed to be given by:

$$\bar{\Gamma}'_i = [(1 - \eta/2) \bar{\Gamma}'_i/\rho'_i + \frac{\eta}{2} \bar{\Gamma}'_j/\rho'_j] (\rho'_i + \rho'_j) \quad (4.5-1)$$

$$\bar{\Gamma}'_j = [(1 - \eta/2) \bar{\Gamma}'_j/\rho'_j + \frac{\eta}{2} \bar{\Gamma}'_i/\rho'_i] (\rho'_i + \rho'_j)$$

The parameter η describes the degree to which mixing takes place during the collision. For $\eta = 0$, no mixing occurs, whereas for $\eta = 1$, the two particles mix perfectly to form two new particles having identical concentrations,

$$\bar{\Gamma}'_i = \bar{\Gamma}'_j = \left(\frac{\bar{\Gamma}'_i}{2\rho'_i} + \frac{\bar{\Gamma}'_j}{2\rho'_j} \right) (\rho'_i + \rho'_j) \quad (4.5-2)$$

The composition of each fluid particle is assumed to be uniform throughout its volume and, between collisions, chemical reactions are assumed to proceed within each fluid element (in accordance with the appropriate rate equations) as though it were a closed system. If the size of each fluid particle is taken to be sufficiently small with

respect to the total flow that the contact time of a collision is comparable to the time scale of molecular diffusion, then η may be assumed to be equal to unity to a good degree of approximation. Thus, the concentrations after mixing are assumed to be given by Eq. (4.5-2)

In this collisional mixing model of the turbulence, the mixing intensity or frequency, β , is interpreted as the frequency at which each particle undergoes a collision. By taking an appropriately large sample of equal mass particles, N , an ensemble average of the species production may be computed, viz.

$$\frac{d\langle\Gamma_t\rangle}{dt} = \frac{1}{N} \sum_{i=1}^N \left(\frac{d\Gamma_i}{dt} \right) \quad (4.5-3)$$

where $(d\Gamma_k/dt)_i$ is the chemical rate of production of species k in the i^{th} fluid particle. It is to be noted that the sample does not necessarily represent the total flow, but rather, an ensemble average of the total composition of the flow.

The computational method which is used to compute the mixing history is a Monte Carlo technique in which randomly selected pairs of particles are allowed to collide and mix. If individual interactions are computed sequentially, each collision represents a forward step in time equal to

$$\Delta t = 1/(\beta N) \quad (4.5-4)$$

In order for this method to reasonably represent the physical situation, the initial composition of the fluid elements must be carefully chosen to represent the overall composition of the flow in the combustor and the form of the initial distribution function of the composition.

Figure 16 shows a flow diagram for a computer code designed to

perform the calculations outlined above. The first step in this program is to initialize the composition of each fluid element in the sample of N fluid elements. To model our combustor, a small number of fluid elements, N_a , may be taken to represent the flow admitted through the fuel atomizer and to have the overall equivalence ratio of the atomizer jet, d_a . The small fraction of very rich fluid elements, N_a/N , is equal to the fraction of the total mass flow rate which is admitted through the atomizer. The rich elements, $1 \leq i \leq N_a$, are assumed to be a uniform mixture of vaporized, but unburnt, fuel and pure air, while the remaining elements, $N_a < i \leq N$, are pure air, $\phi = 0$. The value of β is initialized as β_0 , estimated as previously described.

A pseudorandom number generator is used to choose two indices, i and j , with the restriction that i not be the same as j . These are the indices of the two fluid elements to be involved in the first collision. These elements are allowed to mix completely, and then a new partial equilibrium composition is determined for the two identical particles. This equilibrium is subject to m constraints, $X_1, \dots, X_2, \dots, X_m$, such as the specific enthalpy of the fluid element (taking heat transfer into account) and, for thermal fixation of atmospheric nitrogen, the moles of NO per unit mass contained within the elements (which is zero for the first collision since no combustion has occurred prior to this time). Note that the fluid may be either too rich or too lean for any combustion to occur. Thus, the first forward time step of $\Delta t = (\beta N)^{-1}$ is completed and the value of the time must be increased by this increment, i.e., set t to be equal to $t_0 + (\beta N)^{-1}$, and a new

value of β is computed.

Then, for each fluid element, the constraint equations are integrated from time, t , to the time of the next collision, $t + (\beta N)^{-1}$. A new pair of elements is then chosen randomly to describe the next collision, and the mixing process is repeated.

4.6 Evaluation of the Distribution Function

Our combustor has been described in detail in a previous section. The fuel is admitted through a pneumatic atomizing nozzle. The fuel is assumed to be vaporized upon injection into the combustor and to be perfectly mixed with the atomizing air. The combustion air is supplied around the circumference of the atomizing jet; however, for simplicity it is assumed that the mixture is spatially homogeneous at the inlet to the combustor. The initial distribution is therefore bimodal in nature with a small amount of very rich fluid and a large amount of pure air. The effects of recirculation are neglected so that the flow may be assumed to be a one-dimensional plug flow.

The proportion of the total number, N , of equal mass fluid elements in the sample which initially have the very high equivalence ratio of the atomizer jet is equal to the fraction of the total mass flow rate admitted through the atomizer. The remaining elements are pure air, $\phi = 0$. These elements are allowed to mix randomly as described by the Monte Carlo model, and their composition trajectories are followed through the burner. Figure 17 shows the decay of the dimensionless mass mean, $\langle \phi \rangle / \phi_0$, and variance of the distribution function, $\langle (\phi - \langle \phi \rangle)^2 \rangle / \phi_0^2$, as a function of the dimensionless mixing time

$$\Theta(t) = \int_0^t \beta(\tau) d\tau \quad (4.6-1)$$

Θ is the mean number of collisions which each fluid element has suffered, i.e.,

$$\Theta(t) = N_{\text{coll}}(t) / N \quad (4.6-2)$$

where $N_{\text{coll}}(t)$ is the total number of collisions which have occurred prior to time t . These results were calculated for stoichiometric combustion using 1000 sample elements in the statistical collision model. For Θ greater than about 2 the mean equivalence ratio is equal to the overall equivalence ratio and $\langle(\phi - \langle\phi\rangle)^2\rangle/\phi_0^2$ becomes the "unmixedness" parameter, s^2 .⁽¹⁷⁾ Furthermore, a comparison of the distribution function calculated using the statistical collision model with a gaussian distribution which has the same variance, shown in Figure 17, indicates that for Θ greater than 2 the distribution function becomes very nearly gaussian in nature.

Complete combustion does not occur until the fuel and air are mixed to some extent. The range of equivalence ratios in which complete combustion is likely to take place is not well defined. However, based upon estimated flammability limits of the kerosene fuel⁽⁴⁷⁾ it is assumed that complete combustion occurs if $0.3 \leq \phi \leq 3$. There is assumed to be no combustion outside these limits. The oxygen profile during stoichiometric combustion has been computed using the above assumptions and is shown in Figure 19.

From the calculated dependence of s and $[O_2]$ on Θ and oxygen profiles measured along the length of the combustor during stoichiometric combustion, the mixing history in the combustor may be estimated. Figure 20 shows

the dimensionless mixing time, Θ , as a function of the distance down the combustor for three different atomizing pressures. Extrapolating these results to lower atomizing pressures, it is estimated that even at 12 psig the distribution function is gaussian in nature, i.e., Θ is approximately 3, within the first two diameters of the combustor length.

Figure 21 shows the rate of NO formation via the Zel'dovich mechanism, taken from Reference 17, as a function of the local equivalence ratio. Clearly the vast majority of the NO formation occurs between $\phi = 0.8$ and $\phi = 1.2$. The mass fraction of the flow which has a local equivalence ratio in the range $\phi_\ell < \phi < \phi_u$ is

$$\int_{\phi_\ell}^{\phi_u} f(\phi) d\phi$$

This mass fraction, calculated for stoichiometric combustion and three ranges of ϕ , is shown in Figure 22. The points have been calculated using the statistical collision model, whereas the lines have been computed using the gaussian distribution. At short mixing times, Θ less than 3, the mass fraction within the range $0.8 < \phi < 1.2$ is small, less than 20 per cent of the total fluid. Thus, the discrepancy between the gaussian and the distribution given by the statistical collision model has a small net effect. As the fluid becomes more uniformly mixed and the mass fraction within the range becomes significant, the error due to the assumed gaussian rapidly decreases. Thus, the simple mixing model appears to provide a reasonable description of the net NO formation.

The carbon monoxide has been shown to be in thermodynamic equilibrium

at the local fuel:air equivalence ratio.⁽¹⁷⁾ Therefore, only a distribution function and net heat transfer are necessary to compute [CO]. The major contribution to [CO] is due to rich fluid (see Figure 23). In Figure 22 the two determinations of the mass fraction of fluid with equivalence ratio greater than 1.05 are shown. Clearly at a value of about $\Theta = 3$ the simple mixing model calculation of CO will start being a good approximation.

5.0 Fuel Nitrogen Conversion in a Practical Combustor

5.1 Introduction

The rate limiting step in the fuel nitrogen conversion process has been shown to be the formation of N_2 via reactions 1-6. Since these reactions are second order in $[NO]$, the local rate of change of $[NO]$ is strongly dependent upon the local NO concentration and, therefore, upon the past history of the fluid element. Thus, a more detailed mixing model than has been applied to CO and thermal NO formation is required to accurately model the fuel nitrogen conversion process.

The statistical collision model is well-suited to this task. The application of the collision model to the combustor used in the fuel-nitrogen experiments has been described in the previous section. The only additions to these calculations which are necessary are the kinetics of the fuel-nitrogen conversion and the details of the heat transfer. Recall that, between collisions, chemical reactions are assumed to proceed within each fluid element as though it were a closed system. Thus, the kinetics may be modelled in the same manner as in the premixed flame experiments.

In as much as the reduced gas temperature due to heat transfer results in significant reductions of $[N]$ and $[NH]$ and the eventual freezing of the single nitrogen kinetics in this combustor, the heat transfer from the hot gas to the burner walls must be considered. Radiative heat transfer from the fluid elements may be treated in the manner of Hottel and Sarofim. (48)

In the absence of significant soot formation, i.e., in a nonluminous flame, the predominant radiating species are CO, CO₂, and H₂O. The concentrations of these species are determined in the partial equilibrium calculations and their emissivities have been measured.⁽⁴⁸⁾ so the heat transfer due to radiation from each fluid element may readily be estimated.

Unfortunately, the major mode of heat transfer in our combustor is conduction from the hot gas to the walls.⁽¹⁷⁾ This process involves the rapid cooling of a small amount of gas in close proximity to the burner walls. The effect is then transmitted to the remainder of the gas by the turbulent mixing process. The conduction to the walls may be included in the turbulent mixing model by allowing random collisions of fluid elements with the burner walls. During each such collision some degree of thermal equilibration is achieved between the wall and the fluid element. Thus, a new empirical parameter, a measure of this degree of equilibration, must be introduced into the statistical collision model. In as much as detailed heat transfer measurements have not been made in our combustor, it is not possible to evaluate such a parameter at the present time. We shall, therefore, use a simple model of the effects of mixing process in the following section to model fuel nitrogen conversion.

5.2 A Simple Mixing Model for Fuel-Nitrogen Conversion

It has been demonstrated that a simple mixing model of the type applied to thermal NO or CO formation is not a reasonable approximation for fuel nitrogen conversion. We shall, therefore, adopt a heuristic

model which will be justified in an a posteriori fashion.

The mean NO concentration due to fuel nitrogen was observed to reach a plateau at about two diameters down the combustor (see Figure 5). The NO concentration as a function of the local fuel air equivalence ratio at this point is computed in a very simple manner. It is assumed that, on the average, the NO concentration in a fluid element at any local equivalence ratio is described by applying the kinetic model to that fluid element and allowing no mixing to occur. This NO concentration is shown in Figure 24 for three different additive concentrations. Also shown are the 100 per cent conversion levels and the equilibrium NO at two diameters down the combustor. At rich conditions, the reduction due to the slow removal mechanisms is significant. At lean conditions, the initial superequilibrium N and NH concentrations result in a rapid reduction of NO. On a longer time scale the Zel'dovich mechanism results in additional NO formation. At very lean conditions, $\phi < 0.5$, and very rich conditions, $\phi > 2$, very little of the fuel nitrogen is oxidized.

The mean NO concentration is calculated by integrating the product of the local NO concentration and a gaussian distribution function

$$\langle [\text{NO}] \rangle = \int_0^{\infty} [\text{NO}]_{x_p} f(\phi, x_p) d\phi \quad (5.2-1)$$

at $x_p = 20$ cm (2 diameters) down the burner. The calculated NO concentrations are compared with the experimental measurements in Figures 25a - 25c. (For clarity, only the pyridine data is shown.) The values of the "unmixedness" parameter, $s = \langle \gamma_{\phi}^2 \rangle^{1/2} / \phi_0$, were

determined from the statistical collision model calculations previously presented. Both the levels and the trends of the experimental data are predicted using this simple model of the flow nonuniformities.

The success of this calculation may be understood in part by considering the two extreme mixing conditions. At an atomizing pressure of 29 psig (well mixed), the flow in the combustor is very nearly uniform in composition after short flow time. Hence, these experimental conditions are closely approximated by the kinetic model calculations for a uniform flow. In Figure 26 the results of the kinetic model calculations are seen to agree with the high atomizing pressure data. The width of the distribution function is so large at low atomizing pressures (poor mixing) that all effects of the details of the local nitric oxide profiles are integrated out. The nearly constant NO levels over the full range of ϕ make this readily apparent in the 12 psig data shown in Figures 25a - 25c. Thus, even if the levels of NO are only approximately correct the calculations should yield reasonable estimates of [NO]. The intermediate atomizing pressures show varying degrees of smoothing out the details of the NO vs. ϕ profile.

5.3 An Approximate Model of the Fuel-Nitrogen Conversion

Boilers and other large scale combustion sources may generally be characterized by poor fuel:air mixing. Thus, the details of the local NO concentrations should not have a large effect on the mean NO emissions. A simple approximation to the local NO concentration which requires no kinetic calculations may yield reasonable estimates of the NO emissions.

Rather than applying the kinetic model we assume that all of the

fuel-nitrogen is initially oxidized to form NO. If the NO thus formed is at a level greater than equilibrium, it is assumed that the reactions which result in N_2 formation reduce the local NO concentration to its full equilibrium value. If, on the other hand, the NO concentration is less than equilibrium, it is assumed that the Zel'dovich mechanism proceeds unaffected by the fuel-nitrogen. The NO levels obtained under these conditions are the full thermal fixation calculated (or measured) for a nitrogen free fuel plus all of the fuel nitrogen. This NO vs. ϕ profile is, thus, the lower of either the equilibrium NO concentration or the sum of the total fuel nitrogen level plus the full thermal NO concentration. The mean NO concentration is calculated as described in the previous section using this estimate of the local nitric oxide concentration.

Figures 27a to 27e compare the results of this calculation with the measured NO concentrations. The trends of the calculated concentrations are in close agreement with the measured values at low atomizing pressures. At higher pressures the agreement is not so close, especially for rich conditions. Also, since the rapid reduction mechanism has not been taken into account, the predicted levels are higher for well mixed lean combustion. This very simple calculation does, however, adequately predict the emissions when the fuel:air mixing is poor.

5.4 An Estimate of the Unoxidized Fuel Nitrogen

Exhaust concentrations of hydrogen cyanide or a cyanide-type species amounting to about 30 ppm have been measured for stoichiometric combustion and poor fuel:air mixing with 1/2 per cent by weight of

bound-nitrogen in the fuel. This suggests that some of the bound-nitrogen in the fuel is surviving the flame reaction zone and being emitted in an unoxidized form. The statistical collision model makes it possible to estimate an upper bound on the emissions unburnt fuel-nitrogen.

At adiabatic flame conditions any fuel-nitrogen existing in fluid with an equivalence ratio greater than about 2 is not expected to be oxidized. As the flame gases are cooled it is anticipated that leaner combustion conditions are required to oxidize any remaining bound-nitrogen. No attempt is made to describe this effect in detail, and the arguments which follow are entirely speculative.

Figure 28 shows the fraction of the total fuel (or fuel-nitrogen) contained in fluid with a local equivalence ratio greater than 2 as a function of the dimensionless mixing time, Θ . At an atomizing pressure of 12 psig the value of Θ at the point at which the NO level reaches a plateau is about 3. This suggests that 10 per cent of the fuel nitrogen has not been oxidized at this time, or about 65 ppm of the total of 650 ppm of fuel nitrogen.

For an atomizing pressure of 12 psig, the value of Θ at the exhaust is about 4.5. Thus, if the flow were adiabatic, all of the fuel-nitrogen might be oxidized. The upper limit of the range of equivalence ratio in which the fuel-nitrogen is fully oxidized may, however, be reduced by heat transfer. For example, if this limit were reduced to $\phi = 1.5$, as much as 6 or 7 per cent (40 to 45 ppm in the exhaust) of the fuel nitrogen might be emitted in some form other than NO or N_2 . Thus, the

measured HCN concentration appears to be reasonable, although a significantly higher concentration would not be anticipated.

6.0 Conclusions

Experimental measurements have been presented which indicate that, in a practical combustor where the fuel and air are not premixed, the formation of nitric oxide from fuel-nitrogen is strongly dependent upon the turbulent mixing process. Thus, in order to predict the nitric oxide emissions from practical systems burning nitrogen containing fuels, it has been necessary to model both the chemical kinetic and turbulent mixing aspects of the problem.

A kinetic model for fuel-nitrogen conversion has been deduced from the results of premixed flame experiments. At relatively high temperatures (1905°K to 2535°K) and rich combustion conditions ($\phi = 1.1$ to $\phi = 1.72$) the model accurately predicts the experimentally observed yields of NO for additive concentrations between 710 ppm and 13200 ppm. At both lean combustion conditions ($\phi = 0.9$, $T = 1910^\circ\text{K}$ to 1985°K , 350 ppm to 11000 ppm) the trends are predicted but the levels are not. These discrepancies at lean conditions are due to the assumption of rapid equilibration of the hydrocarbon system prior to any fuel-nitrogen oxidation. At rich conditions, the discrepancy is due to the assumption that equilibration among the single nitrogen species occurs simultaneously with the hydrocarbon system equilibration whereas the single nitrogen equilibrium is probably not achieved. Since the oxidation of the fuel-nitrogen probably occurs on the same time scale as the oxidation of the carbon, improvements in the kinetic model require more detailed modelling of the hydrocarbon oxidation kinetics.

A statistical collision model for the interactions of turbulent

mixing with chemical kinetics has been formulated and used to study the development of the distribution function in our combustor. These calculations allow us to understand the reasons for the success of simple mixing models which have been applied to the thermal fixation of atmospheric nitrogen and to carbon monoxide oxidation.⁽¹⁷⁾ Unfortunately, difficulties associated with modelling the primary mode of heat transfer in our burner, conduction from the hot gas to the burner walls, prevented direct application of the collision model to the conversion of fuel-nitrogen. Instead, a simple approximate model of the flow nonuniformities has been used to model the experiments, predicting exhaust nitric oxide concentrations within 30 per cent of the measured values over a wide range of equivalence ratio ($\phi = 0.5$ to $\phi = 1.5$) and mixing conditions (ranging from nearly uniform composition to poorly mixed).

The results of this study have significant implications to combustion modification methods for the control of NO_x emissions from stationary sources. First, increasing fuel atomizer and turbulent mixing efficiency without other changes will increase the conversion of fuel-nitrogen to nitric oxide.

Reduction of combustion temperatures is expected to have little effect on the exothermic oxidation of fuel-nitrogen. Thus, combustion modification techniques such as cooled flue gas recirculation or the injection of steam or water will probably prove ineffective in reducing NO_x formation from fuel-nitrogen. Turner and Siegmund⁽⁶⁾ have recently demonstrated the ineffectiveness of flue gas recycle in experiments performed on a compact industrial boiler supporting this conclusion.

On the other hand, methods which result in increased hot gas residence time at rich conditions may result in increased N_2 formation from the fuel-nitrogen with a corresponding reduction in NO emissions. Thus, two-stage combustion is expected to reduce NO emissions due to fuel-nitrogen conversion as well as thermal fixation. This conclusion is also supported by the experiments of Turner and Siegmund.⁽⁶⁾ The reduction possible through two stage combustion has its limits, however. If the conditions of any significant portion of the flow in the first stage of combustion were too rich, the fuel-nitrogen might be retained in an unoxidized form, only to be oxidized in the second stage where N_2 formation is likely to be less significant. It is also possible that some of the fuel-nitrogen would not be oxidized in the second stage and, thus, would be emitted in another, perhaps more hazardous, form such as NH_3 , HCN, or other nitrogenous hydrocarbons. Some optimization of the two stage combustion technique is, therefore, required to minimize the nitric oxide emissions. Some of the tools necessary to study this method and its optimization are provided in the forms of the kinetic model and the statistical collision model for the turbulent mixing process.

TABLE IKerosene Fuel Analysis

Gravity API @ 60°F.	41.4
BTU per pound HHV	19783
Carbon	85.9%
Hydrogen	13.4%
Nitrogen	0.05%
Oxygen by difference	0.65%

TABLE II

Conditions of Premixed Flame Experiments

ϕ	OI	Additive	Fuel	T_{ad} ($^{\circ}$ K)	T_m ($^{\circ}$ K)	X_{RN} (ppm)	Ref.
0.9	0.176	NH_3 , C_4H_5N	ethylene	1910-2090	1900	525-22000	15
1.25	0.166	C_4H_5N , CH_3NH_2	ethylene	1985-2035	1920	350-11000	
1.25	0.195	NH_3 , CH_3NH_2	ethylene	2190-2225	2070	4700-13200	
1.5	0.178	C_4H_5N , C_5H_5N , CH_3NH_2	ethylene	1930-1980	1870	420-11000	
1.5	0.216	NH_3 , CH_3 , NH_2	ethylene	2180-2195	2030	3700-7600	
1.72	0.190	C_5H_5N	ethylene	1935	1860	490-830	
1.72	0.305	NH_3	ethylene	2535-2555	2240	2190-5750	
0.9	0.209	NH_3	methane	2130-2145	—	693-4432	16
1.1	0.209	NH_3	methane	2155-2195	—	713-4675	
1.2	0.209	NH_3	methane	2060-2115	—	753-4932	
1.3	0.209	NH_3	methane	1980-2035	—	809-5294	
1.4	0.209	NH_3	methane	1905-1941	—	859-5625	

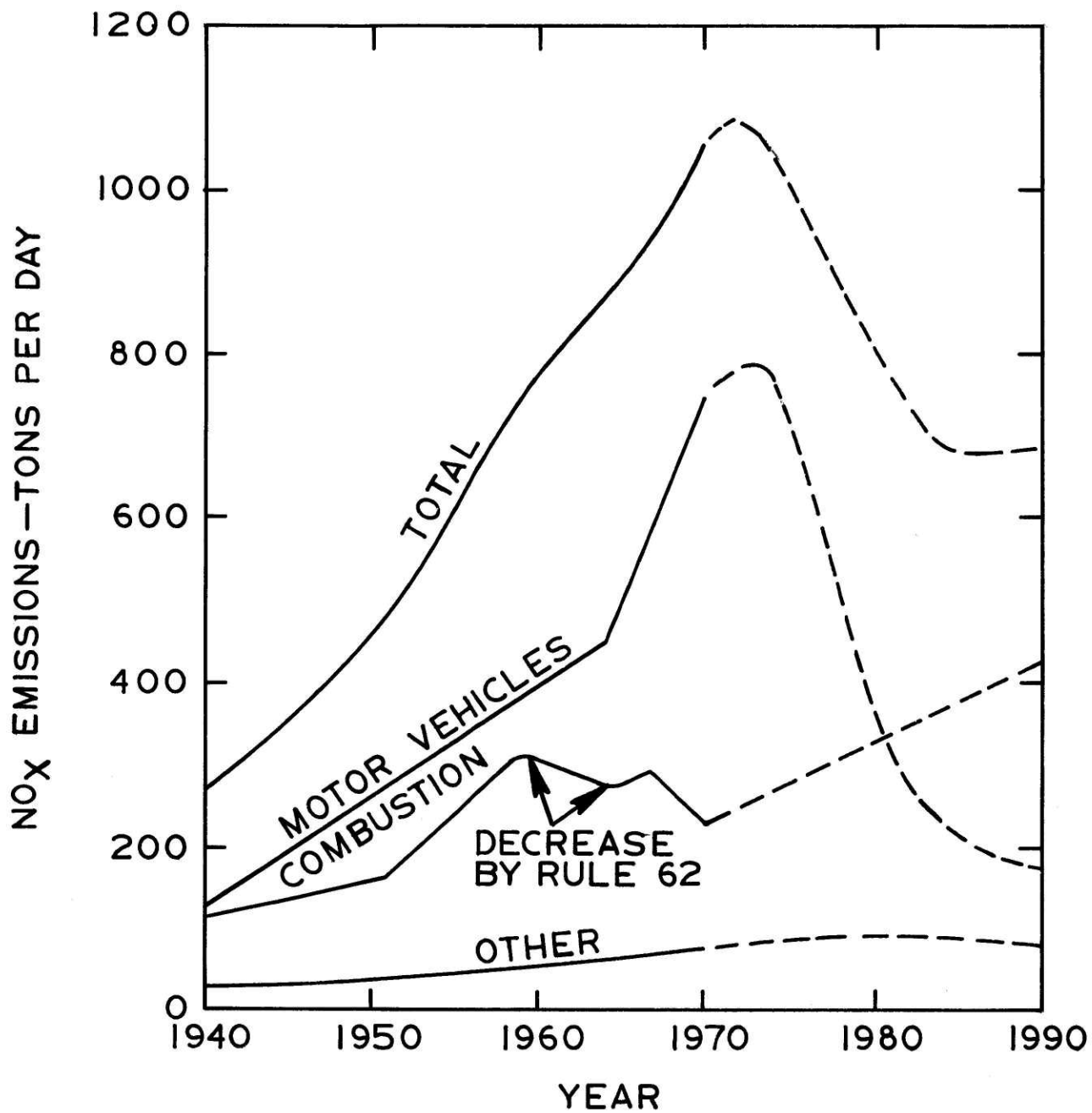
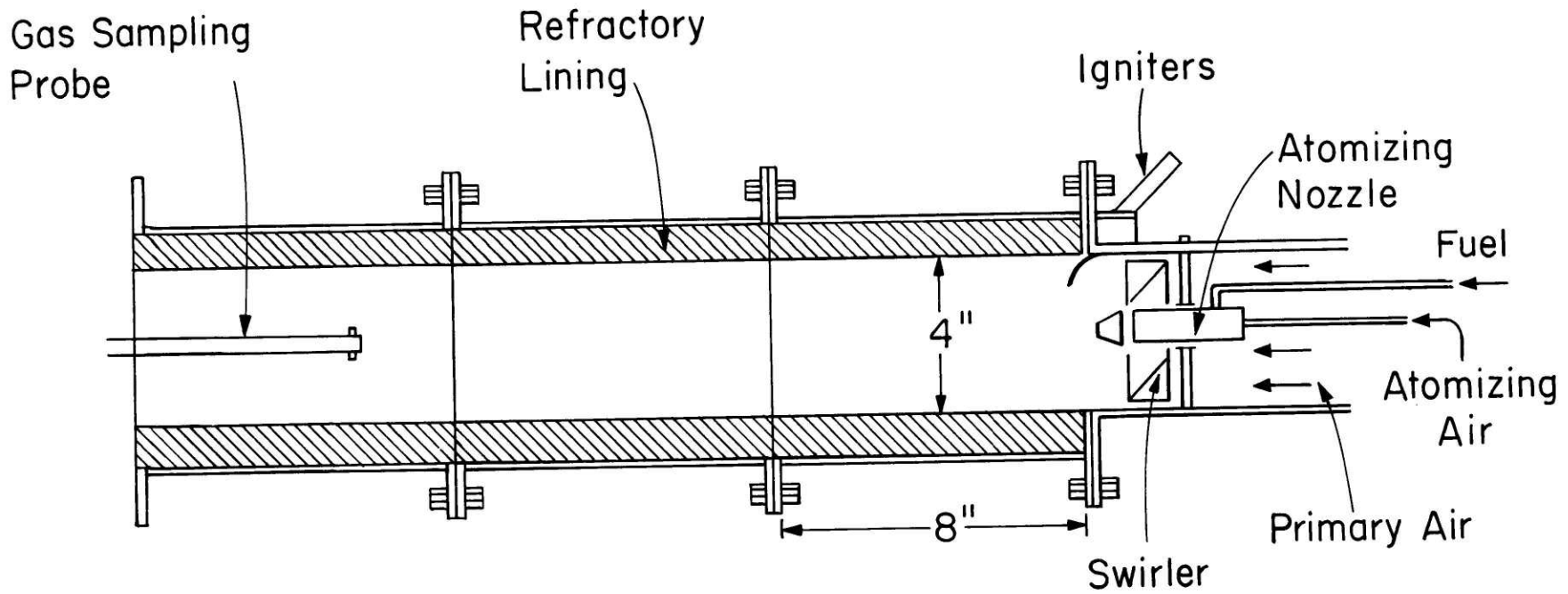


Figure 1. Estimated daily NO_x emissions (calculated as NO₂) from all sources in the Los Angeles County Air Pollution Control District.



Atmospheric Pressure Burner

Figure 2. Schematic diagram of the burner and component equipment

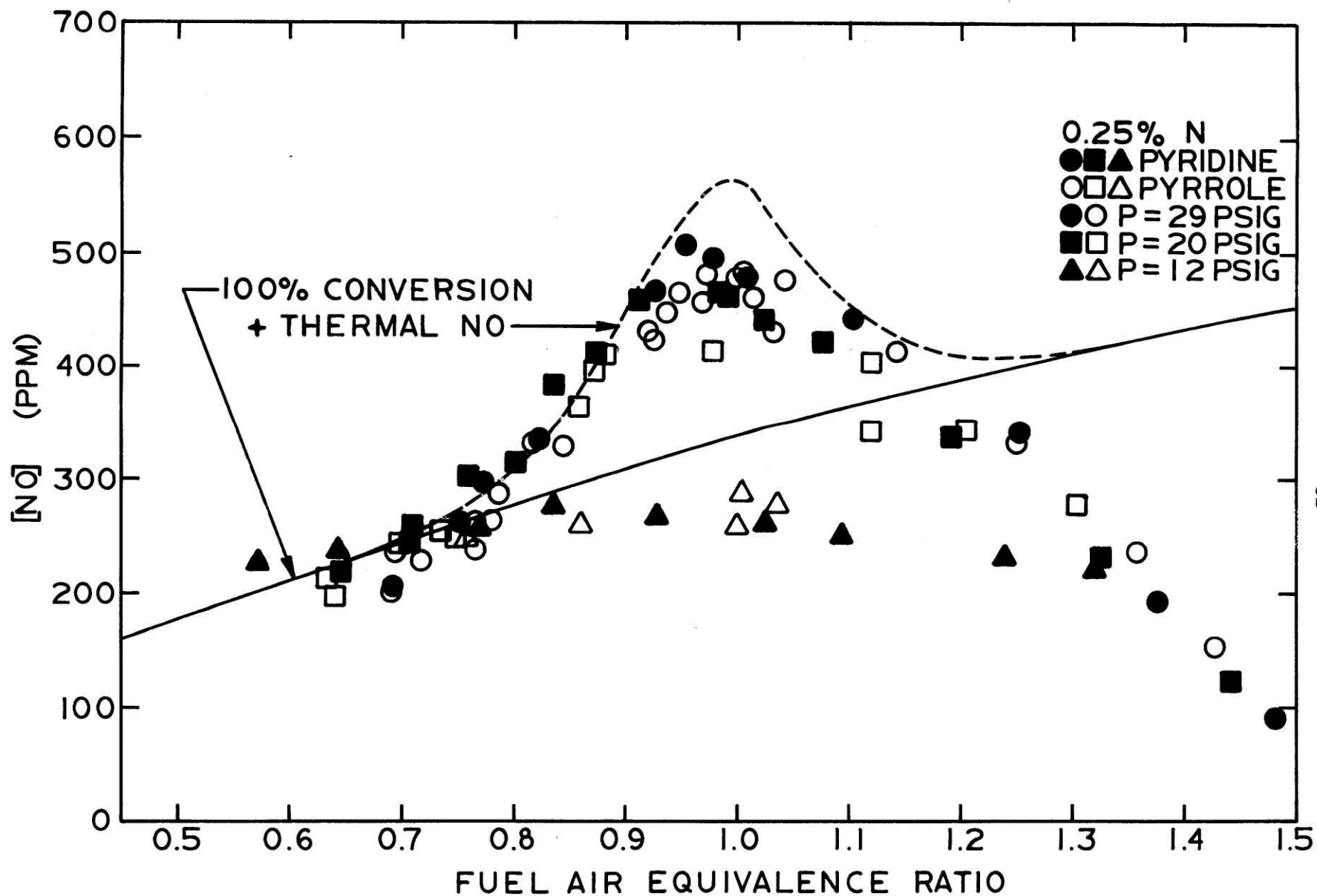
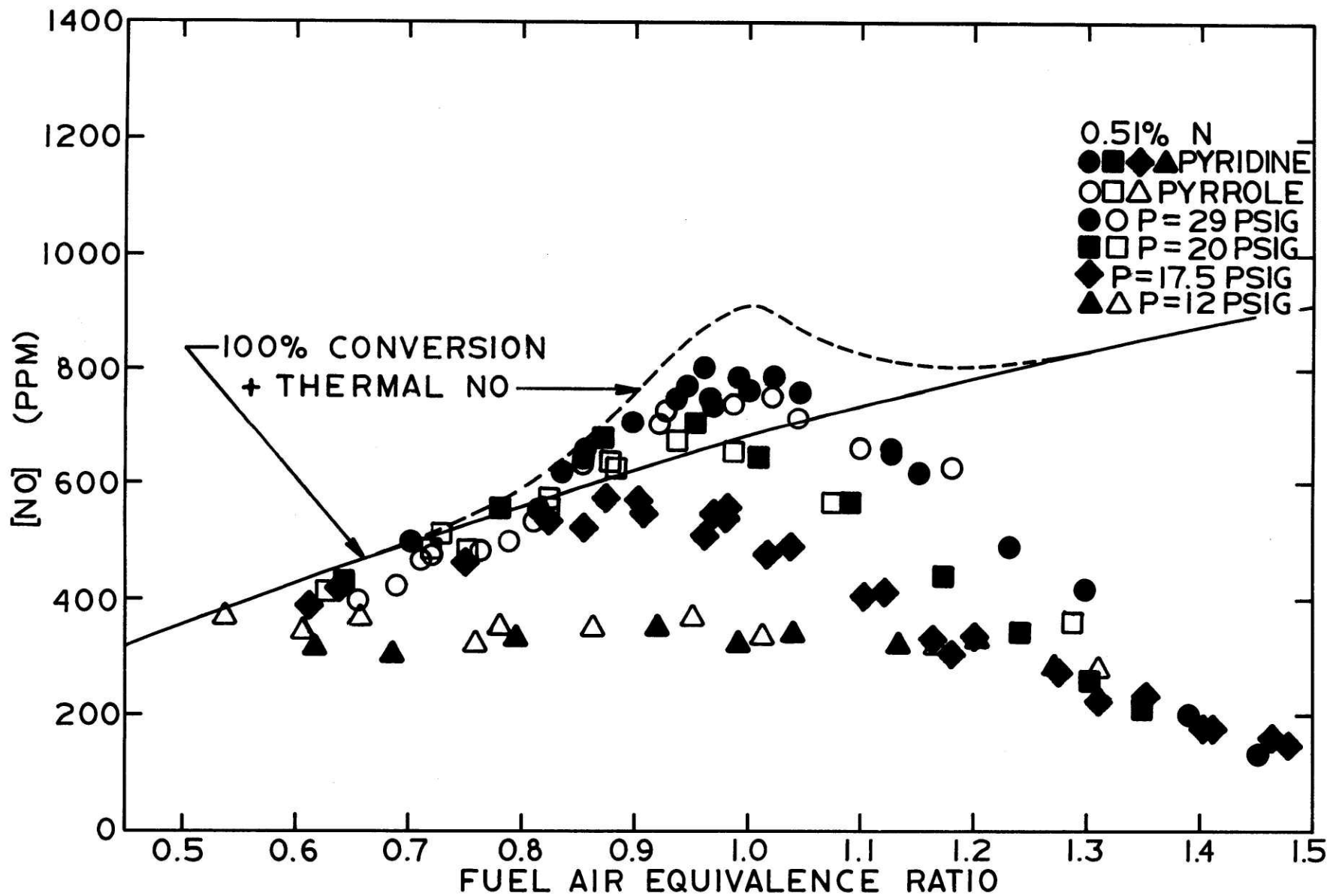
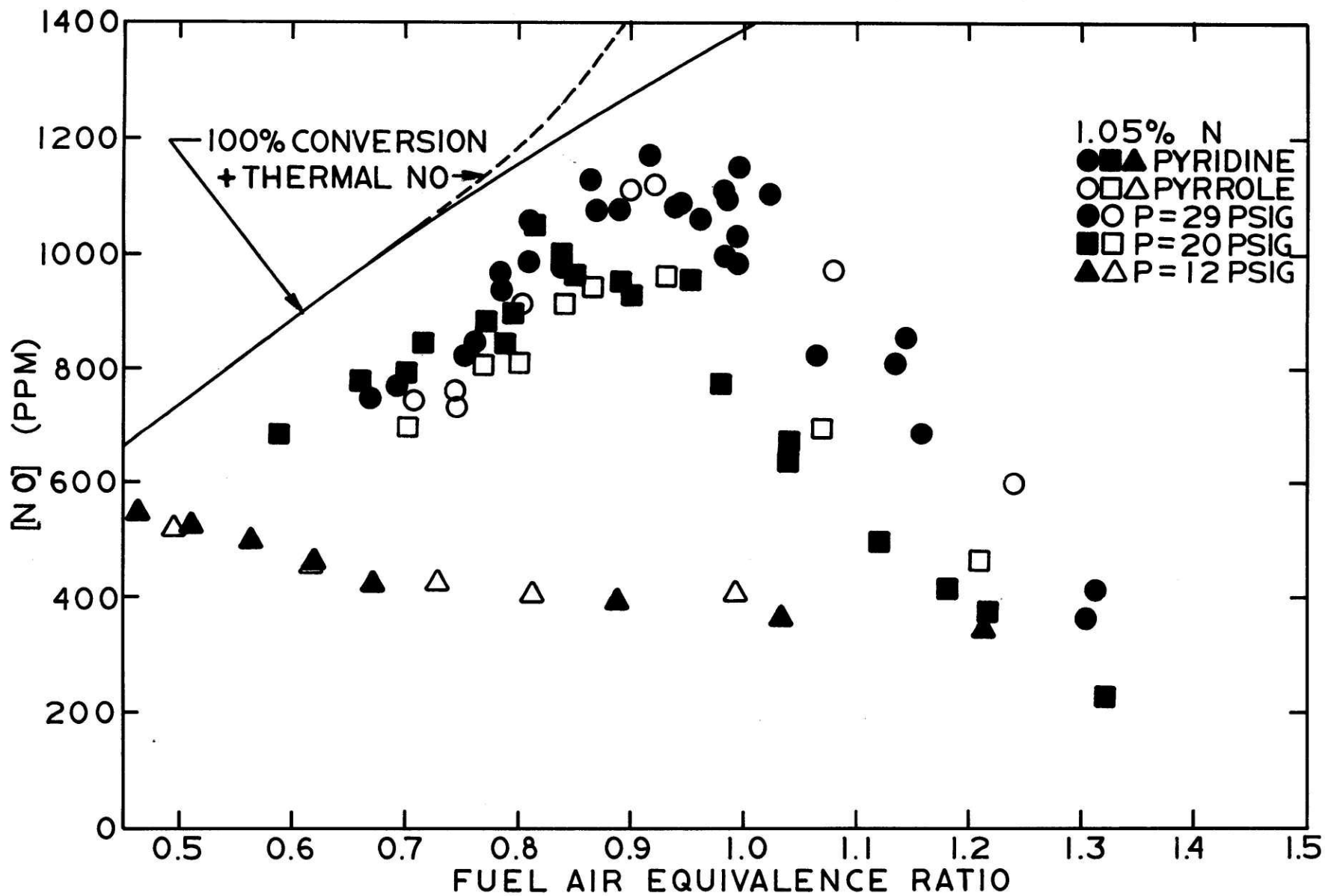


Figure 3. Exhaust NO concentrations (ppm, wet basis) during combustion of nitrogen doped fuels.

(A) 0.25 per cent nitrogen by weight.



(B) 0.51 per cent nitrogen by weight.



(C) 1.05 per cent nitrogen by weight.

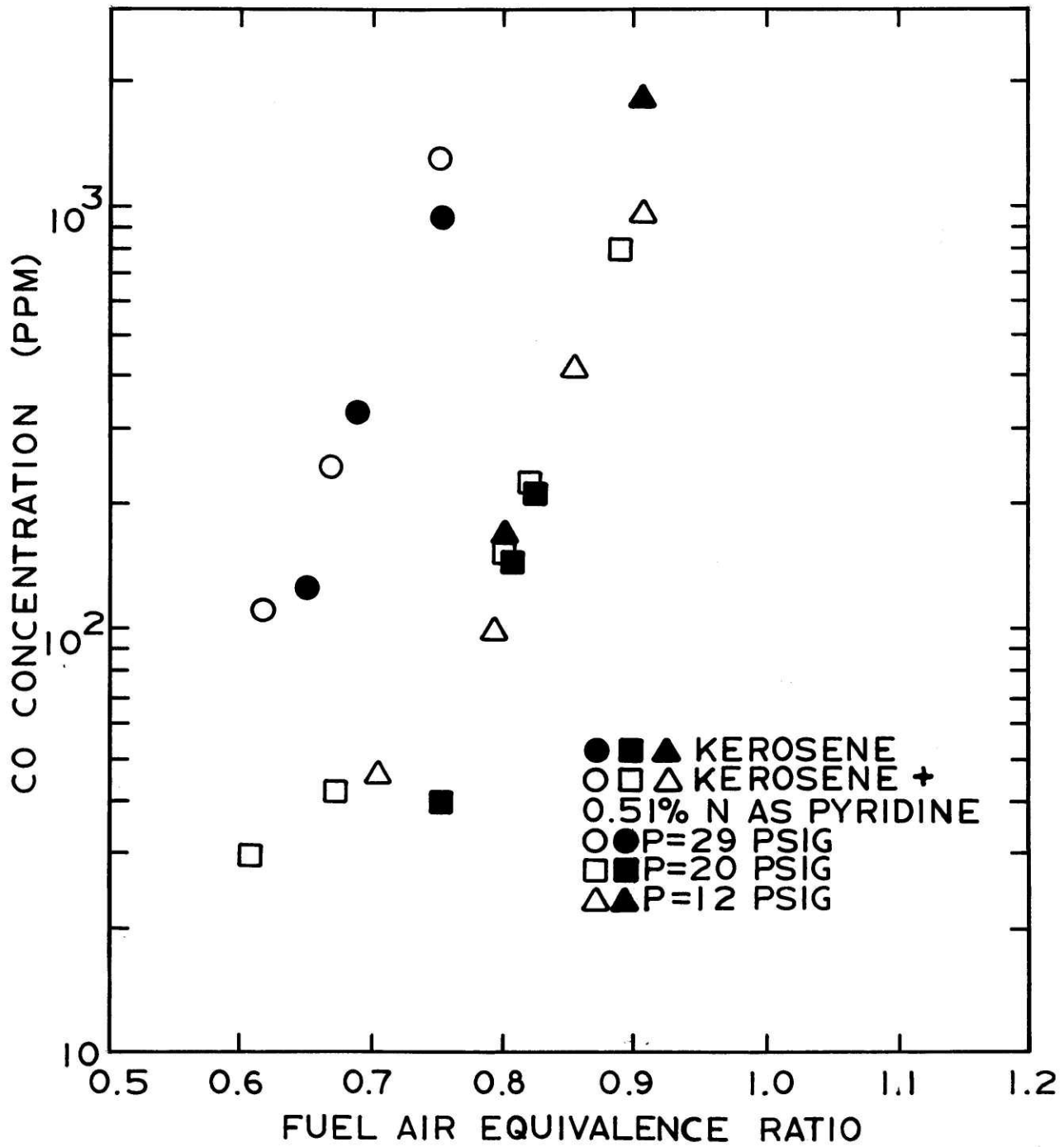


Figure 4. Exhaust CO concentrations (ppm, wet basis).

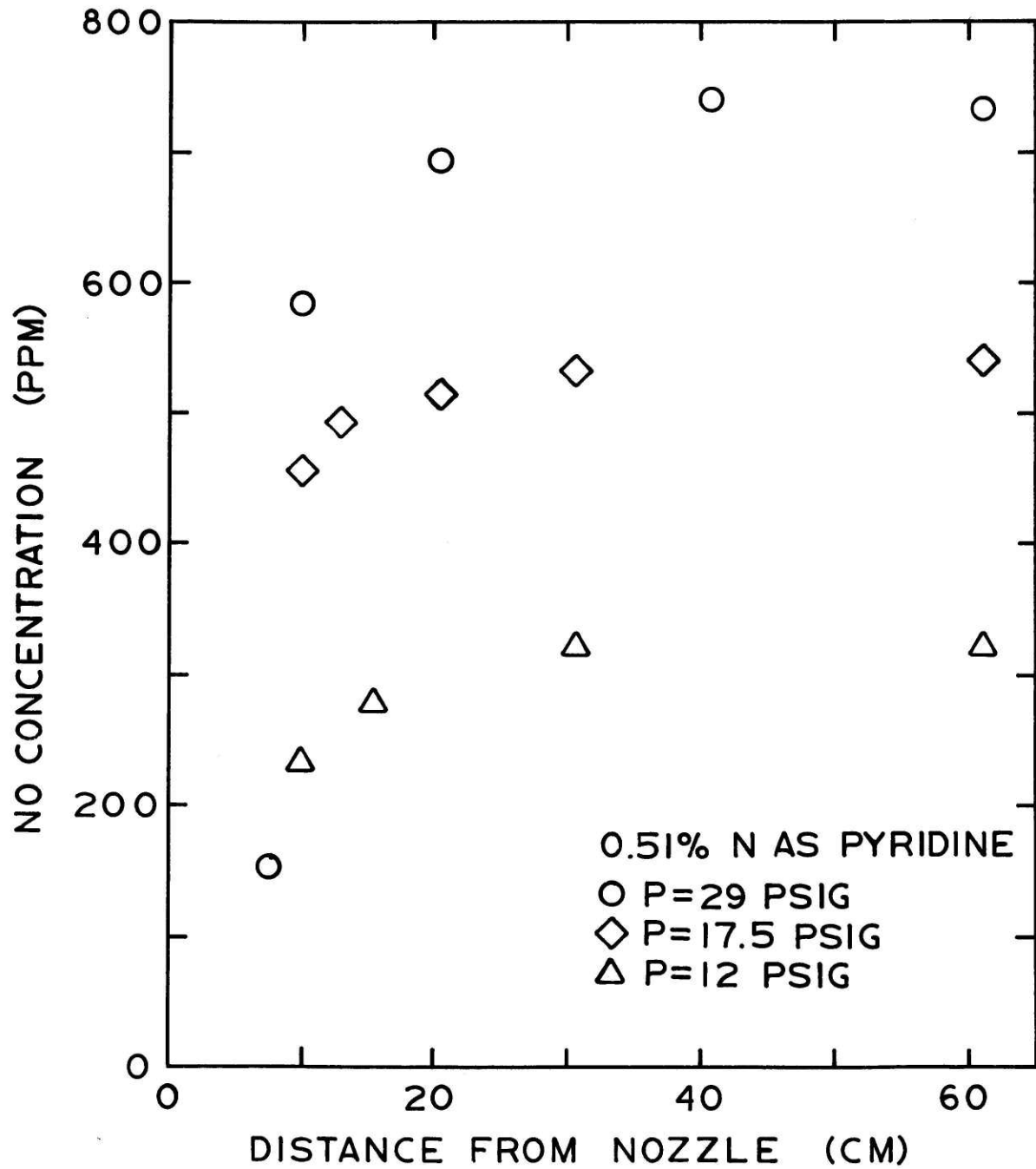


Figure 5. Axial variation of the NO concentration for combustion of kerosene doped with 0.51 per cent N by weight as pyridine.

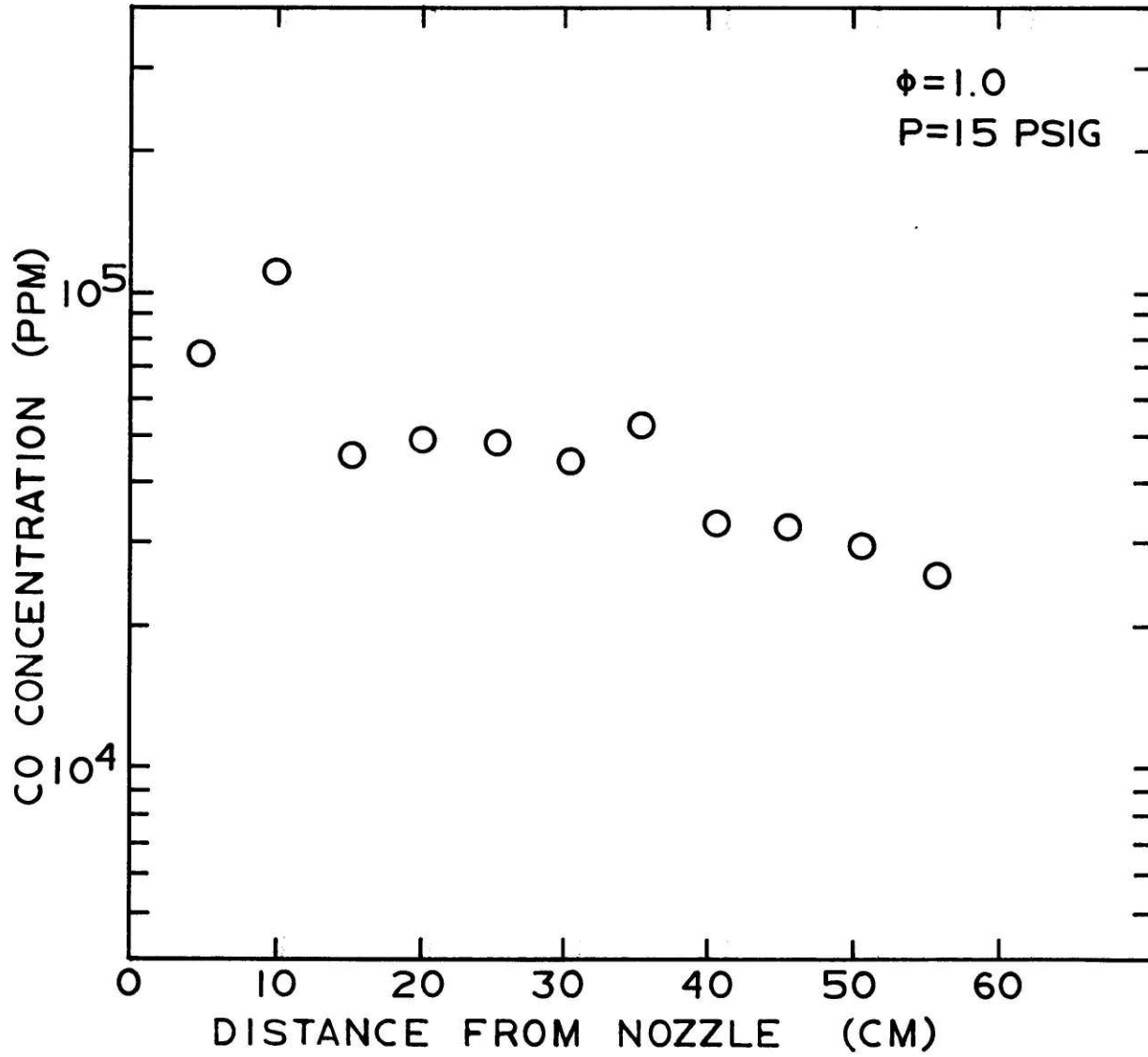


Figure 6. Axial variation of the CO concentration. $p=15$ psig, $\phi=1.0$.

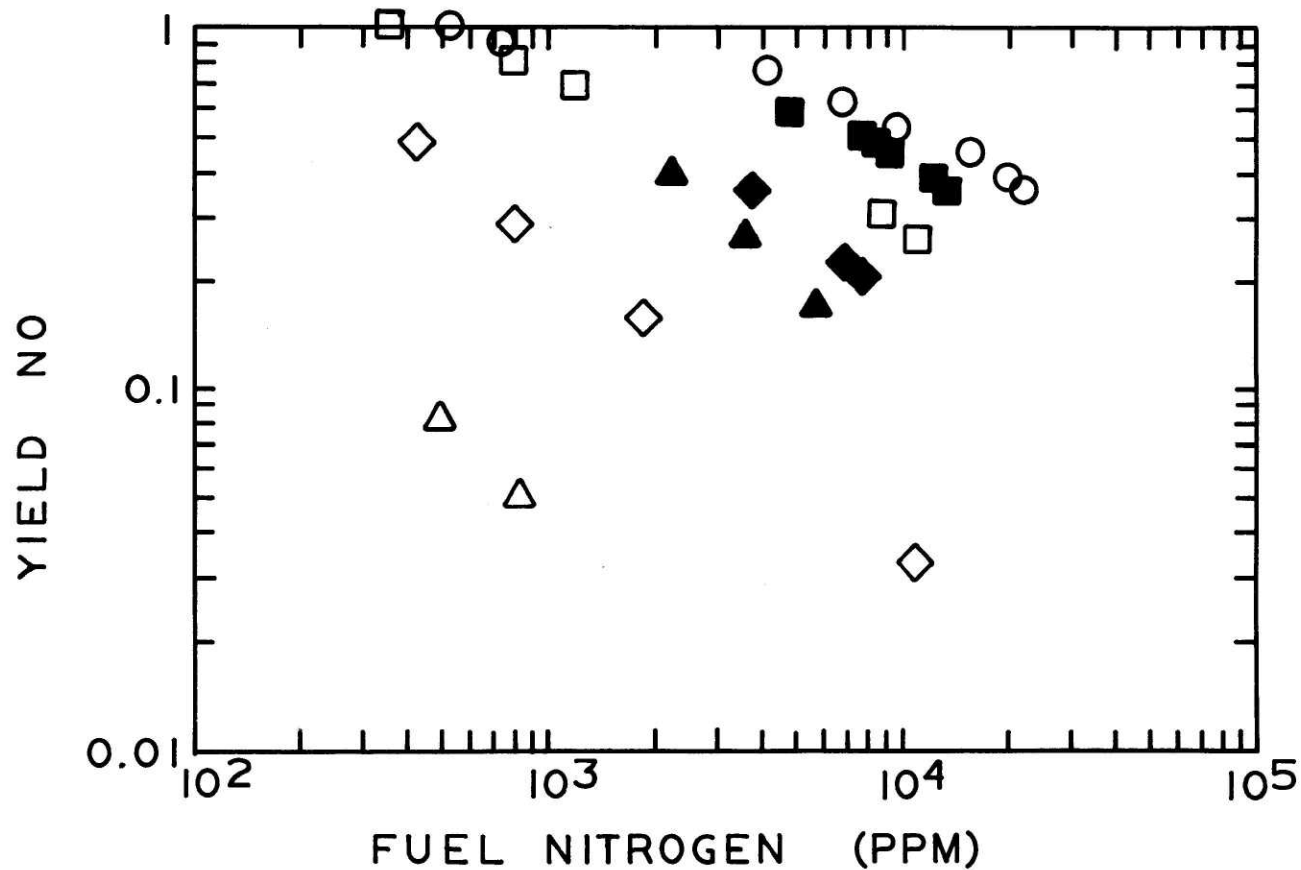
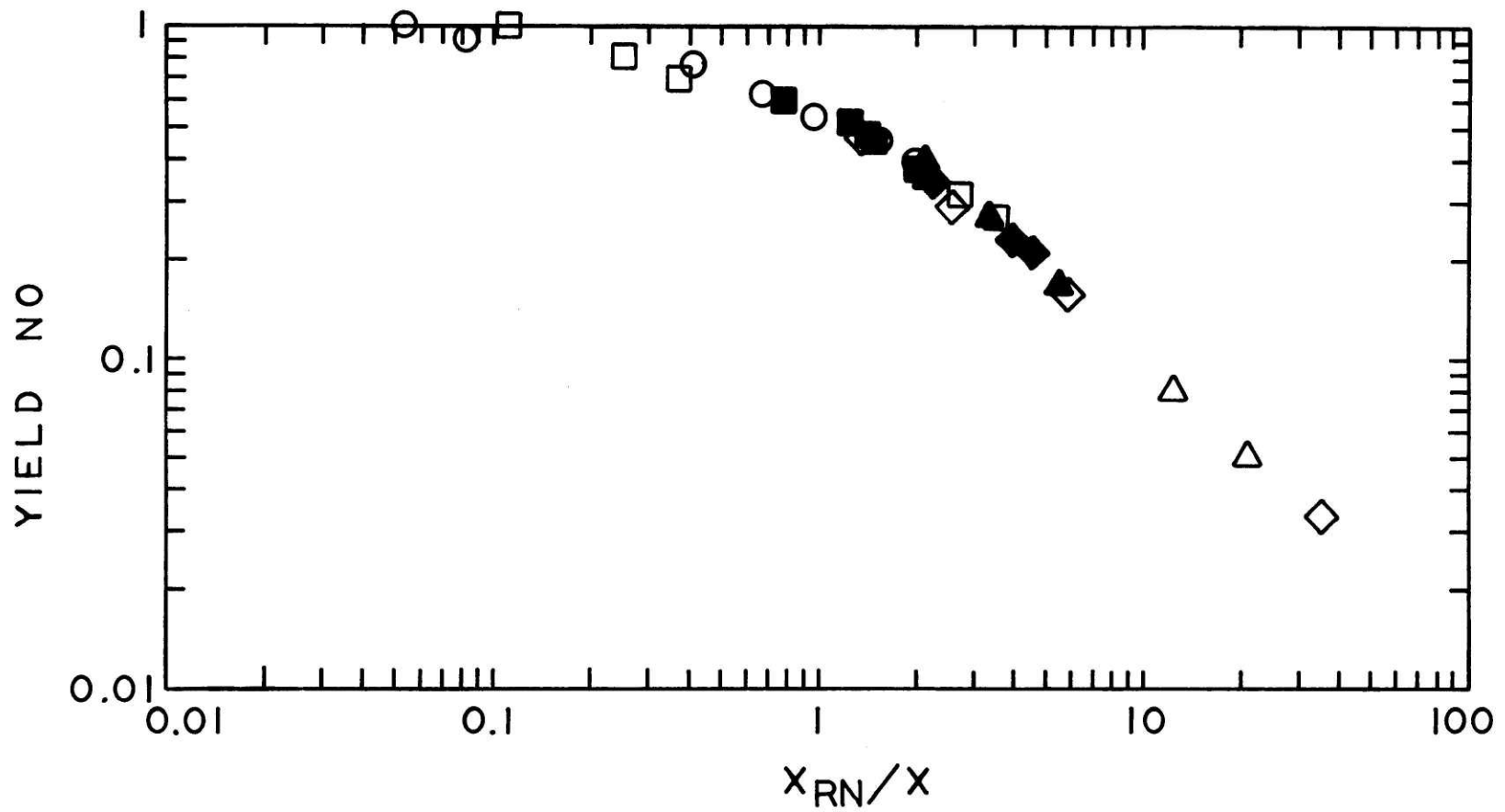


Figure 7. Fractional yield of NO in premixed ethylene flames.

○: $\phi=0.9$, $T=2000^\circ\text{K}$; ■: $\phi=1.25$, $T=2210^\circ\text{K}$; □: $\phi=1.25$, $T=2010^\circ\text{K}$; ◆: $\phi=1.5$, $T=2190^\circ\text{K}$;
 ◇: $\phi=1.5$, $T=1950^\circ\text{K}$; ▲: $\phi=1.72$, $T=2545^\circ\text{K}$; △: $\phi=1.72$, $T=1935^\circ\text{K}$ (adiabatic flame temperatures).

(A) Yield of NO vs. total fuel nitrogen.



(B) Correlation of NO yields in (A) with the ratio of the total fuel nitrogen concentration, X_{RN} , to the empirically determined flame property X.

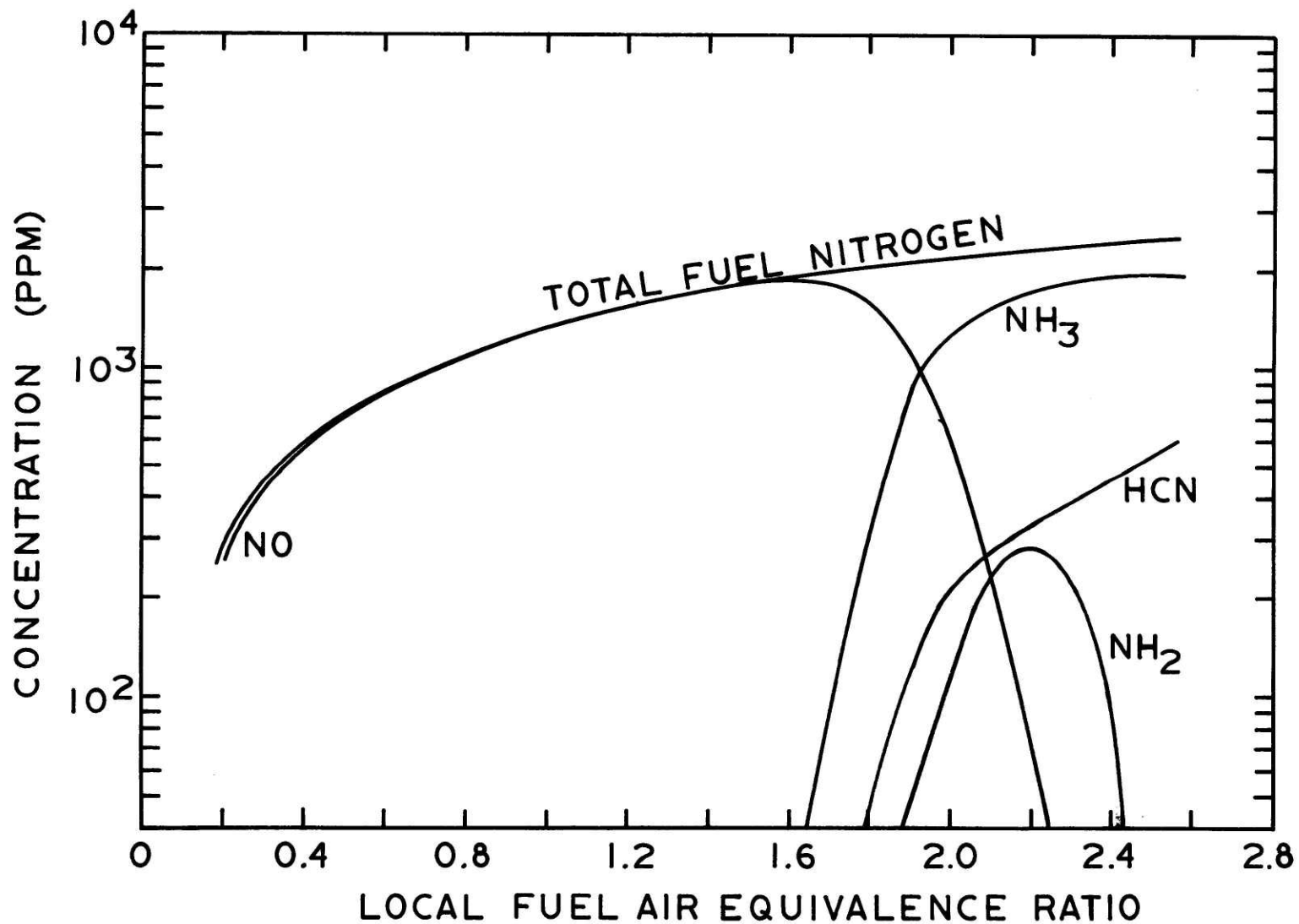


Figure 8. Partial equilibrium concentrations of major single nitrogen species calculated using one constraint for 1.05 per cent N by weight of pyridine in a kerosene fuel.

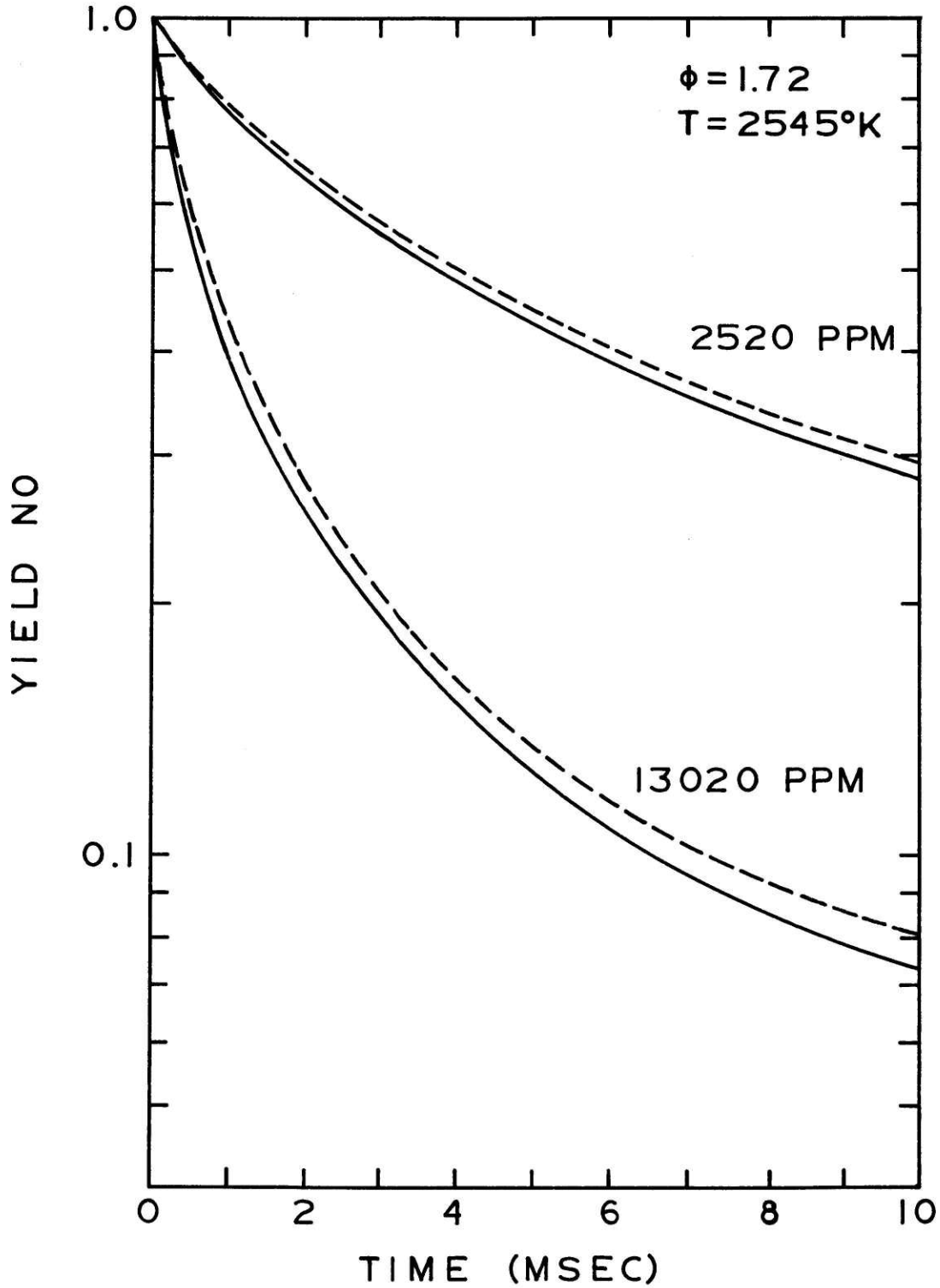
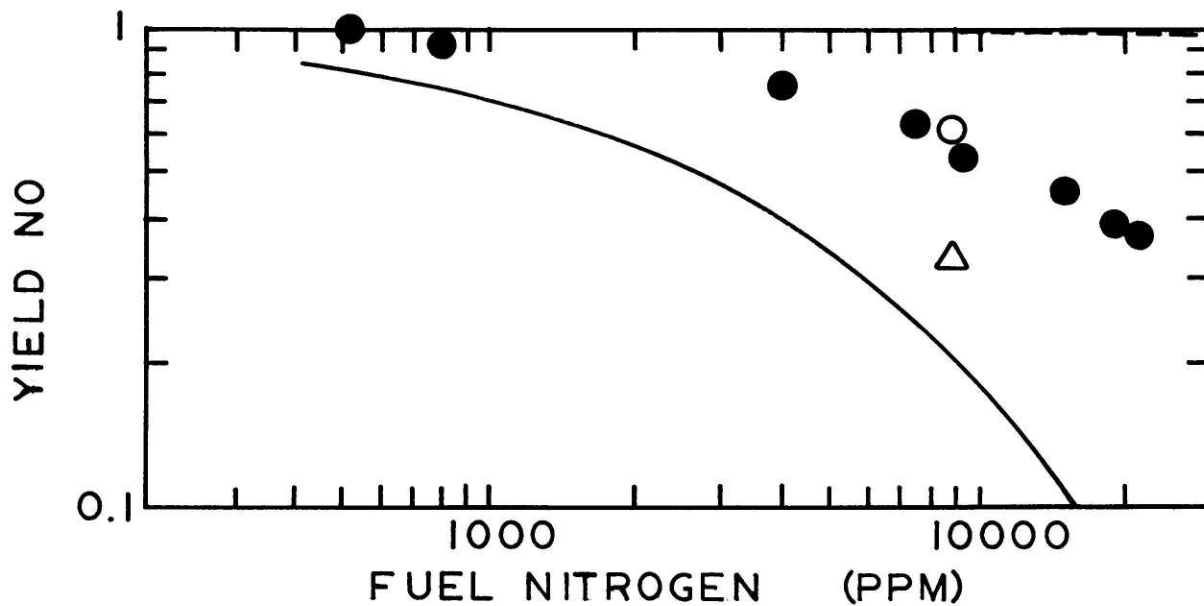
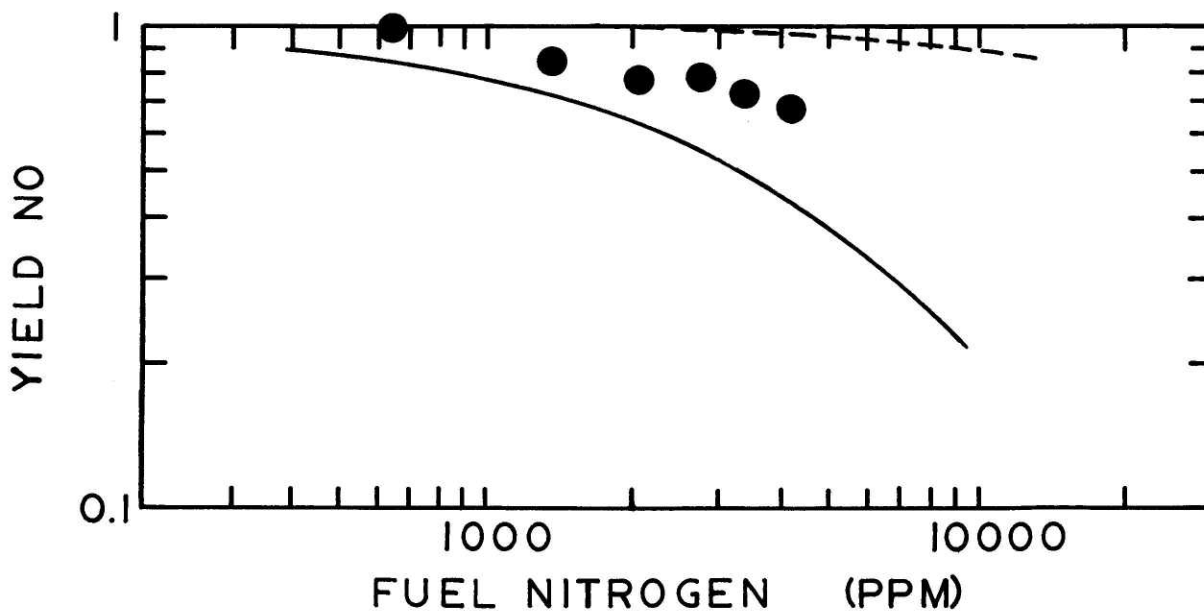


Figure 9. Comparison of exact (—) and approximate (-----) calculations of the fractional yield of NO using one constraint on the single nitrogen species. $\phi=1.72$, $T=2545^\circ\text{K}$, ethylene flame.



(A) $\phi=0.9$, $T=2000^\circ\text{K}$, ethylene flames of Ref. 15.



(B) $\phi=0.9$, $T=2140^\circ\text{K}$, methane flames of Ref. 16.

Figure 10. Fractional yield of NO in lean premixed flames. ●: experimental measurements; -----: calculations using one constraint; —: calculations using three constraints; \triangle : calculation with [O], [OH], and [H] increased 3 times the equilibrium values and using 3 constraints; \circ : calculation with [O], [OH], and [H] increased 10 times equilibrium.

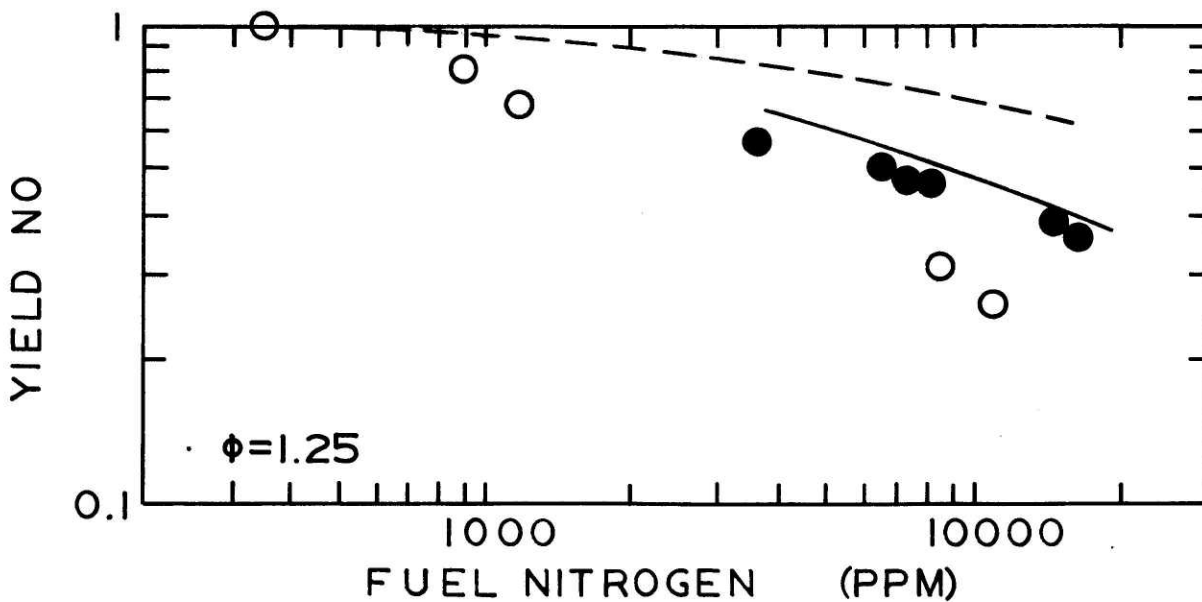
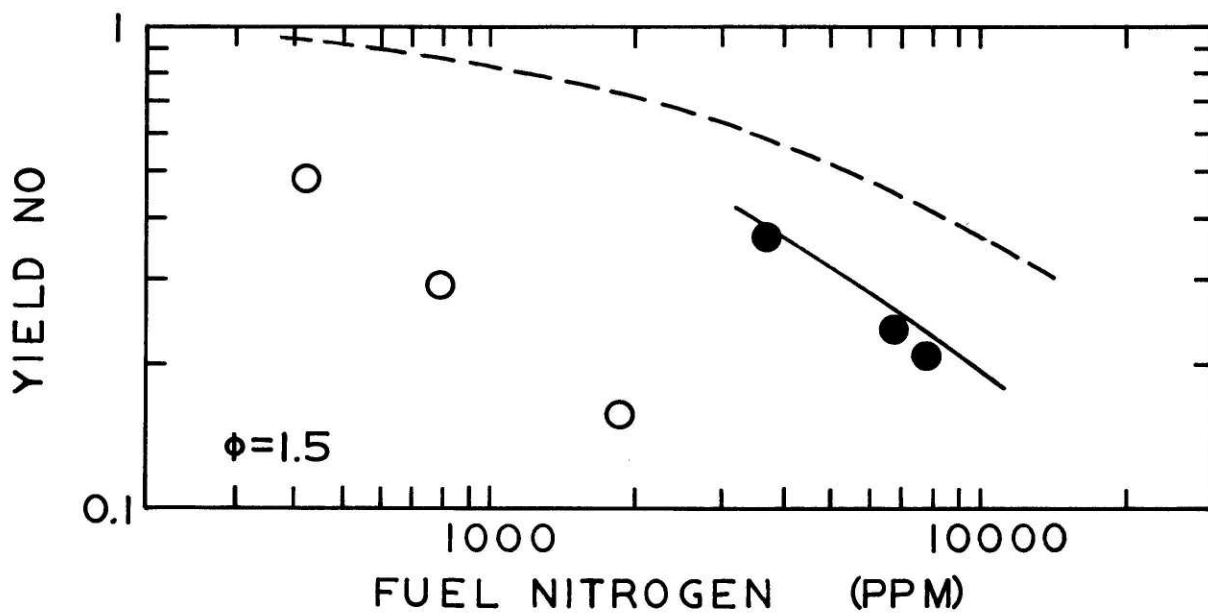
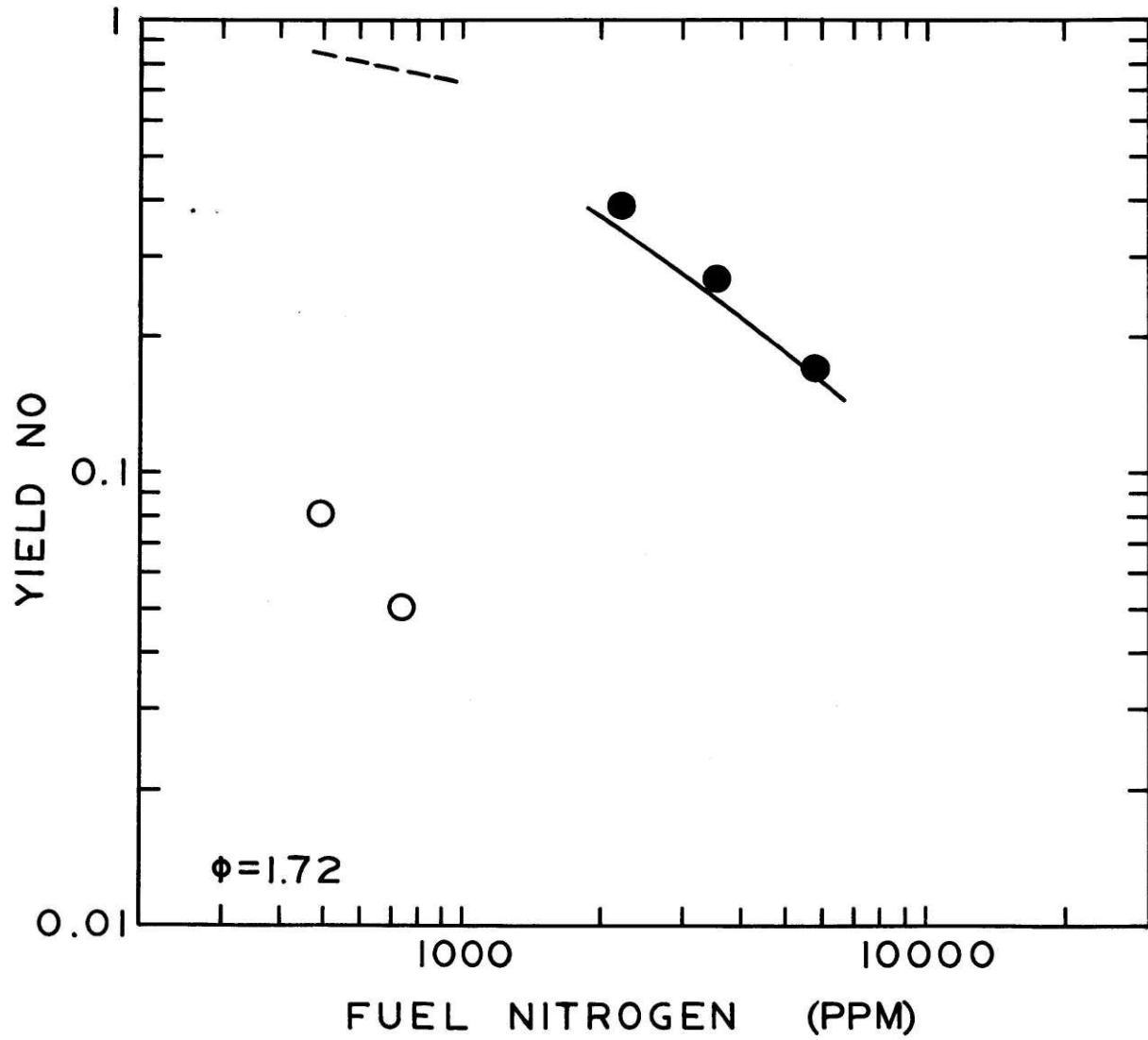
(A) $\phi=1.25$, $T=2010^{\circ}\text{K}$ and $T=2210^{\circ}\text{K}$ (B) $\phi=1.5$, $T=1955^{\circ}\text{K}$ and $T=2190^{\circ}\text{K}$

Figure 11. Fractional yields of NO in rich premixed ethylene flames of Ref. 15. \circ ,-----: low temperature, $t=2$ msec.; \bullet ,——: high temperature, $t=4$ msec.



(C) $\phi=1.72$, $T=1935^\circ\text{K}$ and $T=2545^\circ\text{K}$

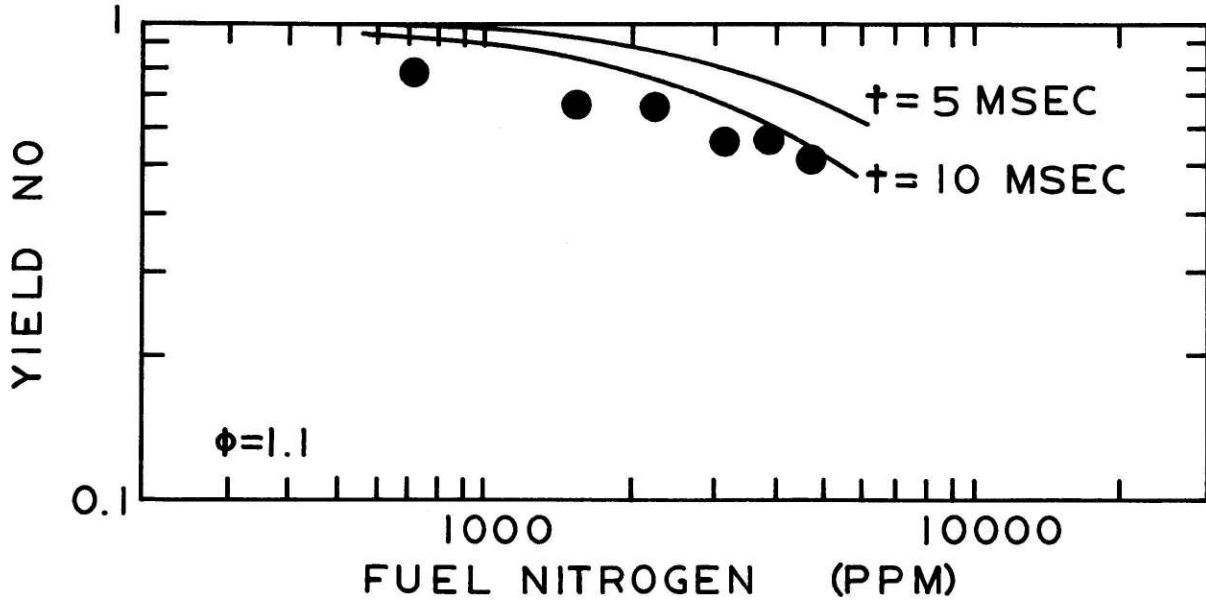
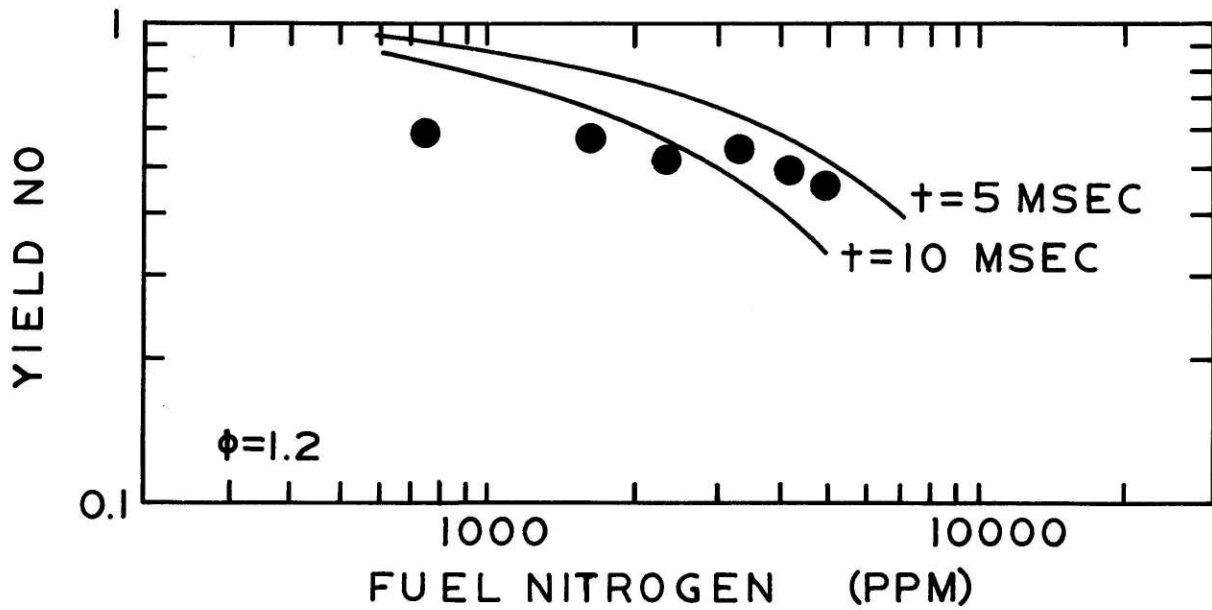
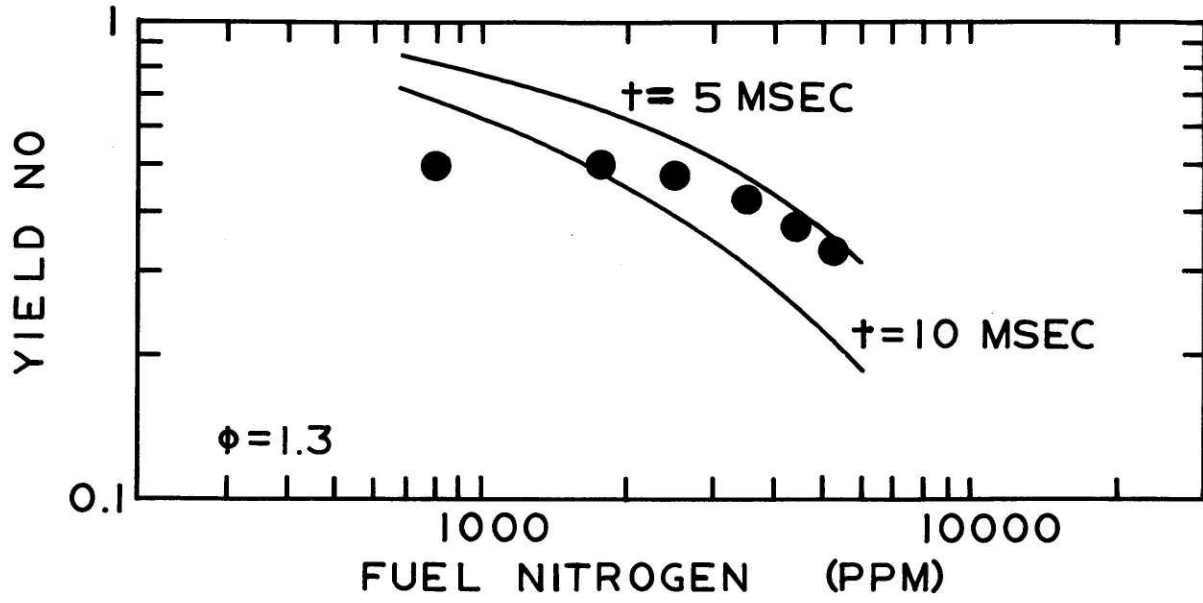
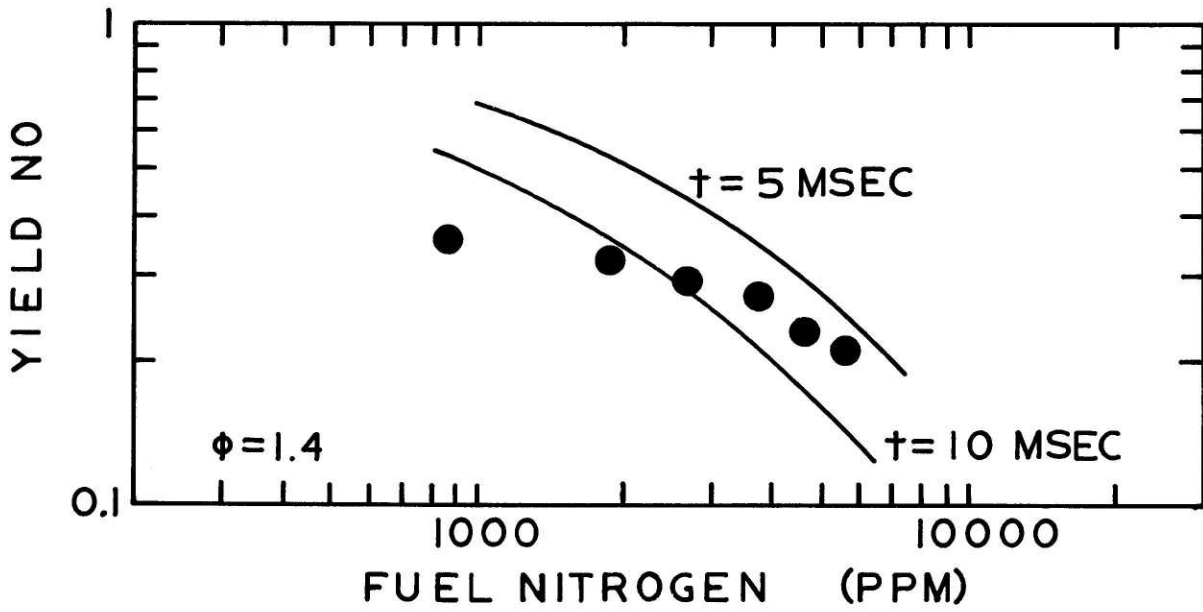
(A) $\phi=1.1$ (B) $\phi=1.2$

Figure 12. Fractional yield of NO in rich premixed methane/air flames doped with ammonia. ●: measured values; —: calculations using one constraint to the indicated residence times.

(C) $\phi = 1.3$ (D) $\phi = 1.4$

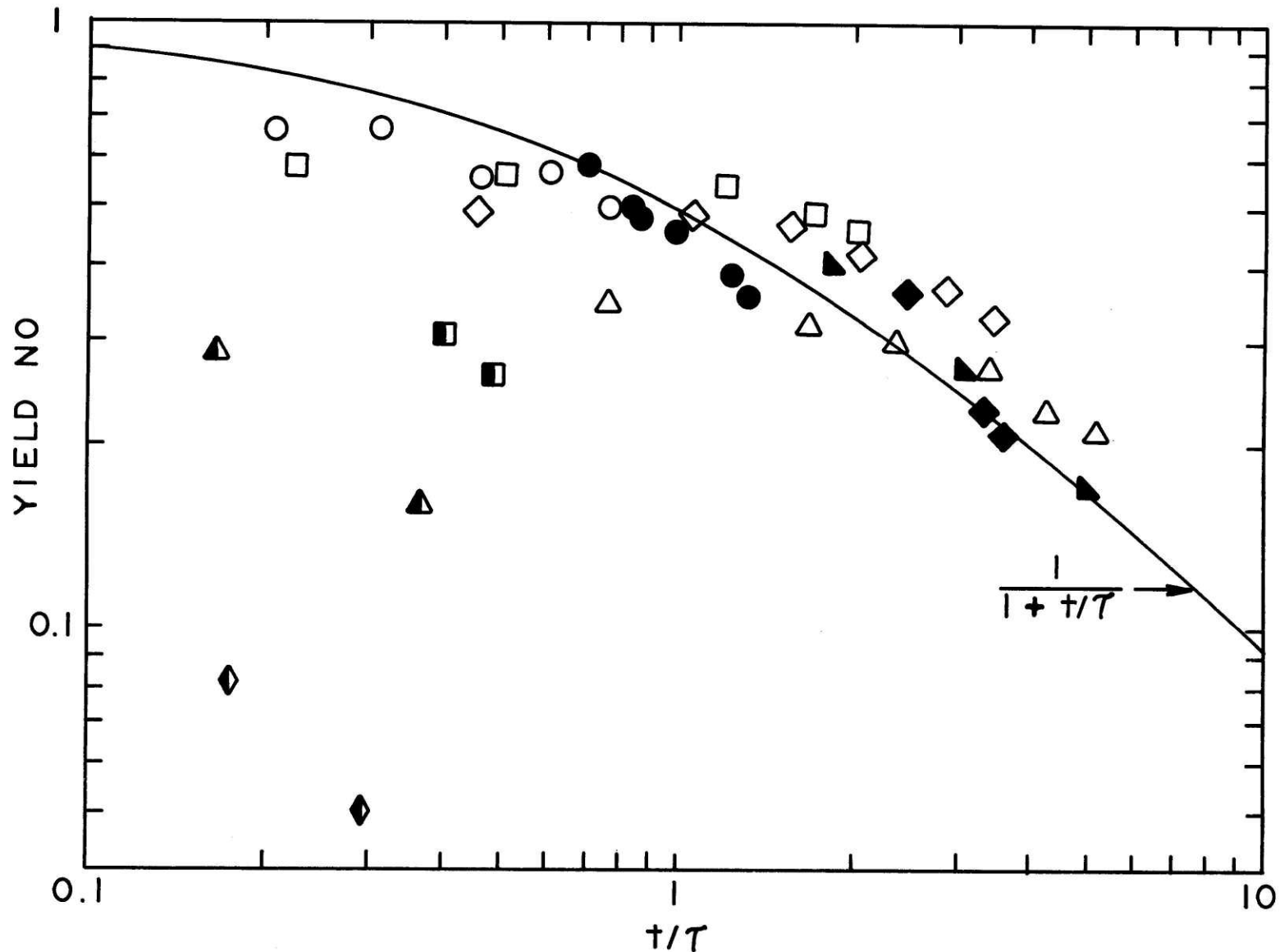


Figure 13. Correlation of the fractional yield of NO with the ratio of the residence time to the characteristic time of the N_2 forming reactions for rich conditions. Ethylene flames (Ref. 15). High temperature data ($t=4\text{msec.}$): \bullet : $\phi=1.25$, $T=2210^\circ\text{K}$; \blacklozenge : $\phi=1.5$, $T=2190^\circ\text{K}$; \blacktriangle : $\phi=1.72$, $T=2545^\circ\text{K}$. Low temperature data ($t=2\text{msec.}$): \blacksquare : $\phi=1.25$, $T=2010^\circ\text{K}$; \blacktriangle : $\phi=1.5$, $T=1955^\circ\text{K}$; \blacklozenge : $\phi=1.72$, $T=1935^\circ\text{K}$. Methane flame data of Ref. 16 ($t=10\text{msec.}$): \circ : $\phi=1.1$, $T=2175^\circ\text{K}$; \square : $\phi=1.2$, $T=2080^\circ\text{K}$; \diamond : $\phi=1.3$, $T=2015^\circ\text{K}$; \triangle : $\phi=1.4$, $T=1925^\circ\text{K}$.

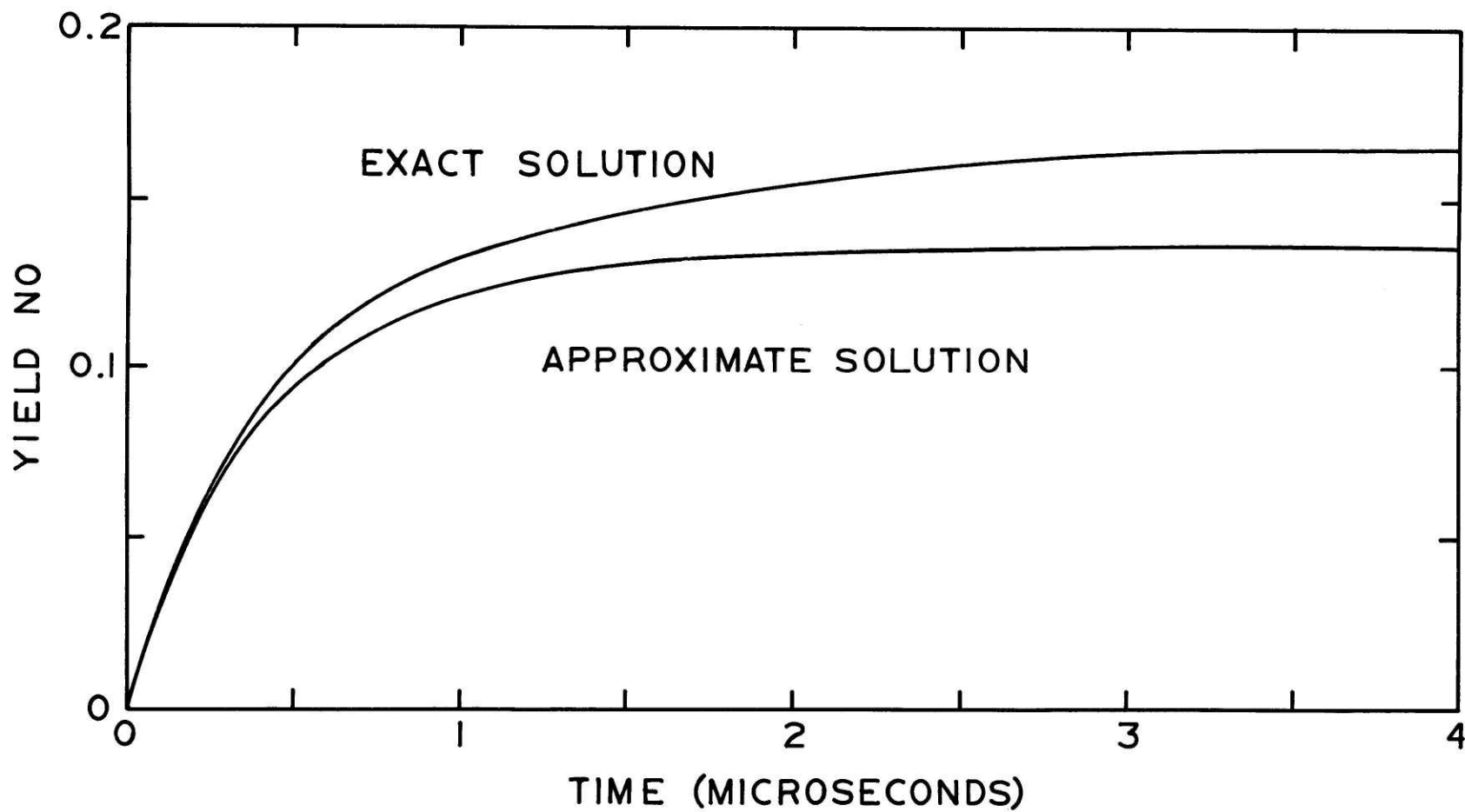


Figure 14. Calculations of the yield of NO using the exact and approximate (constant temperature) solutions using three constraints. $\phi=0.9$, $T=2000^{\circ}\text{K}$, 16150 ppm NH_3 (exhaust concentration) in an ethylene flame.

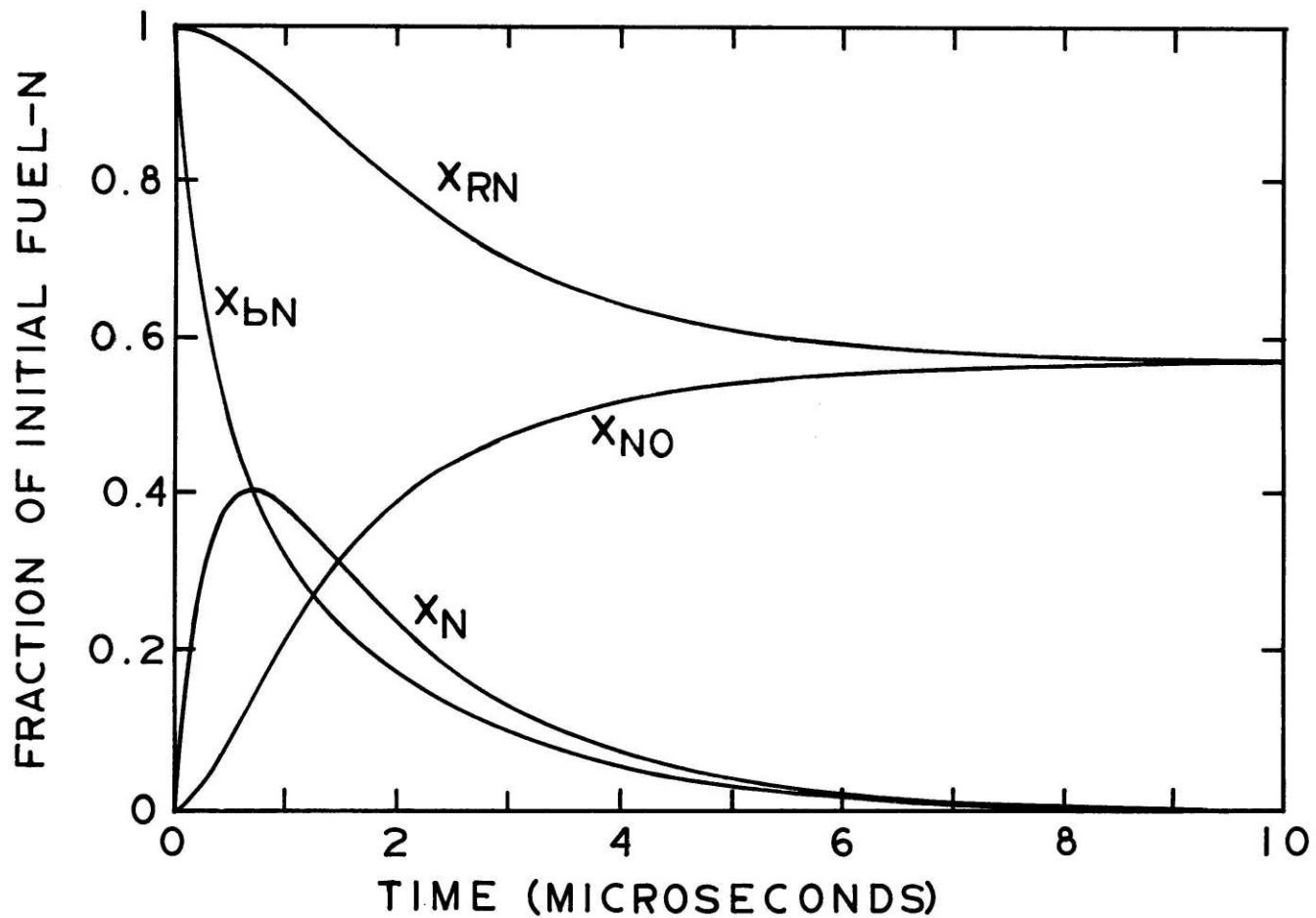


Figure 15. Characteristic behavior of the four constraints during the rapid reduction of X_{RN} . Methane/air flame with 2500 ppm ammonia added. $\phi=0.9$, $T=2140^\circ\text{K}$.

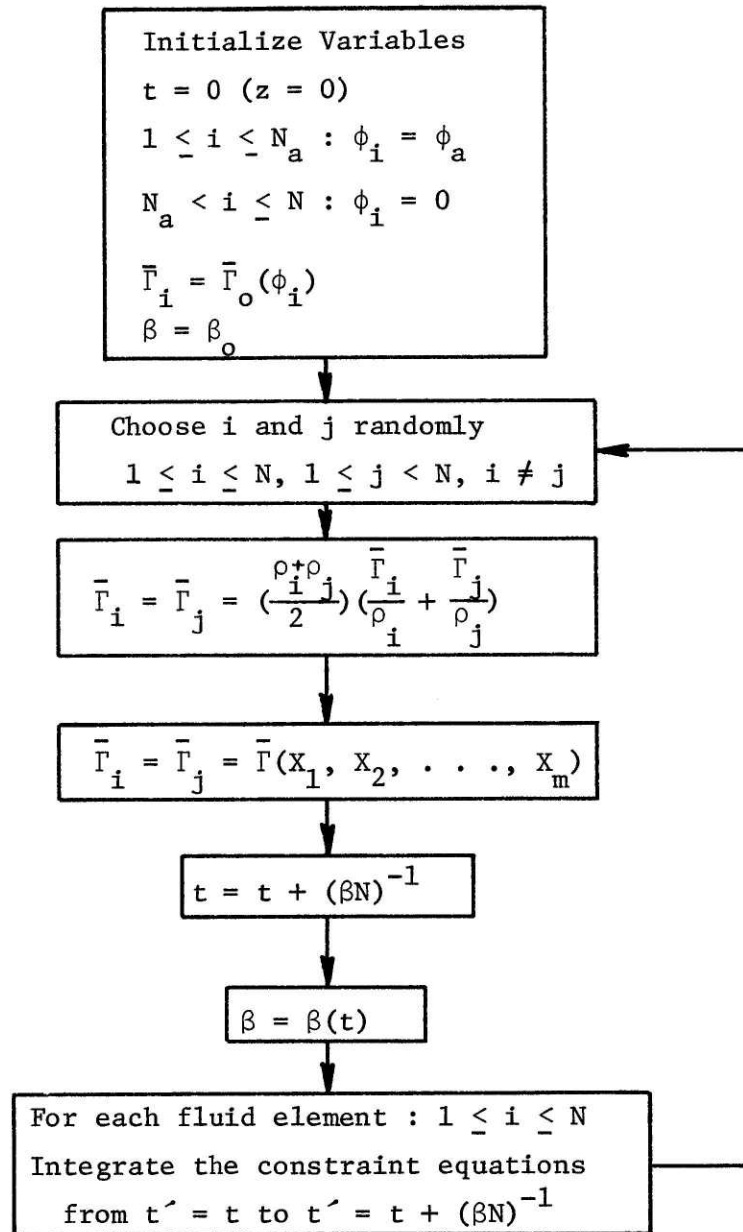


Figure 16. Flow Diagram for Mixing Model Computer Code

Note: $\bar{\Gamma}_i = \{\Gamma_{1i}, \Gamma_{2i}, \dots, \Gamma_{ki}\}$, where Γ_{ji} is the concentration of the j th species in the i th fluid element.

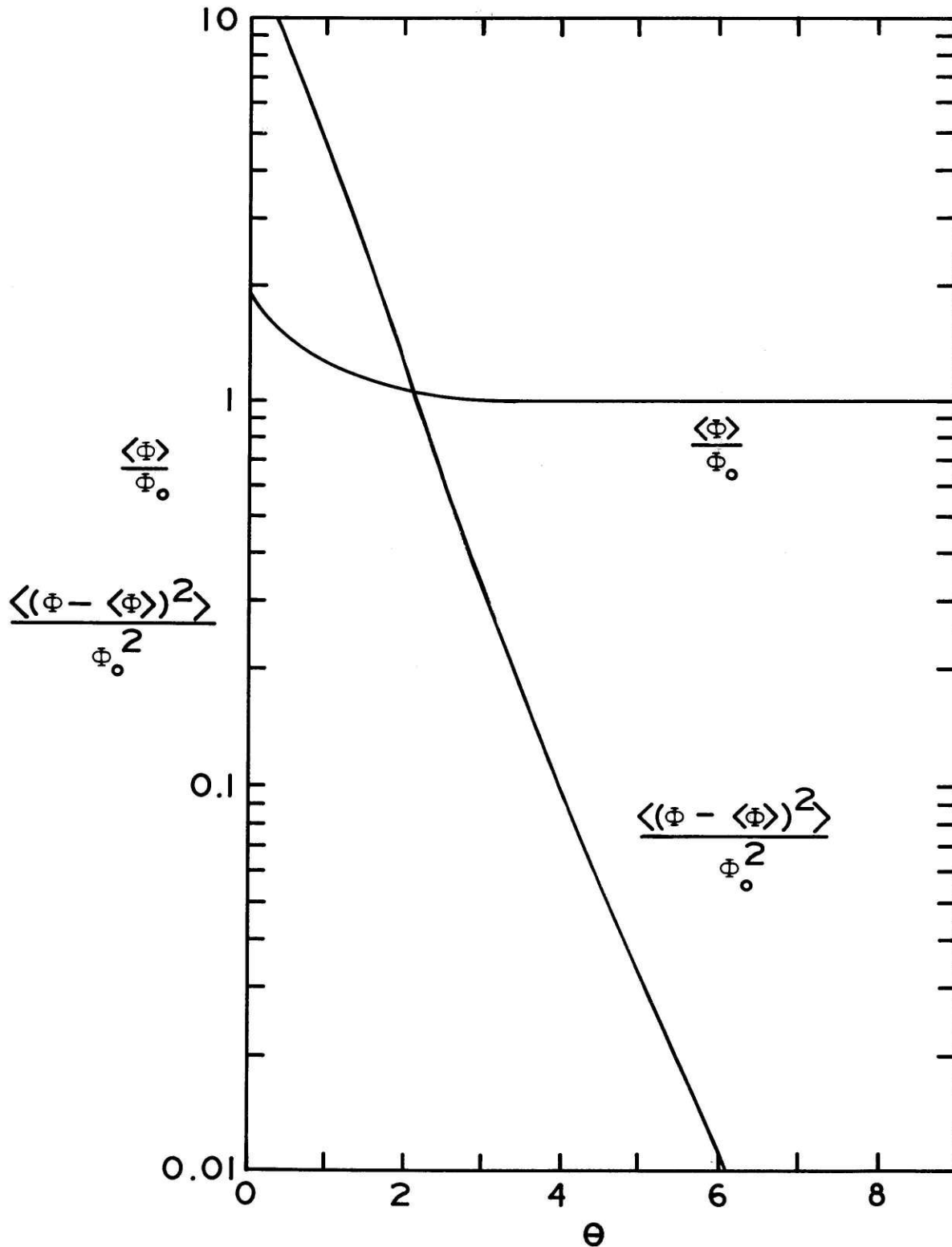


Figure 17. Dimensionless moments of the distribution function in ϕ calculated using the statistical collision model of the turbulent mixing process. θ is a dimensionless mixing time. ($N=1000$, $\phi=1$).

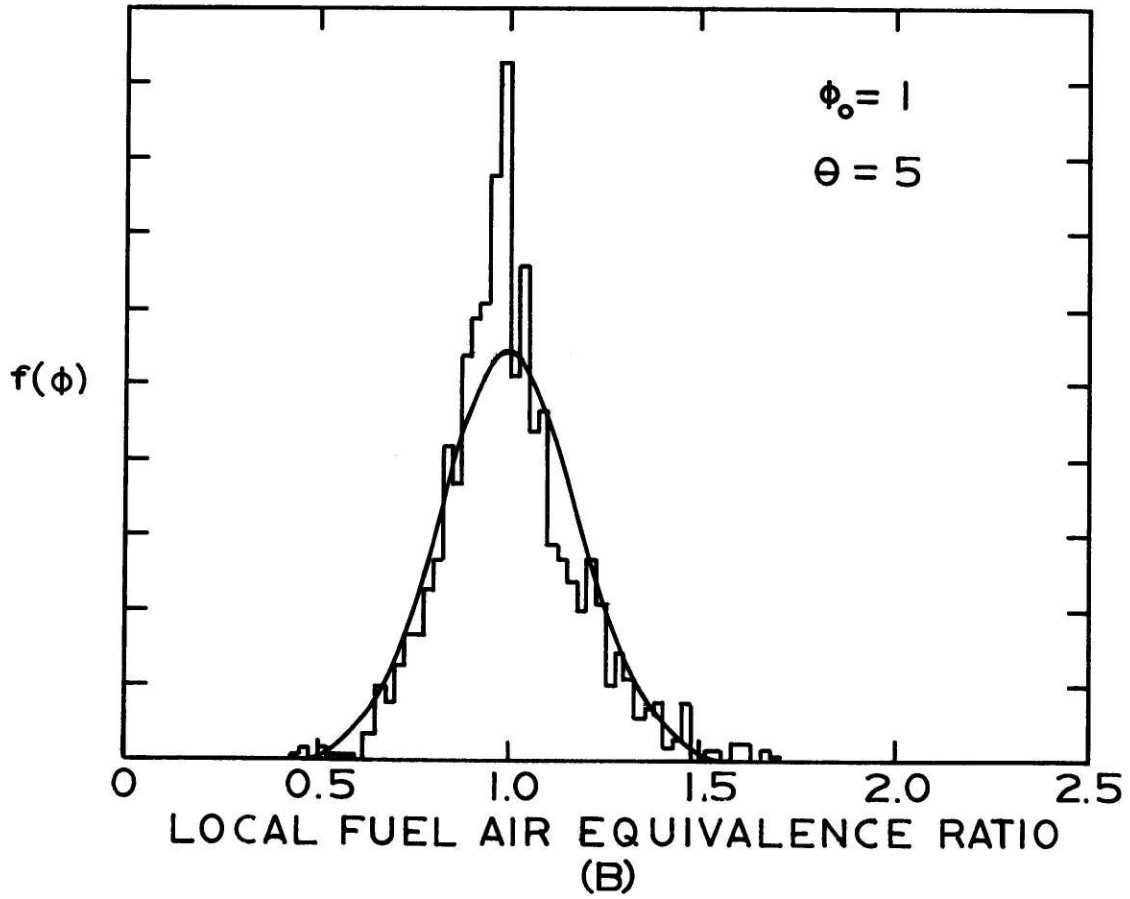
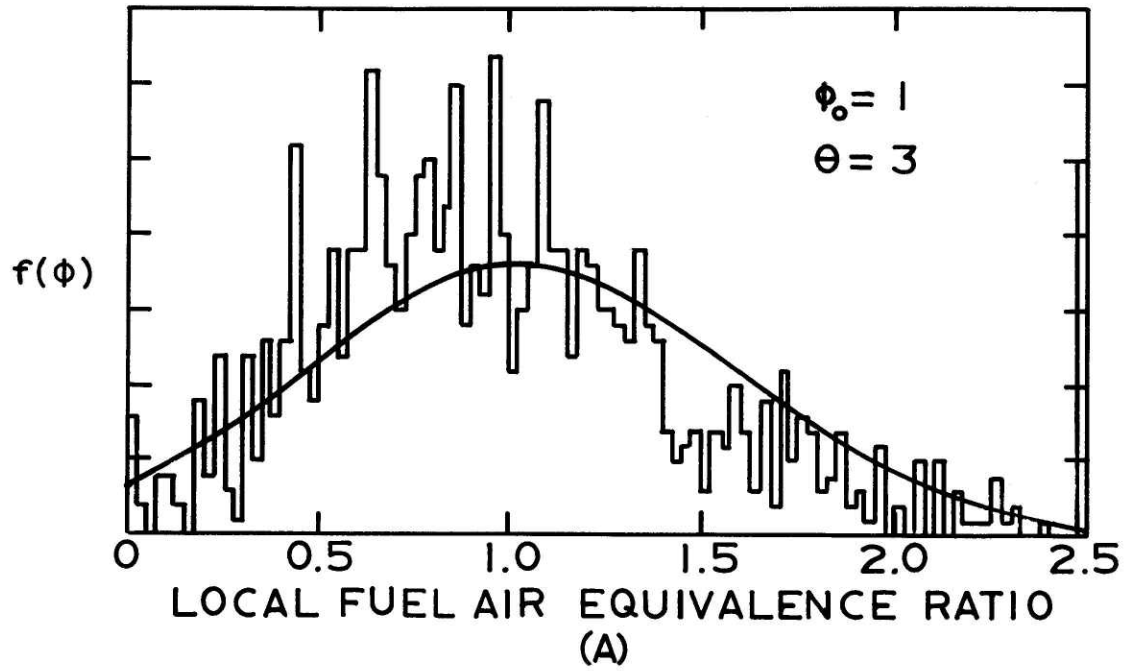


Figure 18. Comparison of the distribution function calculated using the statistical collision model with a gaussian distribution of the same variance. $N=1000$, $\phi_0=1$.

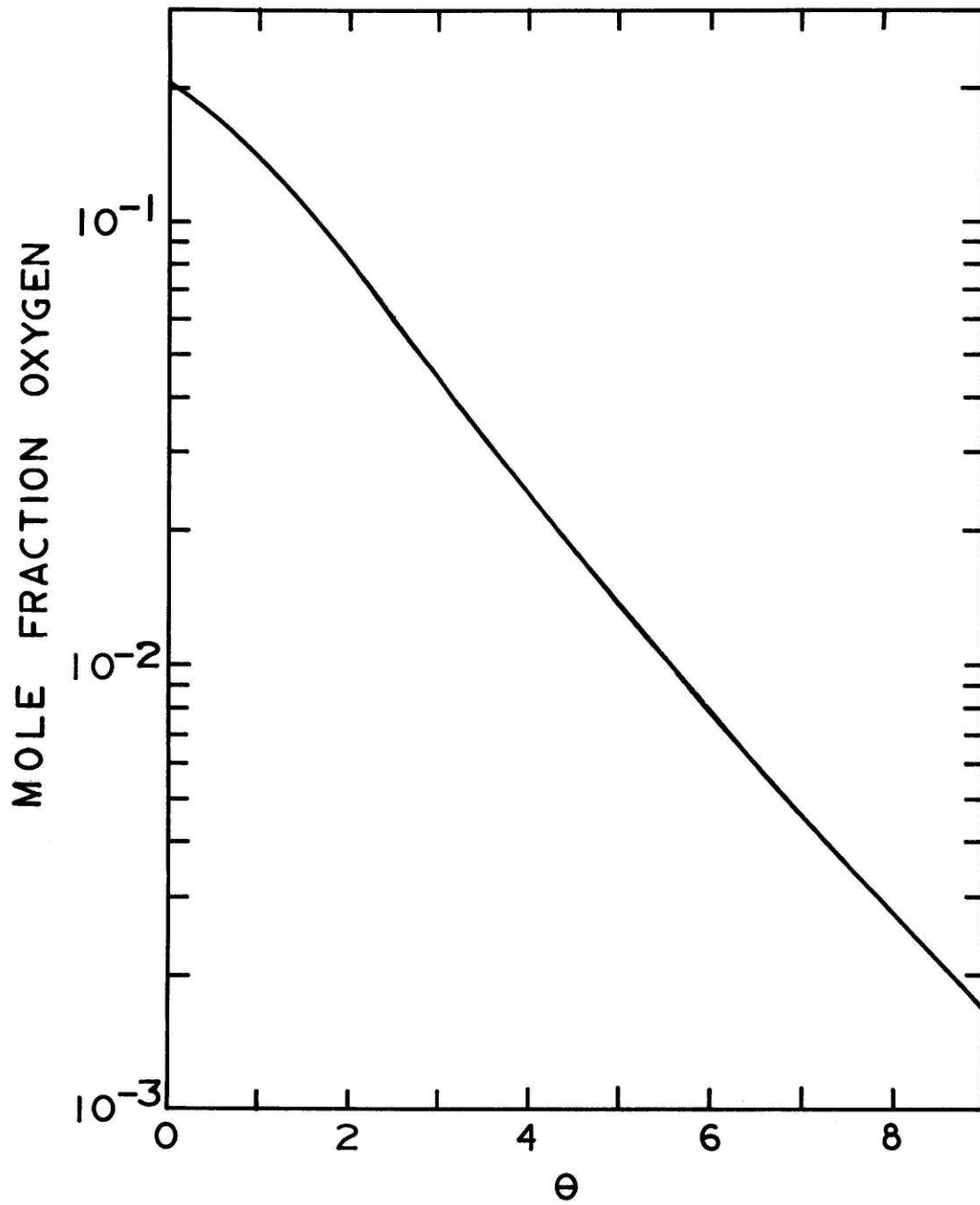


Figure 19. Oxygen concentration calculated using the statistical collision model for stoichiometric combustion. $N=1000$.

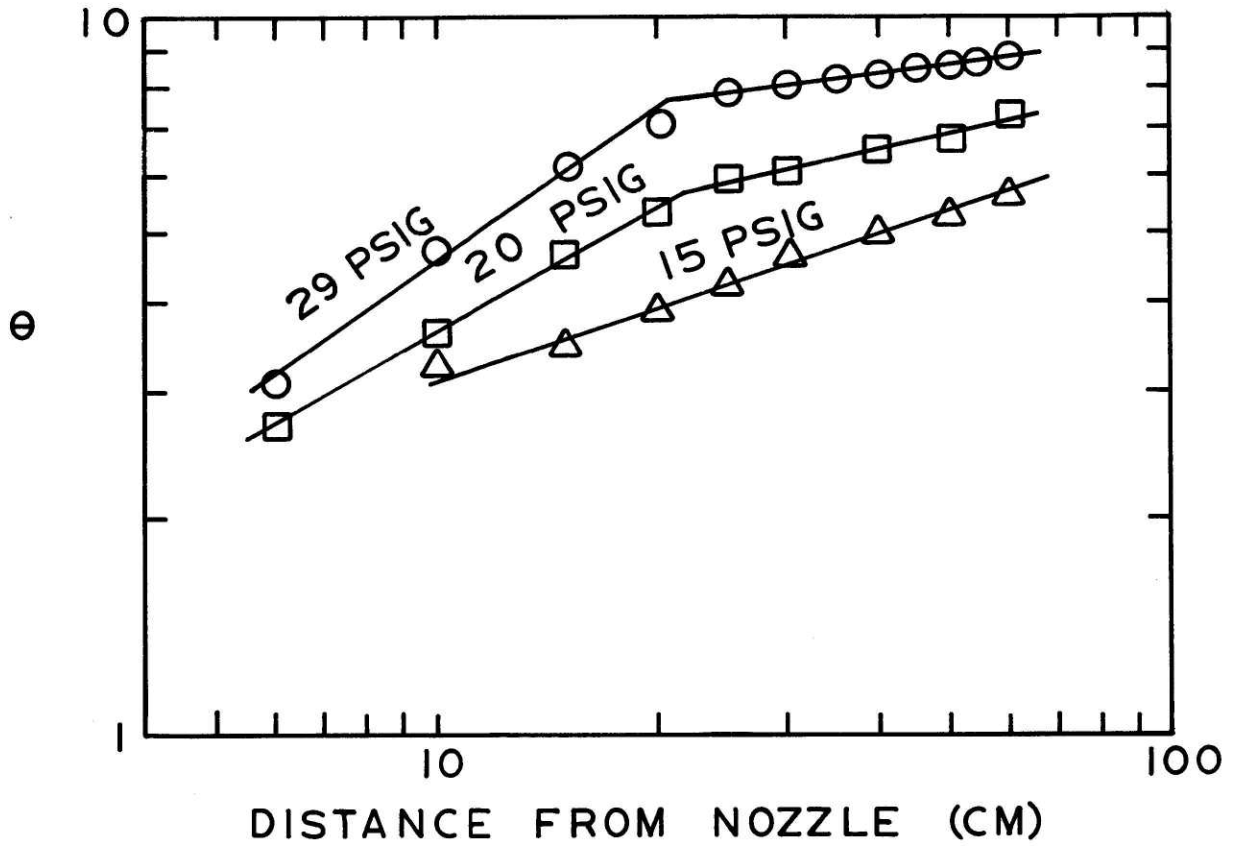


Figure 20. Dimensionless mixing time as a function of the axial distance down the combustor.

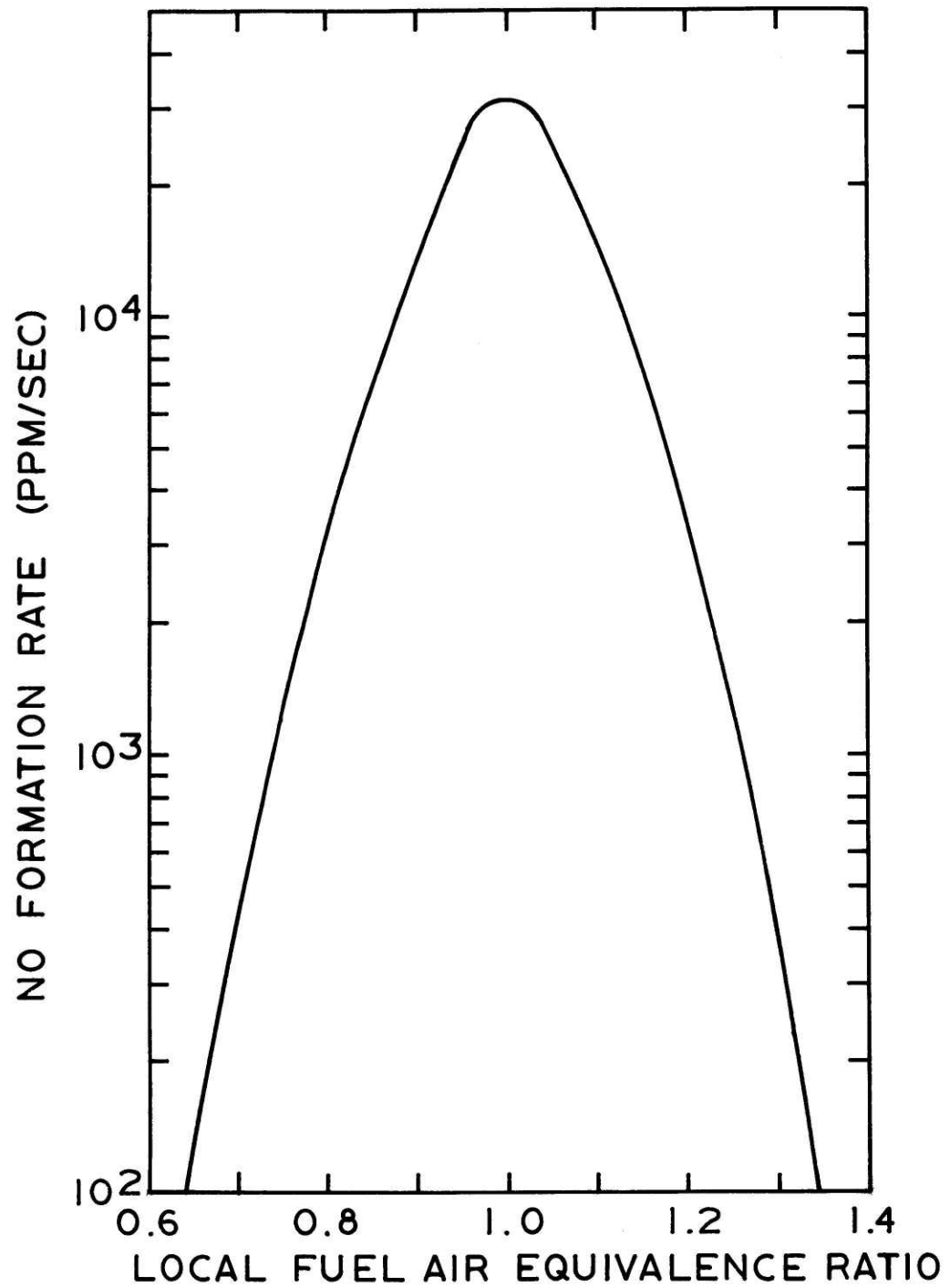


Figure 21. Rate of NO formation as a function of the local fuel air equivalence ratio (from Ref. 17).

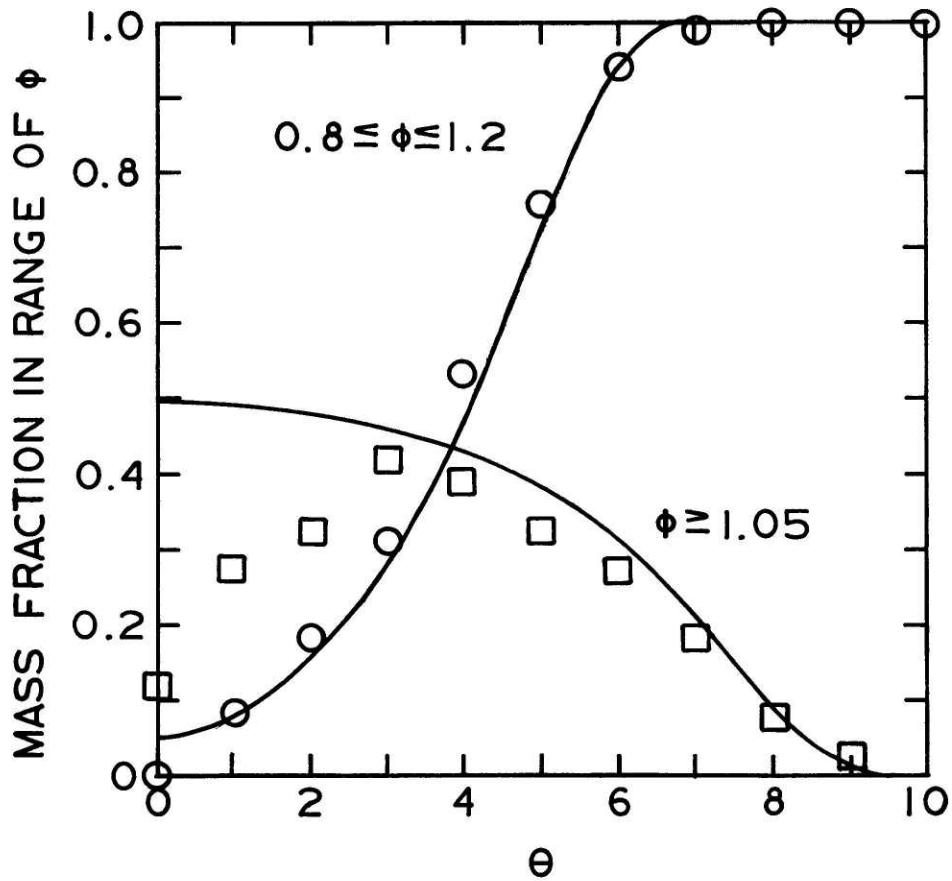


Figure 22. A comparison of the contribution of a gaussian distribution function within the noted ranges of ϕ (—) with the results of the statistical collision model (\circ, \square).

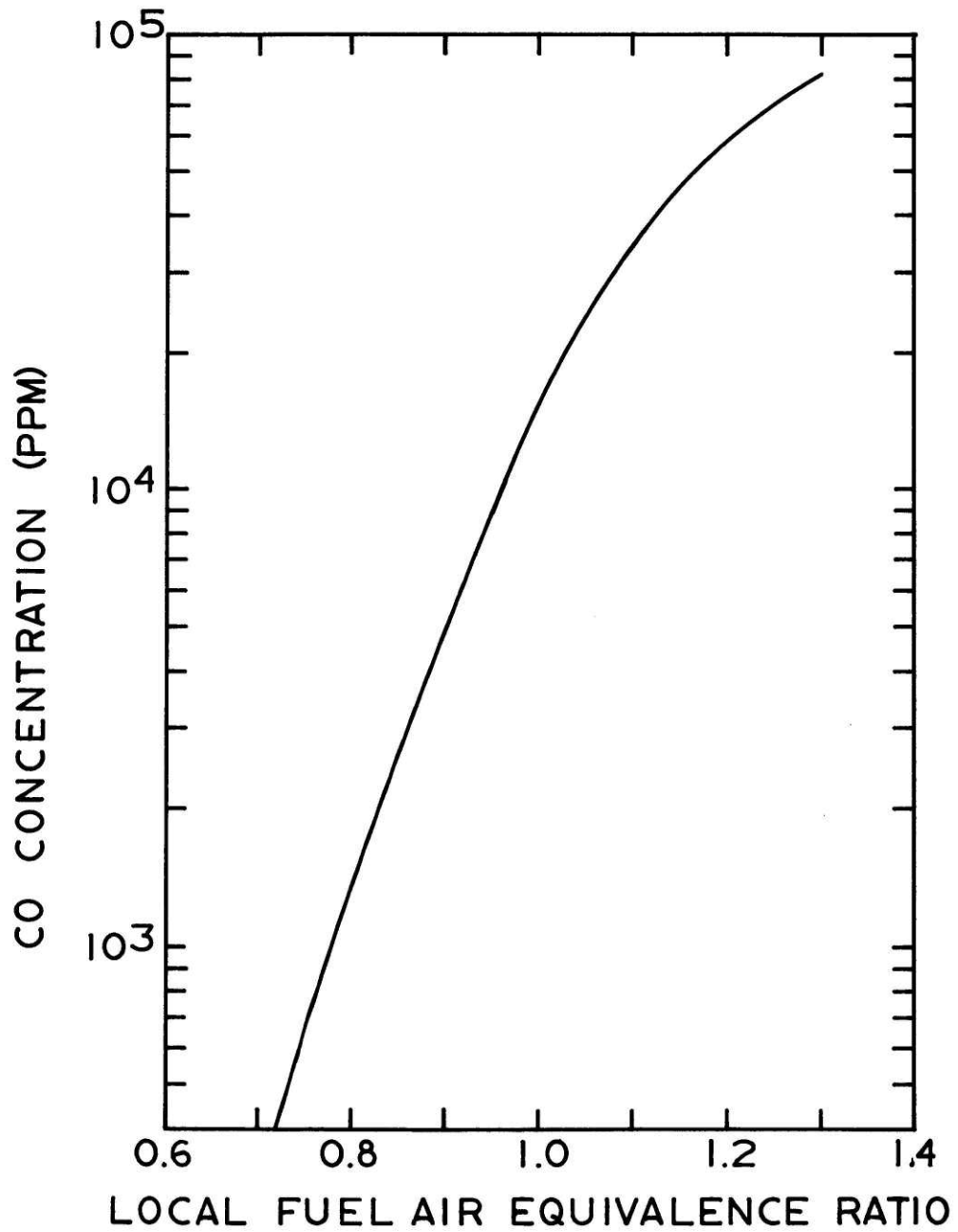


Figure 23. CO concentration as a function of the local fuel air equivalence ratio (from Ref. 17).

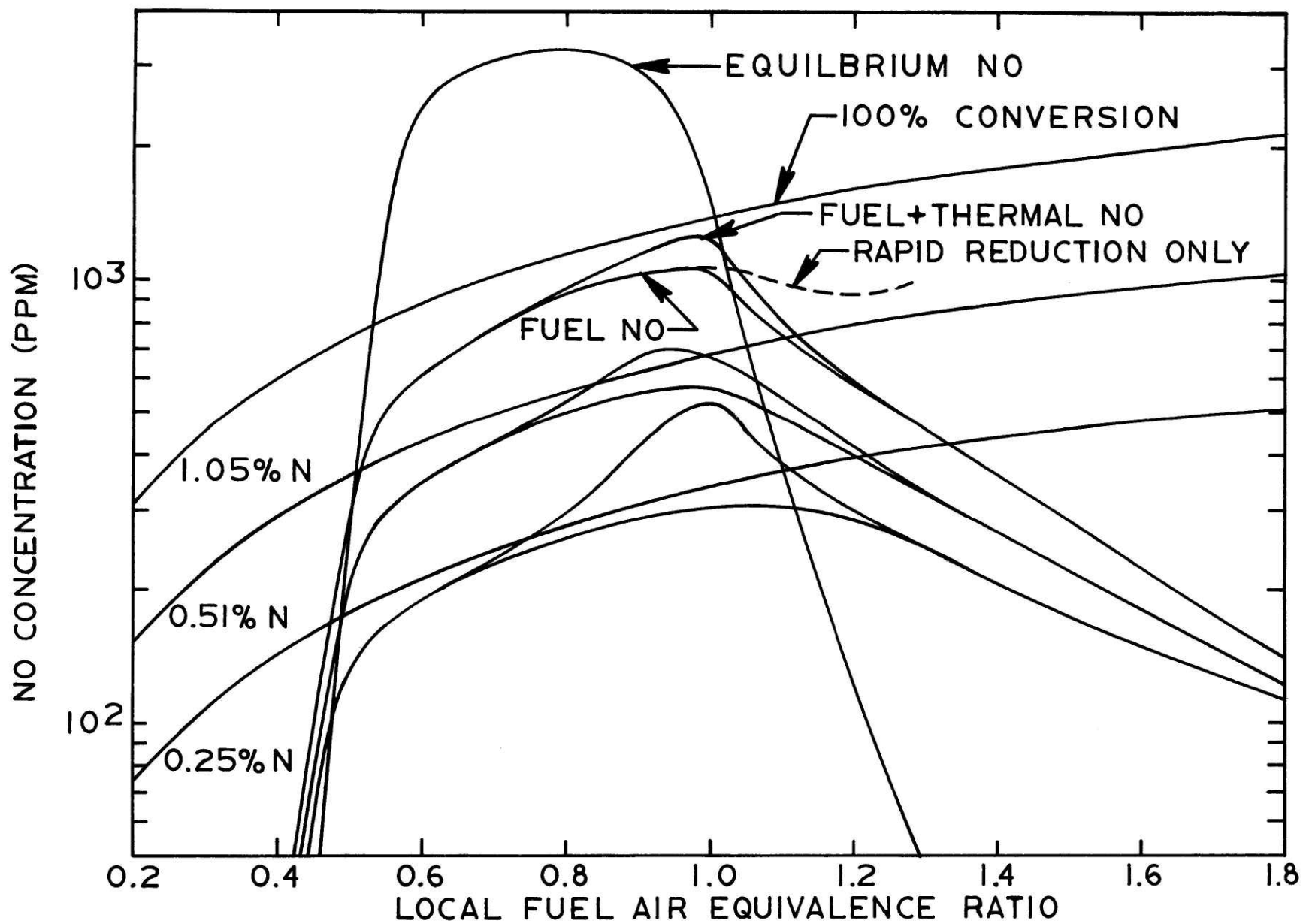


Figure 24. Local NO concentration from fuel nitrogen as calculated using the kinetic model with no mixing.

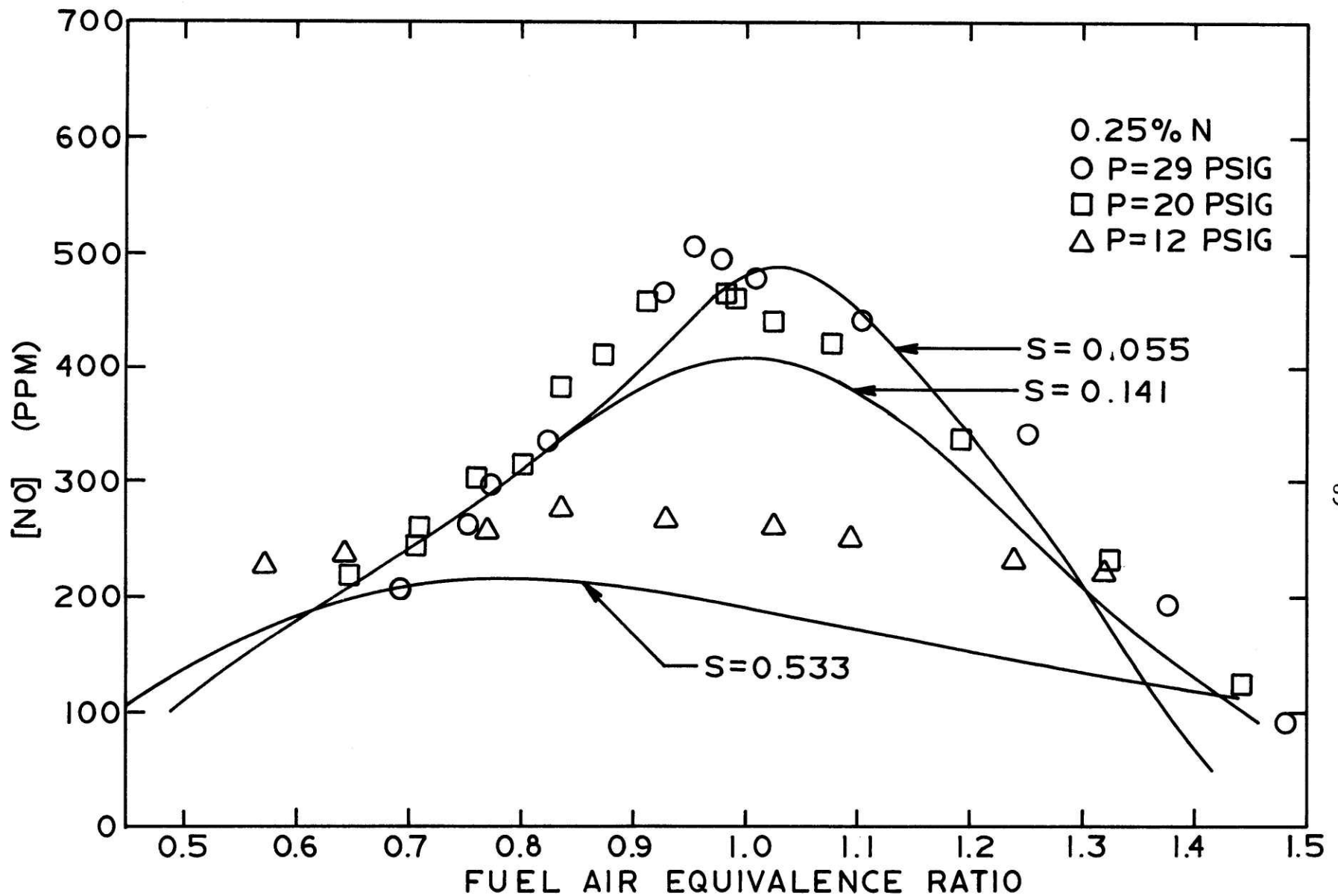
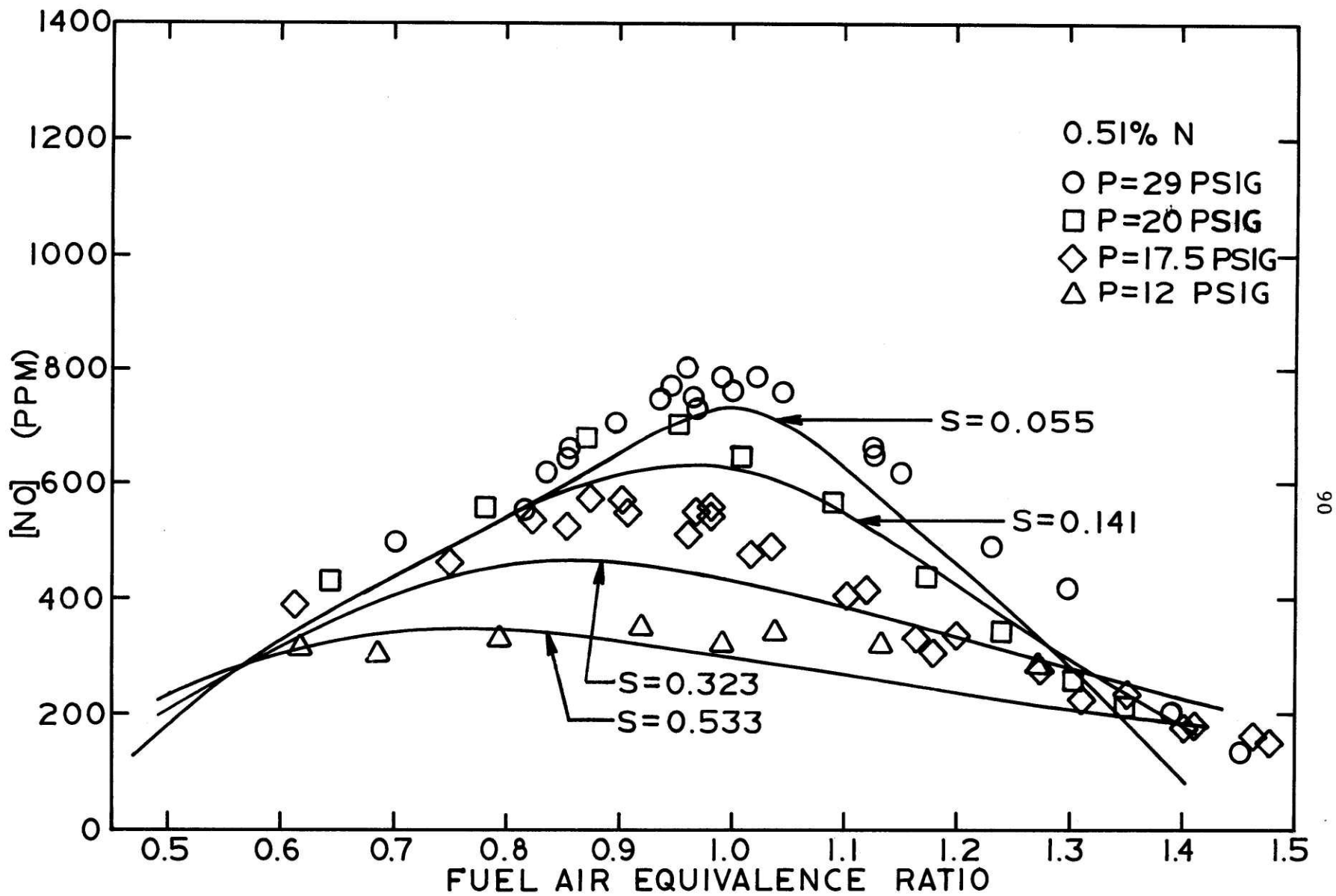
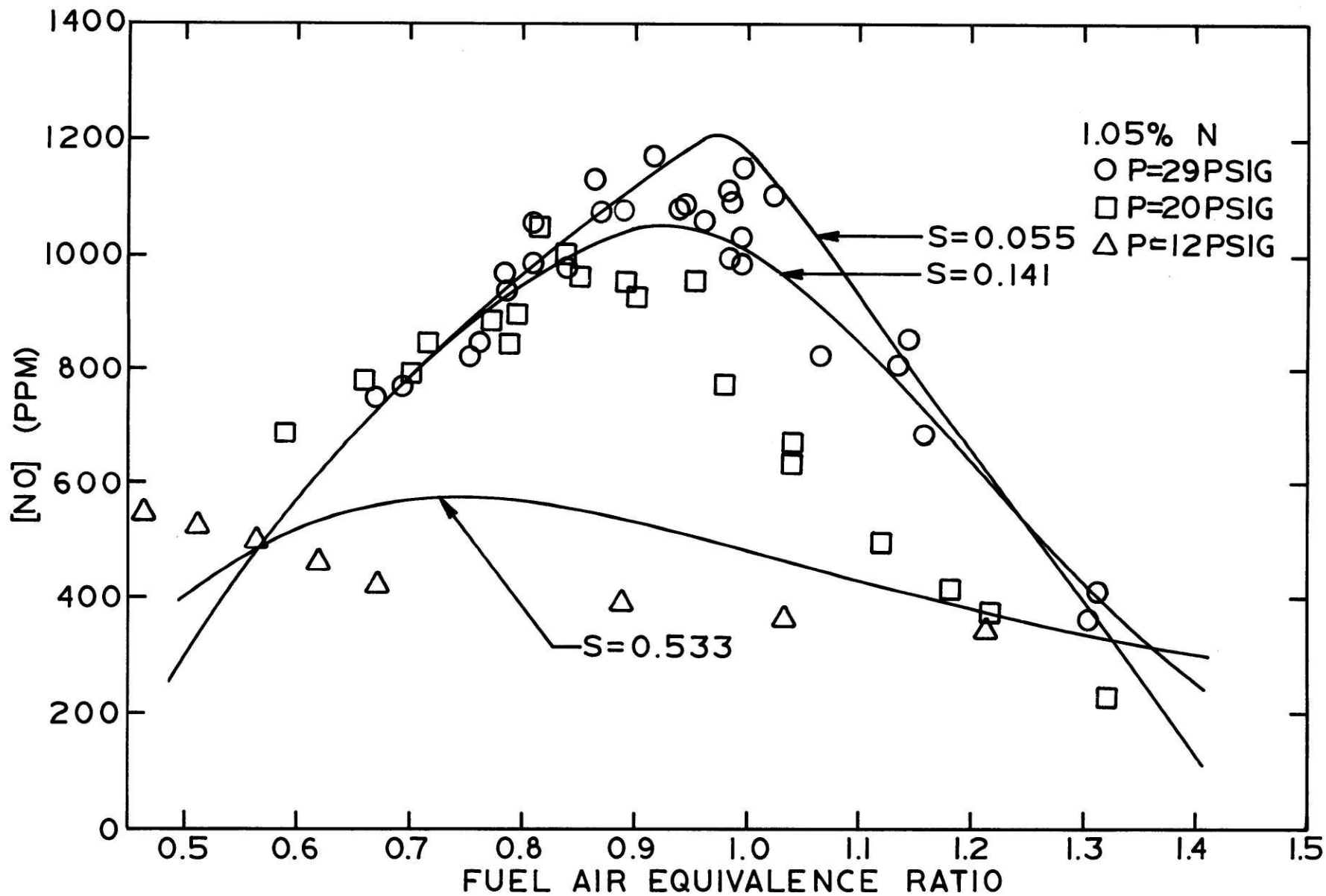


Figure 25. Comparison of the results of the kinetic model calculations with NO concentrations measured in the combustor exhaust during the combustion of pyridine doped fuel. (A) 0.25 weight per cent nitrogen.



06

(B) 0.51 weight per cent nitrogen.



(c) 1.05 weight per cent nitrogen.

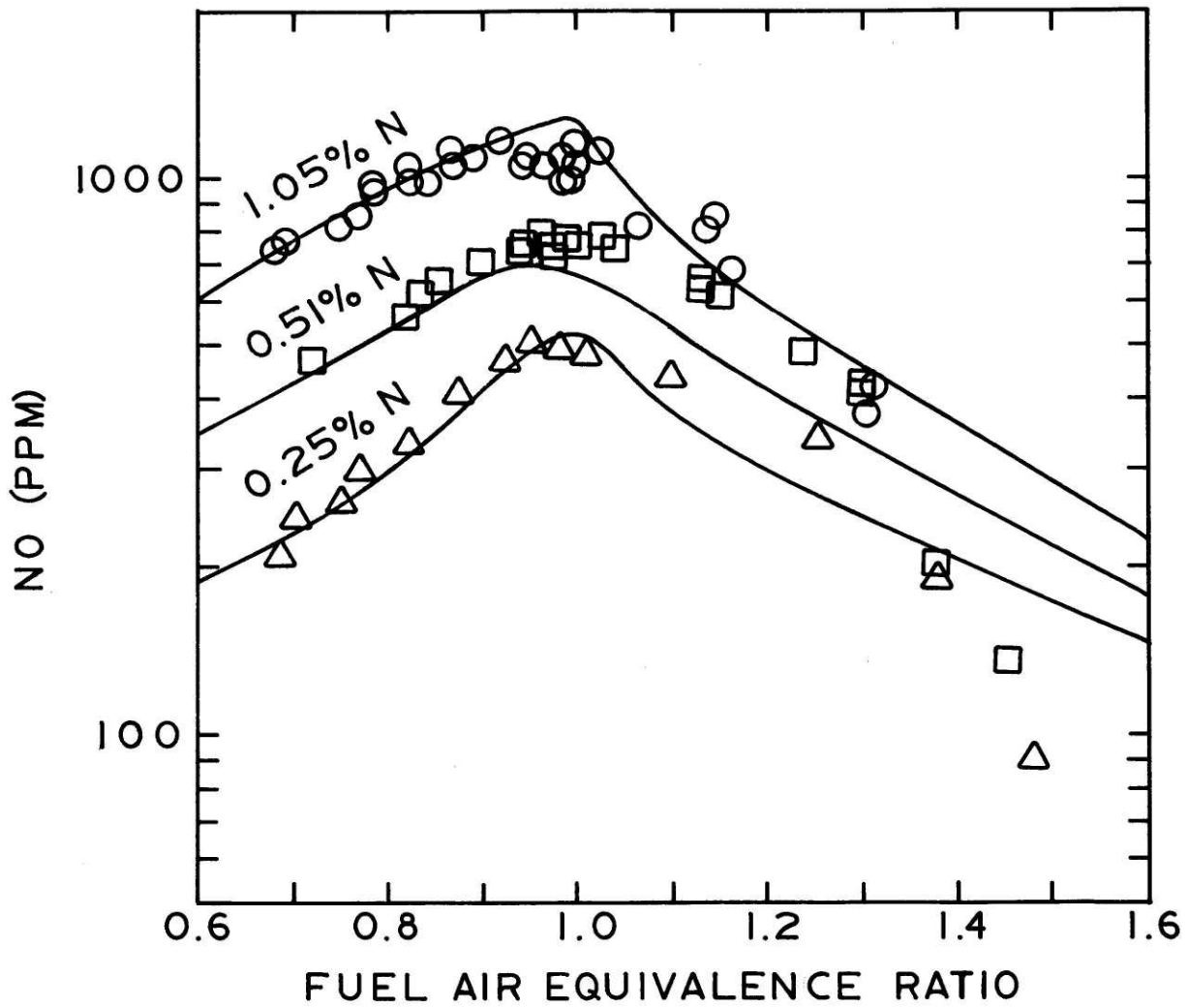


Figure 26. Comparison of exhaust NO concentrations for well mixed ($p=29$ psig) combustion with the results of the kinetic model for uniform flow.

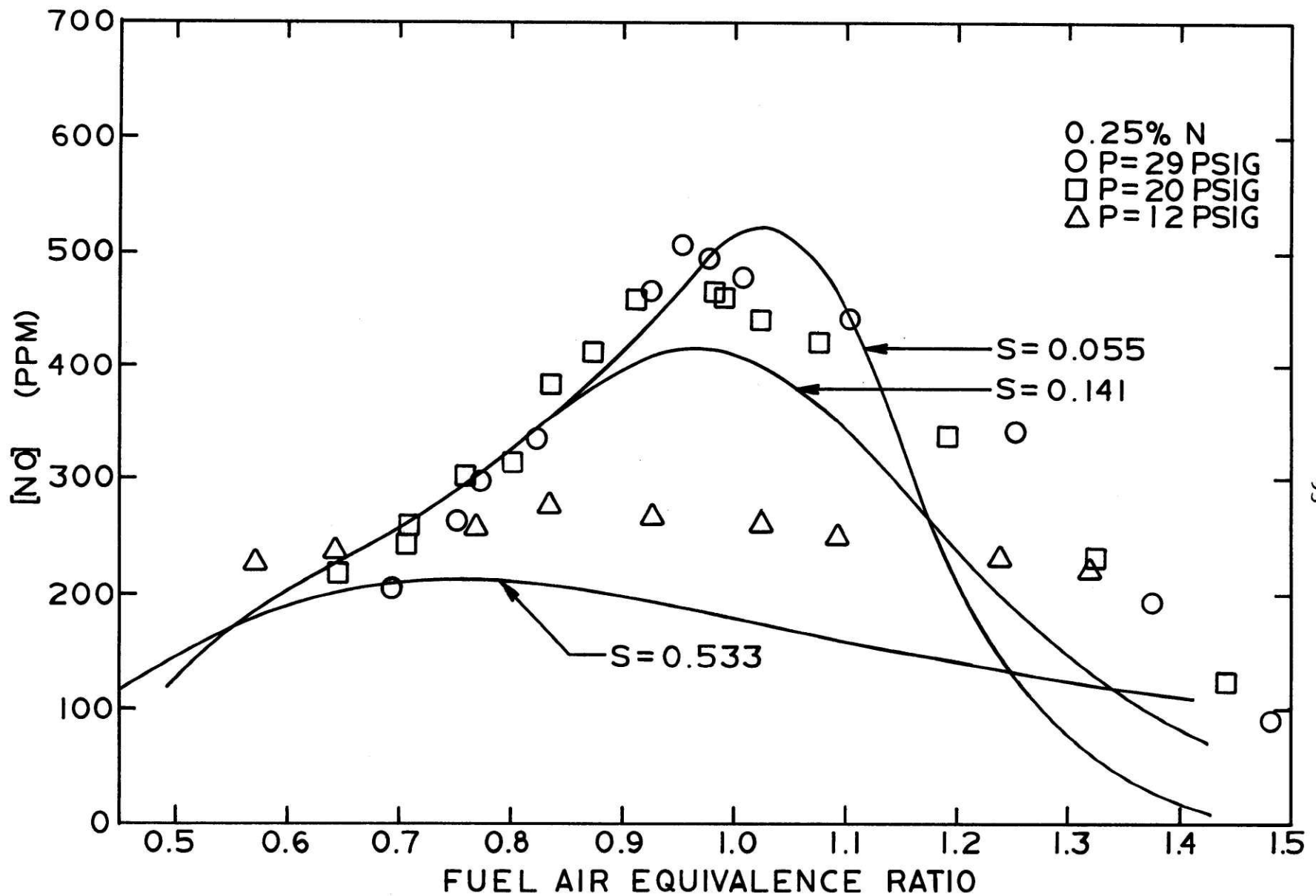
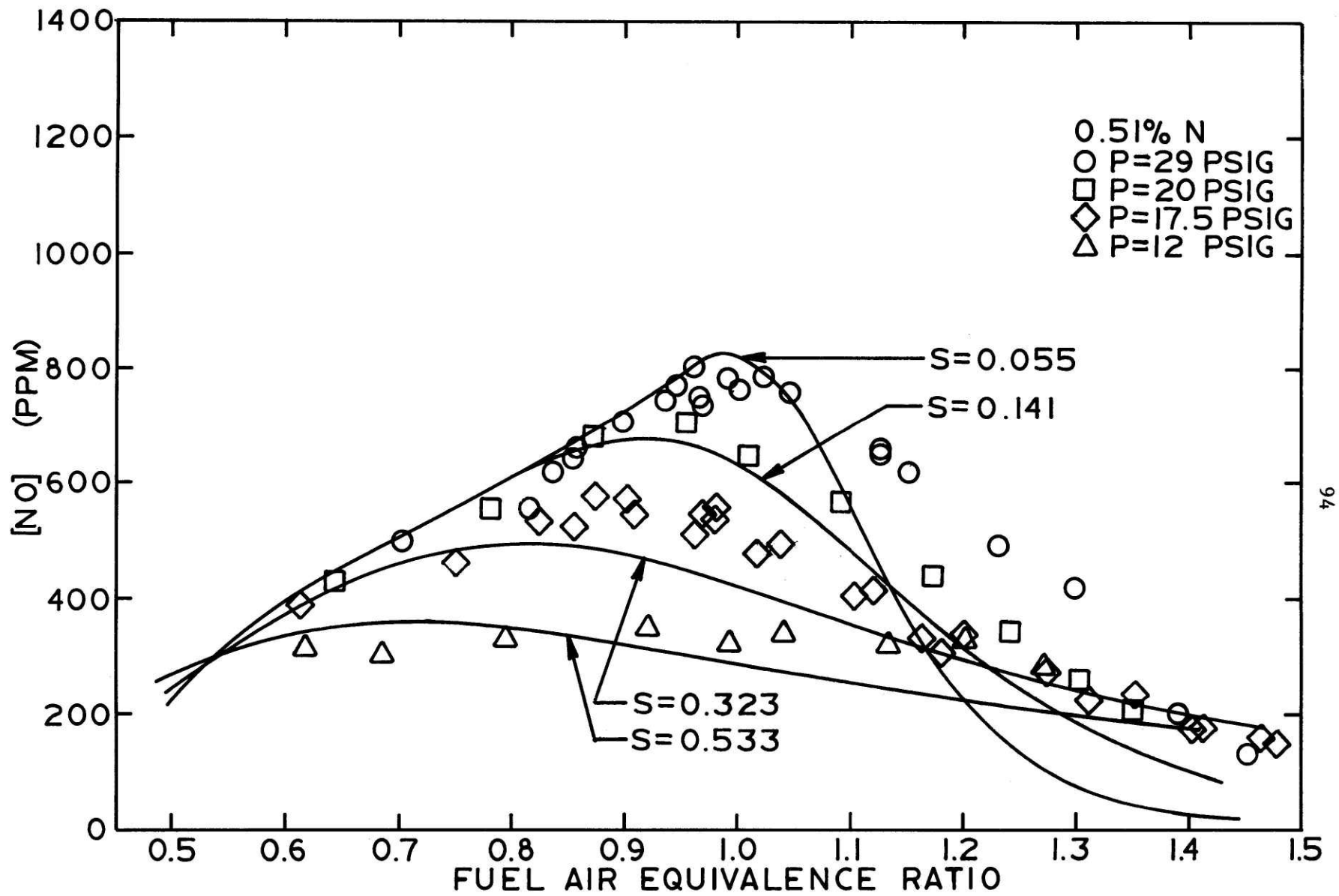
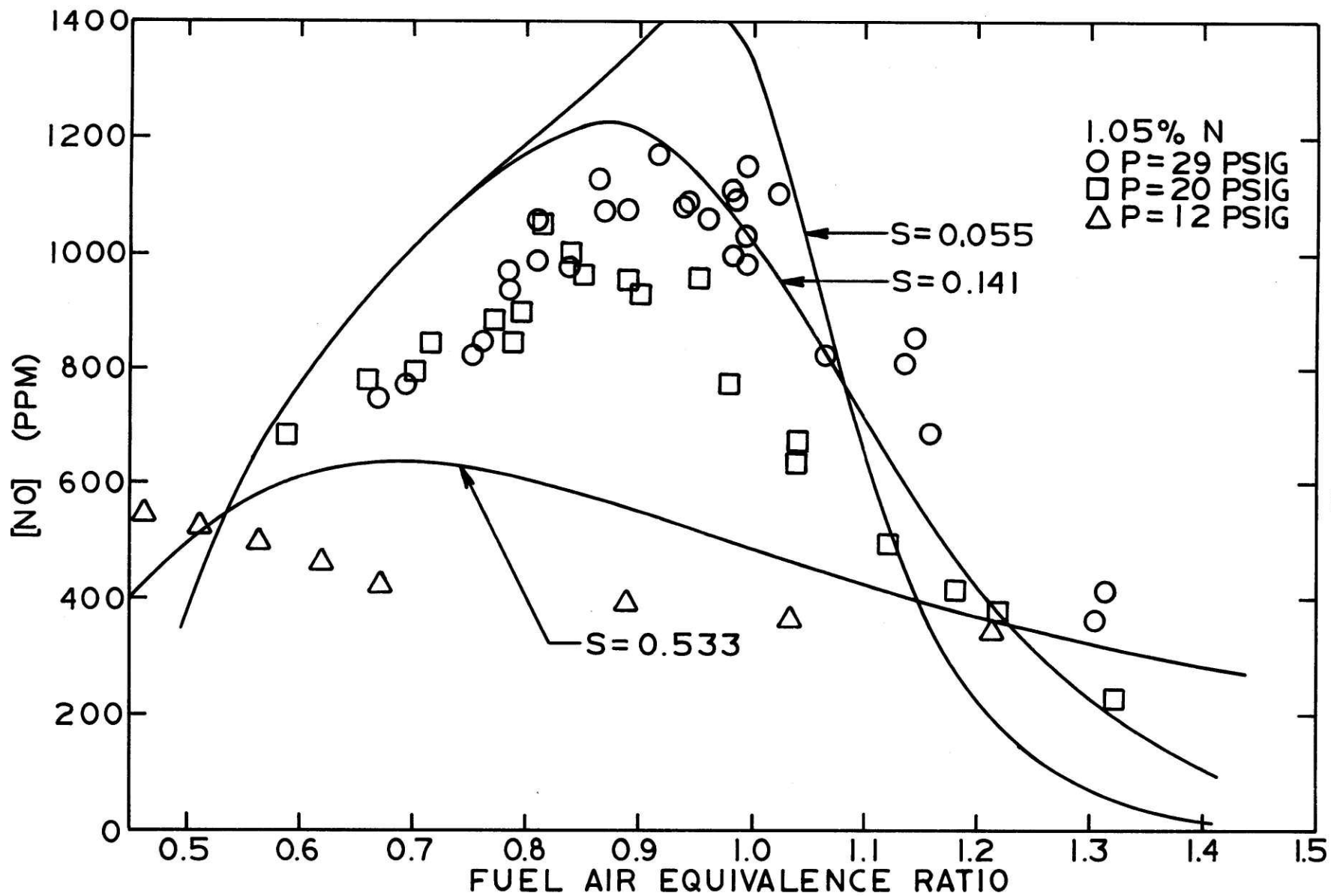


Figure 27. Comparison of the results of the simplified calculation of NO formation (100 per cent conversion plus thermal NO or equilibrium NO) with exhaust measurements for pyridine doped fuel. (A) 0.25 weight per cent nitrogen.



(B) 0.51 weight per cent nitrogen.



(C) 1.05 weight per cent nitrogen.

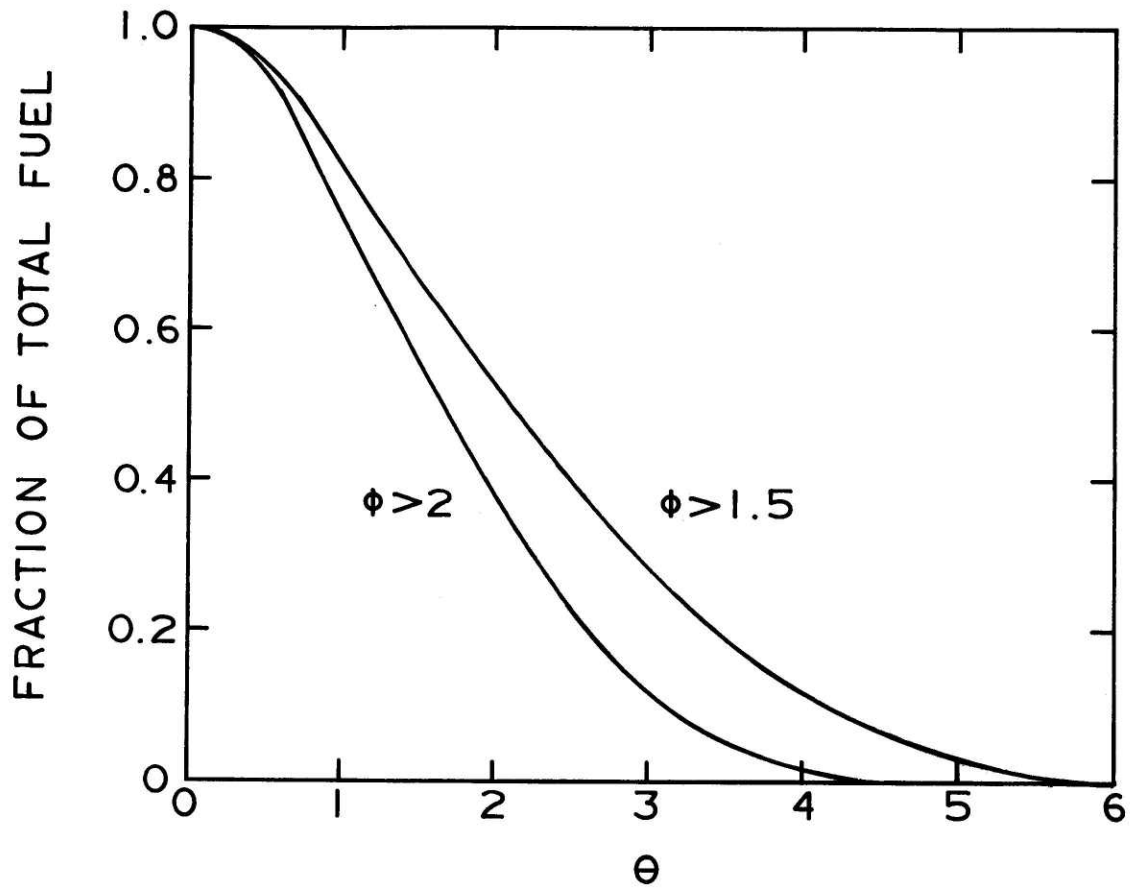


Figure 28. Fraction of fuel (or fuel nitrogen) at very rich conditions during stoichiometric combustion calculated using statistical collision model.



77 Massachusetts Avenue
Cambridge, MA 02139
<http://libraries.mit.edu/ask>

DISCLAIMER NOTICE

The pagination in this thesis reflects how it was delivered to the Institute Archives and Special Collections.

Missing page 97

REFERENCES

1. W. Bartok, A.R. Crawford, and A. Skopp, "Control of NO Emissions from Stationary Sources," Chem. Eng. Prog. 64, (1971).
2. W. Bartok, A.R. Crawford, A.R. Cunningham, H.J. Hall, E.H. Manny, and A. Skopp, "System Study of Nitrogen Oxides Control Methods for Stationary Sources," Final Report No. GR-2-NOS-69, NAPCA Contract No. PH 22-68-55, Esso Research and Engineering Co. (FCSTI PB 192 789) November 1969.
3. W. Bartok, V.S. Engleman, R. Goldstein, and E.G. del Valle, "Basic Kinetic Studies and Modeling of Nitrogen Oxide Formation in Combustion Processes," presented at Symposium on Combustion Processes and Air Pollution Control, A.I.Ch.E. 70th Annual Meeting, Atlantic City, August 29, 1971.
4. G. Blair Martin, and E.E. Berkau, "An Investigation of the Conversion of Various Fuel Nitrogen Compounds to Nitrogen Oxides in Oil Combustion," presented at Symposium on Combustion Processes and Air Pollution Control, A.I.Ch.E. 70th Annual Meeting, Atlantic City, August 30, 1971.
5. J.T. Shaw and A.T. Thomas, "Oxides of Nitrogen in Relation to Combustion of Coal," presented at 7th International Conference on Coal Science, Prague, Czechslovakia, June 1968.
6. D.W. Turner and C.W. Siegmund, "Staged Combustion and Flue Gas Recycle: Potential for Minimizing NO_x from Fuel Oil Combustion," presented at the American Flame Research Committee Flame Days, Chicago, Illinois, September 6-7, 1972.
7. A.A. Jonke, E.L. Carls, R.L. Jarry, L.J. Anatasia, M. Haas, J.R. Pavlik, W.A. Murphy, C.B. Schoffstoll, and G.N. Vargo, "Reduction of Atmospheric Pollution by Application of Fluidized Bed Combustion," Annual Report ANL/ES-CEN-1002 (June 1969-June 1970), Argonne National Laboratory.
8. W. E. Morrison and C.L. Readling, "An Energy Model for the United States," Bureau of Mines Information Circular 8384, 1968. W.E. Morrison, "Simulated Models of Future Energy Demand-Probabilities and Contingencies for 1980 and 2000 A.D.," A.S.M.E. Publication 68-PWR-4, 1968.
9. W.E. Haines, G.L. Cook, and G.U. Dinneen, "Techniques for Separating and Identifying Nitrogen Compounds in Petroleum and Shale Oil," 7th World Petroleum Congress Proceedings, 9, 83 (1967).

10. H.M. Spiers, Technical Data on Fuels, 6th Edition, pp. 297-298. The British National Committee, World Power Conference, 1962.
11. -- "Profile of Air Pollution Control, "Air Pollution Control District, County of Los Angeles, Los Angeles, 1971.
12. -- "Rules and Regulations," Air Pollution Control District, County of Los Angeles, Los Angeles, 1969.
13. -- Resources and Man, National Academy of Sciences - National Research Council, W.H. Freeman and Co., 1969.
14. -- "Control Techniques for Nitrogen Oxide Emissions from Stationary Sources," National Air Pollution Control Administration Publication No. AP-67, 1967.
15. C.P. Fenimore, Comb. and Flame 19, 289 (1972).
16. C.T. Johnson, Jr., "The Conversion of Fuel Bound Nitrogen to Nitric Oxide in Low Volatile Pulverized Coal Flames," S.B. Thesis, Department of Chemical Engineering, Massachusetts Institute of Technology, March, 1973.
17. F. Pompei and J.B. Heywood, Comb. and Flame 19, 407 (1972).
18. R.C. Flagan, F. Pompei, and J.P. Appleton, "Atmospheric Pressure Burner Studies II: Nitric Oxide Formation by Combustion of Nitrogen Containing Fuels," presented at Central States Section Meeting, The Combustion Institute, Bartlesville, Oklahoma, March, 1972.
19. J.P. Appleton and J.B. Heywood, "The Effects of Imperfect Fuel-Air Mixing in a Burner on Formation from Nitrogen in the Air and in the Fuel," Fourteenth Symposium (International) on Combustion, August, 1972 (in press)
20. M.B. Jacobs, The Analytical Toxicology of Industrial Inorganic Poison, p. 433, Interscience Publishers, New York, 1967.
21. A.A. Noyes and E.H. Swift, Qualitative Chemical Analysis of Inorganic Substance, p. 329, Macmillan Co., New York, 1942.
22. C.P. Fenimore, personal communication.
23. C.D. Hurd, A.R. Macon, J.I. Simon, and R.V. Levetan, Am. Chem. Soc. J., 84, 4509 (1962).
24. J.C. Keck and D. Gillespie, Comb. and Flame 17, 237 (1971).
25. S. Galant, "Thermodynamics of Constrained Equilibrium," S.M. Thesis Department of Mechanical Engineering, Massachusetts Institute of Technology, January 1973.

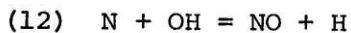
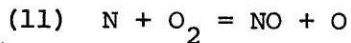
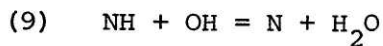
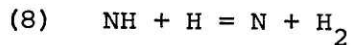
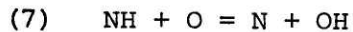
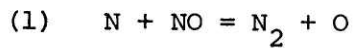
26. D.L. Baulch, D.D. Drysdale, D.G. Horne, and A.C. Lloyd, "Critical Evaluation of Rate Data for Homogeneous, Gas Phase Reactions of Interest in High-Temperature Systems," Report No. 4, Department of Physical Chemistry, The University, Leeds, England, Dec. 1969.
27. C.P. Fenimore and G.W. Jones, *J. Phys. Chem.* 65, 298, (1961).
28. W.E. Kaskan and D.E. Hughes, "Mechanism of Decay of Ammonia in Flame Gases from an NH_3/O_2 Flame," accepted for publication in *Comb. and Flame*.
29. D.I. MacLean and H. Gg. Wagner, 11th Symposium on Combustion, pp. 871-878, The Combustion Institute, 1967.
30. G.S. Bahn, "Reaction Rate Compilation for the H-O-N System," Gordon and Breach, Science Publishers, 1968.
31. I.M. Campbell and B.A. Thrush, *Trans. Faraday Soc.* 64, 1265 (1968).
32. A.A. Westenberg and R.M. Fristrom, Tenth Symposium (International) on Combustion, p. 473, The Combustion Institute, 1965.
33. G.B. Skinner, A. Lifsklitz, K. Scheller, and A. Burcat, *J. Chem. Phys.* 56, 3853 (p. 172).
34. D.J. Seery and C.T. Bowman, *Comb. and Flame* 14, 37 (1970).
35. A.A. Westenberg, *Comb. Sci. and Tech.* 4, 59 (1971).
36. I.I. Galyun and Yu. A. Ivanov, *Combustion, Explosion and Shock Waves* 6, 211 (1973). (*Fizika Goreniya & Vrzyva* 6, 237 (1970)).
37. R.S. Fletcher and J.B. Heywood, "A Model for Nitric Oxide Emissions from Aircraft Gas Turbines," presented at A.I.A.A. 9th Aerospace Sciences Meeting, New York, January 1971.
38. S. Corrsin, *A.I.Ch.E. J.* 3, 329 (1957).
39. S. Corrsin, *Phys. Fluids* 1, 42 (1958).
40. S. Corrsin, *A.I.Ch.E. J.* 10, 870 (1964).
41. R.L. Curl, *A.I.Ch.E. J.* 9, 175 (1963).
42. J.J. Evangelista, S. Katz, and R. Skinnar, *A.I.Ch.E. J.* 15, 843, (1969).
43. J.J. Evangelista, R. Skinnar, and S. Katz, 12th Symposium (International) on Combustion, p. 901, The Combustion Institute, (1968).
44. L.A. Spielman and O. Levenspiel, *Chem. Engr. Science* 20, 247 (1965).

45. S.A. Shain, A.I.Ch.E. J. 12, 806 (1966).
46. D.P. Rao, I.J. Dunn, Chem. Engr. Science 25, 1275 (1970).
47. -- "Basic Considerations in the Combustion of Hydrocarbon Fuels with Air," NACA Report 1300, Propulsion Chem. Div., Lewis Flight Prop. Lab., 1957.
48. H.C. Hottel and A.F. Sarofun, Radiative Transfer, McGraw-Hill, 1967.

APPENDIXA Test for the Partial Equilibrium Approximation

The partial equilibrium assumption implies that the shuffle reactions between any one species and the remainder of the species within a constraint are fast enough that the equilibrium is maintained. This must be true in spite of the fact that the reactions changing the total level of the constraint may act on only a small portion of the total constrained species. If the rates of the shuffle reactions are known or can be estimated, the validity of this assumption may be tested by drawing a parallel between the partial equilibrium and steady-state assumptions.

Take as an example the N atom concentration when all of the bound nitrogen is considered to be described by a single constraint. The important reactions affecting [N] are:



The time rate of change of [N] is given by

$$\begin{aligned} \frac{d[\text{N}]}{dt} = & -k_1^+ [\text{N}] [\text{NO}] + k_1^- [\text{N}_2] [\text{O}] + k_7^+ [\text{NH}] [\text{O}] - k_7^- [\text{N}] [\text{OH}] \\ & + k_8^+ [\text{NH}] [\text{H}] - k_8^- [\text{N}] [\text{H}_2] + k_9^+ [\text{NH}] [\text{OH}] - k_9^- [\text{N}] [\text{H}_2] \\ & - k_{11}^+ [\text{NO}] [\text{O}_2] + k_{11}^- [\text{NO}] [\text{O}] - k_{12}^+ [\text{N}] [\text{OH}] + k_{12}^- [\text{NO}] [\text{H}] \end{aligned}$$

Assuming the steady state approximation has been achieved, $\frac{d[N]}{dt} = 0$

and

$$[N]_{ss} = \frac{k_1^- [N_2] [O] + k_7^+ [NH] [O] + k_8^+ [NH] [H] + k_9^+ [NH] [OH] + k_{11}^- [NO] [O] + k_{12}^- [NO] [H]}{k_1^+ [NO] + k_7^- [OH] + k_8^- [N] + k_9^- [H_2O] + k_{11}^+ [O_2] + k_{12}^+ [OH]}$$

which may be rewritten

$$[N]_{ss} = \frac{R_f}{R_r} \frac{1 + k_1^- [N_2] [O] / R_f}{1 + k_1^+ [NO] / R_r}$$

R_f is the rate of production of N by the exchange reactions responsible for maintaining the equilibrium within the constraint and R_r is the rate of elimination of N by these same reactions. Thus R_f/R_r is the partial equilibrium concentration $[N]_{pe}$. It is readily seen that if either $k_1^- [N_2] [O] / R_f$ or $k_1^+ [NO] / R_r$ is of order unity or larger the partial equilibrium will not be maintained even if it has initially been satisfied.

Biographical Note

The author was born in Spokane, Washington, on June 12, 1947 and attended public schools in Spokane, Toledo, Ohio, Mt. Clemens, Michigan, and Grosse Pointe, Michigan.

He entered the University of Michigan in September, 1965 and received a B.S.E. degree in Mechanical Engineering in May, 1969. During the summers he was employed in summer engineering programs at Chevrolet Engineering Center in 1966 and at Detroit Edison Co. in 1967 and 1968. From September, 1968 to September, 1969 he was a research assistant in the Fluid Dynamics Laboratory of the Mechanical Engineering Department of the University of Michigan. His graduate work was done at M.I.T. from September, 1969 to May, 1973.